AD_____

AWARD NUMBER DAMD17-98-1-8167

TITLE: Characterization of BC1-2, BC1-XL, and Bax Pore Formation and Their Role in Apoptosis Regulation

PRINCIPAL INVESTIGATOR: Sharon L. Schendel, Ph.D.

CONTRACTING ORGANIZATION: The Burnham Institute
La Jolla, California 92037

REPORT DATE: July 1999

TYPE OF REPORT: Annual Summary

PREPARED FOR: U.S. Army Medical Research and Materiel Command
Fort Detrick, Maryland 21702-5012

REPORT DOCUMENTATION PAGE

Form Approved
OMB No. 0704-0188

1. AGENCY USE ONLY *(Leave blank)*	2. REPORT DATE	3. REPORT TYPE AND DATES COVERED
	July 1999	Annual Summary (1 Jul 98 - 30 Jun 99)

4. TITLE AND SUBTITLE
Characterization of BC1-2, BC1-XL and Bax Pore Formation and Their Role in Apoptosis Regulation

5. FUNDING NUMBERS
DAMD17-98-1-8167

6. AUTHOR(S)
Sharon L. Schendel, Ph.D.

7. PERFORMING ORGANIZATION NAME(S) AND ADDRESS(ES)
The Burnham Institute
La Jolla, California 92037

8. PERFORMING ORGANIZATION REPORT NUMBER

9. SPONSORING / MONITORING AGENCY NAME(S) AND ADDRESS(ES)
U.S. Army Medical Research and Materiel Command
Fort Detrick, Maryland 21702-5012

10. SPONSORING / MONITORING AGENCY REPORT NUMBER

11. SUPPLEMENTARY NOTES

12a. DISTRIBUTION / AVAILABILITY STATEMENT
Approved for public release; distribution unlimited

12b. DISTRIBUTION CODE

13. ABSTRACT *(Maximum 200 words)*

The Bcl-2 protein family plays an important role in governing a cell's decision to live or die. Dysregulation of these proteins is observed in many breast cancer cases and thus it is important to understand their mechanism in order to develop new treatments. The Bcl-X_L protein structure showed a strong similarity to pore-forming bacterial toxins, suggesting that Bcl-2 protein family protein may regulate apoptosis by pore formation or membrane insertion. The results obtained this year include characterization of membrane binding of these proteins to lipid vesicles. It was found that conditions that promote membrane association are similar to those where channel activity is observed and that these conditions also induced a conformational change that had a greater exposure of hydrophobic surface are. The BH3 only protein BID was shown by others to be cleaved by Casp8. A recombinant mimic of this truncated form has channel activity that is voltage-gated on both planar bilayers and liposomes Single cysteine mutants of Bcl-X_L have been generated that will be used to probe the topology of the membrane-inserted state.

14. SUBJECT TERMS	15. NUMBER OF PAGES
Breast Cancer apoptosis, Bcl-2 protein family, BID, membrane proteins	41
	16. PRICE CODE

17. SECURITY CLASSIFICATION OF REPORT	18. SECURITY CLASSIFICATION OF THIS PAGE	19. SECURITY CLASSIFICATION OF ABSTRACT	20. LIMITATION OF ABSTRACT
Unclassified	Unclassified	Unclassified	Unlimited

FOREWORD

Opinions, interpretations, conclusions and recommendations are those of the author and are not necessarily endorsed by the U.S. Army.

NA Where copyrighted material is quoted, permission has been obtained to use such material.

NA Where material from documents designated for limited distribution is quoted, permission has been obtained to use the material.

NA Citations of commercial organizations and trade names in this report do not constitute an official Department of Army endorsement or approval of the products or services of these organizations.

NA In conducting research using animals, the investigator(s) adhered to the "Guide for the Care and Use of Laboratory Animals," prepared by the Committee on Care and use of Laboratory Animals of the Institute of Laboratory Resources, national Research Council (NIH Publication No. 86-23, Revised 1985).

NA For the protection of human subjects, the investigator(s) adhered to policies of applicable Federal Law 45 CFR 46.

NA In conducting research utilizing recombinant DNA technology, the investigator(s) adhered to current guidelines promulgated by the National Institutes of Health.

NA In the conduct of research utilizing recombinant DNA, the investigator(s) adhered to the NIH Guidelines for Research Involving Recombinant DNA Molecules.

NA In the conduct of research involving hazardous organisms, the investigator(s) adhered to the CDC-NIH Guide for Biosafety in Microbiological and Biomedical Laboratories.

7/28/99

PI - Signature Date

Table of Contents

Apoptotic cell death plays an important role in tissue homeostasis by clearing aged or damaged cells thus making space for new cells. In certain situations, the Bcl-2 protein family governs a cell's decision to heed or ignore death signals and malfunctions in the Bcl-2 protein family can lead to inappropriate amounts of cell death. Bcl-2, Bcl-X_L, and Bax are each expressed in normal mammary epithelium but in a significant number of mammary carcinomas, Bax and Bcl-2 protein levels are severely depressed or absent. These depressed levels directly correlate with shorter overall survival times. These results highlight the importance of proper regulation of Bcl-2 family protein activity.

Despite the large body of work describing the nature of protein-protein interactions that are predicted to be in important in apoptosis regulation by the Bcl-2 protein family, the biochemical function of these proteins remains unclear. The Bcl-X_L structure did provide a clue to this family's activity by its similarity to pore-forming bacterial toxins such as diphtheria and colicins. This study seeks to address whether form does indeed follow function by studying if these proteins are capable of membrane insertion. The aims of this project are to determine: (i) the structural changes that occur to convert Bcl-2 family proteins from soluble to membrane-inserted proteins; (ii) which regions of these proteins participate in pore formation; (iii) identifying the residues lining the channel lumen and the relative pore size. The attainment of these goals will utilize membrane-protein biochemistry, site-directed mutagenesis, biophysical techniques- including circular dichroism and fluorescence spectroscopy- and generation of cysteine mutants for fluorescence and EPR studies.

In vitro membrane interaction and structural changes upon membrane association. The Bcl-X_L structure showed the protein to have two central ~20 residue predominantly hydrophobic helices. These helices are of sufficient length to span a membrane bilayer whose hydrophobic cross-section is ~30 Å wide. A mechanism for pore-formation by the Bcl-2 protein family members could occur in a fashion similar to that predicted for the pore-forming colicins. The colicin E1 structure suggests that these molecules undergo a transition to a membrane insertion-competent state which exposes the hydrophobic helices, freeing them to insert into the membrane bilayer (Elkins *et al.* 1998). In the case of Bcl-2 and its homologues, the central hydrophobic helices could insert into the membrane either as monomers or coalesce in the membrane bilayers to form dimers or other multimers to complete the conductive channel. Bcl-2, Bcl-X_L, and Bax have each been demonstrated to form channels *in vitro* both in liposomes and planar bilayers (Schendel *et al.*, 1997; Minn *et al*, 1997; Antonsson *et al.*, 1997). For liposomes, an acidic pH is required for pore formation while conductive channels were observed at neutral pH in planar bilayers

indicating that channel formation can occur at physiological pH. The acidic pH requirement necessary to observe channel formation on a macroscopic level (i.e. the majority of molecules participate in channel formation) is most likely not a situation encountered *in vivo*. One explanation for the acidic pH requirement could be that it is necessary to impart upon the protein a protonation state that fosters electrostatic membrane interaction with the membrane surface. *In vivo,* this membrane interaction could occur in the absence of acidic pH because the protein will already be localized to the membrane surface by the C-terminal anchor which is not included in the recombinant version used in these studies. In order to determine whether exposure to acidic pH increases the probably of interaction of Bcl-2 family members with membranes their binding to lipid vesicles was assayed.

Vesicles composed of 30% DOPG, 60% DOPC, and 10% TNP-PE were prepared as described (Zakharov *et al.*, 1997). TNP-PE is a lipid modified at the head group with a trinitrophenyl moiety that quenches the intrinsic fluorescence of tryptophan residues which come within the ~10 Å quenching radius of the TNP group. Therefore, decreased Trp fluorescence implies membrane contact. Fig. 1 shows that in the presence of TNP-doped vesicles, the Trp fluorescence intensity is quenched. This quenching is not reversible after a pH shift from 4 to 8, indicating that this association has a hydrophobic as well as electrostatic component.

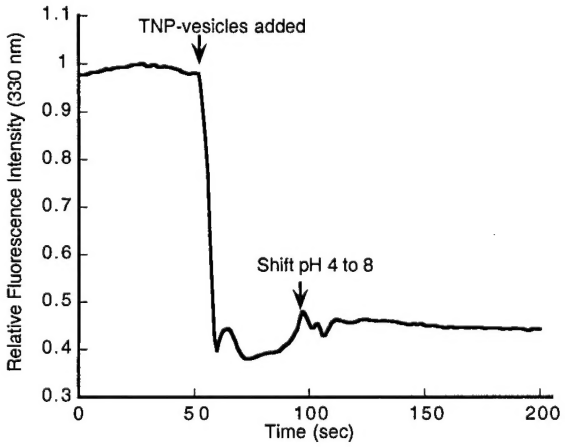

Fig. 1. Relative fluorescence intensity of Bcl-X_L in the presence of 60% DOPC/30%DOPG/10%TNP-PE vesicles. Bcl-X_L (5 μg/mL) was dissolved in 20 mM DMG, 200 mM NaCl, pH 4.0 at t=0. 70 μg/mL TNP lipids were added (arrow) and after stabilization, 60μL 0.3M Tris, 3M NaOH was added which is sufficient to increase the pH to 8.0. Spectra were obtained in the scan mode using a 330 nm excitation wavelength. Slit widths are 8 nm.

In addition, Bcl-2 and Bax were incubated with either 70% DOPC/30% DOPG or 100% DOPC vesicles (on which Bcl-2 family proteins have no activity) at varying pH

values for five minutes after which the vesicles were aggregated by addition of $CaCl_2$. The lipid and soluble fractions were separated by centrifugation and the lipid extracted from the membrane fraction. Soluble and membrane fraction were precipitated with TCA, resolved by SDS-PAGE and detected with polyclonal antibodies specific for each protein.

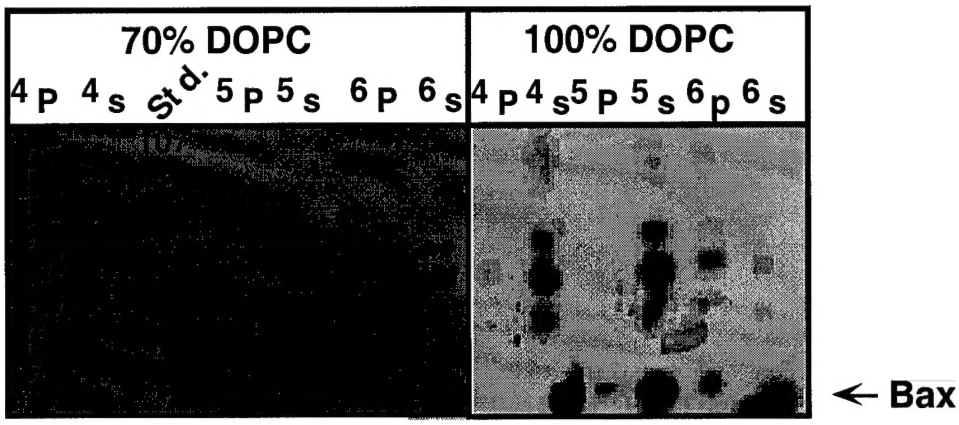

Fig. 2. pH-dependent Bax association with 70% DOPC/30%DOPG or 100% vesicles. Arrow indicates position of presumed monomeric Bax.

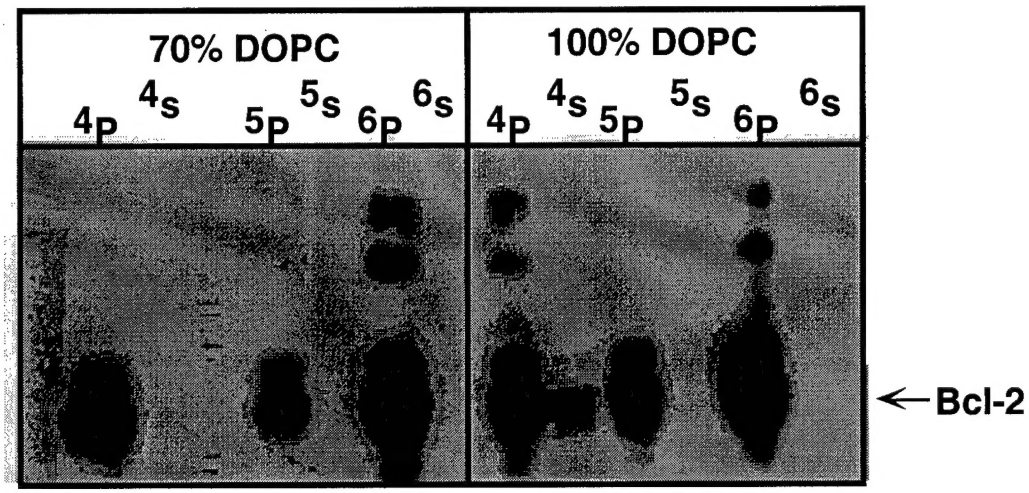

Fig. 3. Bcl-2 association with either 70% DOPC/30% DOPG or 100% DOPC vesicles as a function of pH. Arrow indicates position of presumed monomeric Bcl-2 at M_r ~ 27,000. P and S indicate soluble and membrane fractions, respectively, while numeral indicates pH.

The binding pattern of Bax followed that expected from ion-efflux assays, i.e., association was observed only under conditions where channel activity was detected: at acidic pH in the presence of acidic vesicles (Fig. 2). In contrast, Bcl-2 appeared in the membrane fraction under all conditions tested (Fig. 3) These results suggest that while membrane association is required, it is not sufficient for channel formation.

In addition to membrane association, a conformational change may also be required to form a conductive channel. To address this questions, the intrinsic tryptophan fluorescence was examined both as a function of pH and in the presence of neutral and acidic lipid vesicles. Trp fluorescence is a useful probe of changes in protein tertiary structure as it is dependent upon the degree of solvent exposure of the Trp residues. As the Trp residue becomes more solvent-exposed its fluorescence intensity decreases and when in a less polar environment, such as a lipid membrane, its fluorescence increases.

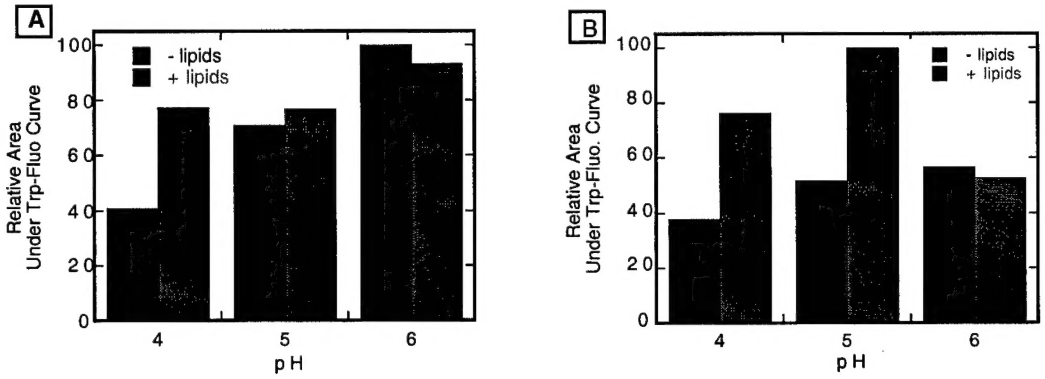

Fig. 4. Relative fluorescence intensity of Bcl-2 (A) and Bax (B) in the absence (black bars) and presence (gray bars) of 70%DOPC/30%DOPG vesicles as a function of pH. Bax or Bcl-2 (5 μg/mL) was added to DMG buffer (alone or in the presence of 50 μg/mL vesicles. The background intensity in the absence and presence of lipid vesicles was subtracted and the area under the resulting curve integrated.

Both Bcl-2 and Bax show a large increase in fluorescence at acidic pH in the presence vesicles having acidic lipids (Fig 4A and B). This result indicates that in the presence of vesicles the Trp residues (which are largely clustered in the hydrophobic central 5th and 6th α-helices) are seeing a less polar environment and are less vulnerable to solvent quenching. No such increase was observed when the proteins were incubated in the presence of neutral vesicles where the proteins have no channel activity (not shown). These results suggest that the Trp residues may be inserted into the lipid bilayer.

Characterization of BID channel activity. Concurrent with these studies, I had been purifying for crystallization studies another member of the Bcl-2 protein family: the BH3-only pro-apoptotic BID. Studies on BID were not included in the original proposal, but this protein has recently taken on increased importance which warranted further study using the abundant amounts of BID I had on hand.

Recently, research presented by Li *et al*, and Luo *et al.*,(1998) showed that upon Fas receptor ligation, pro Casp8 is recruited to the death receptor complex where the caspase is processed to its active form. BID contains within its N-terminal 60 residues a caspase cleavage site and the Casp8-cleaved form of BID (BIDΔ) is a potent inducer of Cyt

c release. Cytosolic Cyt c is a co-factor in activation of other caspases such as Casp3,6. and 7 (Green, 1998) and thus critical to continuation of the apoptotic pathway. The 3-dimensional structure of BID as determined by NMR was also published within the past year (McDonnell *et al.*, 1999) and its structure, like the other Bcl-2 family members, was reminiscent of bacterial toxins, suggesting that BID may also have pore-forming capability.

I created, expressed, and purified a mutant mimic of the cleaved form of BID, BIDΔ, to test on lipid systems previously used to assess Bcl-2, Bcl-X_L, and Bax. This recombinant form removed the possible confounding effects of Casp8. Like intact BID, BIDΔ was highly α-helical as determined by far-UV CD (Fig. 5A).

Planar bilayer and liposome studies indicated that BIDΔ was able to form channels *in vitro*, under conditions similar to that seen for Bcl-2, Bcl-X_L, and Bax (Fig 5B). These channels were voltage-gated and showed conductances of 7.5, 40, and 100pS (not shown, Schendel *et al* 1999). In addition, when full-length BID was cleaved by Casp8, it too demonstrated channel activity similar to that seen with recombinant BID .

Molecular modeling showed that removal of the N-terminal 55 residue segment resulted in an increased exposure of hydrophobic surface area of the central pair of helices which are candidate pore-forming regions of the protein (Schendel *et al.*, 1999). This result implies that removal of the N-terminal region by proteolysis may promote the association of the cleaved BID protein with membrane. Second, excision of the N-terminal segment is predicted to result in increased accessibility of the BH3 dimerization domain by 90 $Å^2$. Since the hydrophobic surface of BH3 domains is known to be involved in Bcl-2 family protein interactions, this result suggests that BID cleavage would also promote its heterodimerization with Bcl-2 family members.

These findings argue that while BID shares very limited amino acid sequence similarity with Bcl-X_L and other pore-forming members of the Bcl-2 protein family, BID may nevertheless be a structurally similar protein that also shares pore-forming capability. The pore-forming activity of BID is unique in that it occurs only following proteolytic cleavage. This mechanism may be required since BID lacks the C-terminal membrane anchoring domain found in other Bcl-2 family proteins currently known to have pore-forming activity. Previously, BH3-only proteins have been viewed as trans-dominant inhibitors that relied exclusively on dimerization with other Bcl-2 family proteins to exert its effects on cell death. These results suggest that some BH3-only proteins may have intrinsic activities as membrane-integrating or channel proteins, suggesting re-valuation of the role of this sub-branch of the Bcl-2 family may be necessary.

A

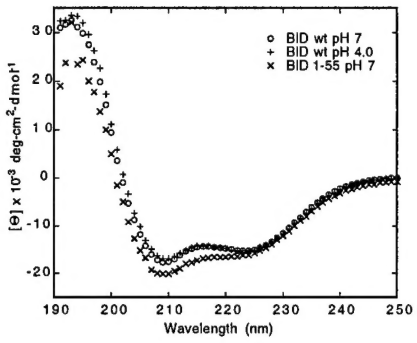

B

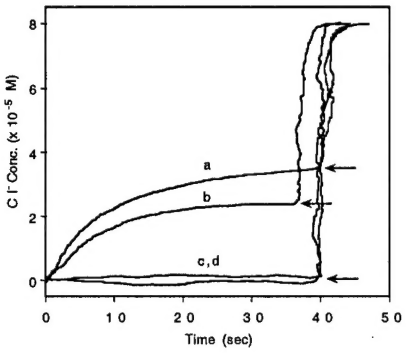

Fig. 5. (A) Far-UV circular dichroism spectra of BID and BIDΔ1-55. BID (o: pH 7.0; +: pH 4.0) and truncated BIDΔ1-55 (x) were dialyzed into 20 mM potassium phosphate, pH 7.0, or 20 mM sodium acetate, pH 4.0, and the spectra scanned from 250 to 190 nm. Protein concentrations were 14 and 10 μM for wild-type and truncated BID, respectively. Spectra represent the average of 3 scans (5 s averaging time) corrected for background intensity by subtraction of the appropriate buffer blank. (B) BIDΔ1-55 induced Cl^--efflux from KCl-loaded vesicles. Either wild-type BID (curves d) or BIDΔ1-55 (curves a,b,c) was added at t=0 to 70% DOPC/30% DOPG vesicles suspended in 10 mM DMG buffer at pH 4.0 (curves a,b,d) or pH 7.0 (curve c) in the presence (curves a,c,d) or absence (curve b) of 15 nM valinomycin (added prior to protein addition). BID and BIDΔ1-55 were added to final concentrations of 1 μg/mL and 0.2 μg/mL, respectively. Arrows indicate the addition of 0.1% Triton X-100 to release residual chloride.

Lastly, a set of six single cysteine mutants of Bcl-X_l has been purified to homogeneity. These proteins have been sent to Wayne Hubbell for EPR analysis. I will also utilize these proteins to perform companion topology studies, employing BODIPY and bichlorobimaine fluorescent probes as gauges of membrane insertion of other helices besides the originally predicted fifth and sixth helices.

Abbreviations: DOPG: dioleoylphosphatidyl glycerol; DOPC: dioleoylphosphatidyl choline; TNP-PE: trinitrophenylphosphatidylethanolamine; BH: Bcl-2 homology; EPR: electroparamagnetic resonance; BODIPY: *N*-(4,4-difluoro-5,7-dimethyl-4-bora-3a,4adiaza-*s*-indacene-3-yl)methyl)iodoacetamide

References

Antonsson B., Contin F, Ciavatta A, Montessuit S, Elwis S, Martinou I, Bernasconi L, Bernard A, Mermod J-J, Mazzei G, *et al.* (1997) Science 277:370-372.

Elkins P, Bunker A, Cramer WA and Stauffacher CV (1997) Structure 5:443-458.

Green, D.R. (1998) *Cell* **94,** 695-698.

Li, H., Zhu, H., Xu, C.-J. and Yuan, J. (1998) *Cell* **94,** 491-501.

Luo, X., Budihardjo, I., Zou, H., Slaughter, C. and Wang, X. (1998) *Cell* **94,** 481- 490.

Minn AJ, Velez P, Schendel SL, Liang H, Muchmore SW, Fesik SW, Fill M and Thompson CB (1997) Nature 285:353-357.

Schendel SL, Xie Z, Montal MO, Matsuyama S, Montal M and Reed JC (1997) Proc. Natl. Acad. Sci. U.S.A. 93: 511-5118.

Schendel SL, Azimov R, Pawlowski K, Godzik A, Kagan BL, and Reed JC. (1999) *J. Biol. Chem. 274*: 21932-21937

Zakharov SD, Heymann JB, Zhang Y-L and Cramer WA (1996). Biophys. J. 70:2774-2783.

Appendix

Key Research Accomplishments:

* Demonstration of *in vitro* pore-forming activity by the BH-3 only Bcl-2 family member, BID.

* Generation and purification of a six member set of single site cysteine mutants in Bcl-X_L.

* Characterization of Bcl-2 and Bax lipid binding properties and qualitative structural changes upon lipid interaction.

Reportable Outcomes:

Publications

Reed JC, Xie Z, Kitada S, Zapata JM, Xu Q, **Schendel SL**, Krajewska M, and Krajewski S. Methods of measuring Bcl-2 family proteins and their functions. In *Apoptosis: A practical approach.*, ed. G. Studzinski. (*in press*)

Schendel SL, Azimov R, Pawlowski K, Godzik A, Kagan BL, and Reed JC. 1999. Ion-channel activity of the BH3-only Bcl-2 family member, BID. *J. Biol. Chem. 274*: 21932-21937

Matsuyama S, **Schendel SL**, Zie X, Reed JC. 1998. Cytoprotection by Bcl-2 requires the pore-forming α5 and α6 helices. *J. Biol. Chem 273*: 30995-31001

Xie Z, **Schendel SL**, Matsuyama S, Reed JC. 1998. Acidic pH promotes dimerization of Bcl-2 family proteins. *Biochemistry 37*:6410-6418.

Schendel SL, Montal M, Reed JC. 1998. Bcl-2 family proteins as ion channels. *Cell Death Differ. 5*:372-380.

Presentations:

The 13th Aspen Cancer Conference Workshop: Mechanisms of Toxicity and Carcinogenesis. 1998. Presentation entitled: Significance of multiple apoptotic pathways in carcinogenesis and Therapy. **Schendel SL**, Matsuyama S, Jürgensmeier J, and Reed JC.

The 5th International Symposium on Dendritic Cells in Fundamental and Clinical Immunology. 1998. Invited speaker.

**Note: Pages 6,7,8 contain unpublished data that should be protected.

THE JOURNAL OF BIOLOGICAL CHEMISTRY
Vol. 274, No. 31, Issue of July 30, pp. 21932–21936, 1999
Printed in U.S.A.

Ion Channel Activity of the BH3 Only Bcl-2 Family Member, BID*

(Received for publication, March 17, 1999, and in revised form, May 26, 1999)

Sharon L. Schendel‡§¶, Rustam Azimov§‖, Krzysztof Pawłowski‡ ‡‡, Adam Godzik‡ ‡‡, Bruce L. Kagan¶§§, and John C. Reed‡¶¶**

From ‡The Burnham Institute, La Jolla, California 92307 and the ‖Neuropsychiatric Institute and West Los Angeles Department of Veterans Affairs Medical Center School of Medicine, University of California, Los Angeles, California 90024

BID is a member of the BH3-only subgroup of Bcl-2 family proteins that displays pro-apoptotic activity. The NH_2-terminal region of BID contains a caspase-8 (Casp-8) cleavage site and the cleaved form of BID translocates to mitochondrial membranes where it is a potent inducer of cytochrome *c* release. Secondary structure and fold predictions suggest that BID has a high degree of α-helical content and structural similarity to Bcl-X_L, which itself is highly similar to bacterial pore-forming toxins. Moreover, circular dichroism analysis confirmed a high α-helical content of BID. Amino-terminal truncated BIDΔ1–55, mimicking the Casp-8-cleaved molecule, formed channels in planar bilayers at neutral pH and in liposomes at acidic pH. In contrast, full-length BID displayed channel activity only at nonphysiological pH 4.0 (but not at neutral pH) in planar bilayers and failed to form channels in liposomes even under acidic conditions. On a single channel level, BIDΔ1–55 channels were voltage-gated and exhibited multiconductance behavior at neutral pH. When full-length BID was cleaved by Casp-8, it too demonstrated channel activity similar to that seen with BIDΔ1–55. Thus, BID appears to share structural and functional similarity with other Bcl-2 family proteins known to have channel-forming activity, but its activity exhibits a novel form of activation: proteolytic cleavage.

Bcl-2 protein family members play an important role in governing a cell's decision to heed or disregard signals to enter pathways for programmed cell death and apoptosis. The Bcl-2 protein family can be divided into two camps: pro- and anti-apoptotic, with proteins such as Bcl-2 and Bcl-X_L acting to prevent cell death and proteins such as Bax and Bak encouraging cell death. The sequences of these proteins share pockets of similarity in regions designated BH1–4.[1]

The three-dimensional structure of Bcl-X_L shows the protein to be a bundle of seven α-helices with two central predominantly hydrophobic helices forming the core of the molecule. This structure is reminiscent of pore-forming bacterial toxins diphtheria and colicins A, E1, and Ia, suggesting that Bcl-X_L may have channel-forming potential (1). Indeed, *in vitro* channel-forming activity was demonstrated for Bcl-X_L, Bcl-2, and Bax (2, 3, 4). Predicted structures for Bcl-2 and Bax can be modeled using the coordinates of Bcl-X_L, suggesting that these proteins share similar structural features (5).

The amino acid sequences of one branch of the Bcl-2 family diverge substantially from Bcl-X_L, Bcl-2, Bax, and many other Bcl-2 family proteins, sharing similarity only within the ~16 amino acid BH3 domain. This "BH3-only" subset includes BID, BAD, BIK, and HRK (reviewed in Ref. 6), which are all pro-apoptotic proteins. These proteins are presently thought to lack intrinsic activity, acting as trans-dominant inhibitors by use of their BH3 domains to interact with the BH3-binding pockets of anti-apoptotic proteins (7). In this view, BH3 proteins may play a passive role in apoptosis promotion by displacing anti-apoptotic proteins such as Bcl-X_L from interactions with Bax, Apaf-1, or other pro-apoptotic proteins, freeing them to exert pro-apoptotic activities.

Mitochondria also play significant roles in apoptosis (reviewed in Ref. 8). Bcl-2 family members possessing a hydrophobic COOH-terminal membrane anchoring domain (*e.g.* Bcl-2, Bcl-X_L) typically localize to mitochondrial membranes (reviewed in Refs. 6 and 8), although some members such as Bax can be transient mitochondrial residents that translocate from the cytosol to the mitochondria in response to several death signals (9, 10). Escape of cytochrome *c* (Cyt *c*) from mitochondria represents a critical event in initiating the caspase activation cascade, through its interaction with Apaf-1, which induces processing and activation of the cell death protease caspase-9 (Casp-9) (11, 12). The portal through which Cyt *c* passes into the cytoplasm is unknown, although Bax and the mitochondrial permeability pore complex appear to play important roles in Cyt *c* release (13, 14).

In response to Fas receptor ligation, pro-Casp-8 is recruited to the death-receptor complex where local aggregation allows Casp-8 processing (15). This activation is followed by Cyt *c* release and subsequent activation of downstream caspases such as Casp-3, -6, and -7 (16). Recently, the participation of BID in Cyt *c* release from mitochondria in Fas-stimulated cells was demonstrated (17, 18).

BID is a 195-residue, 22-kDa protein that lacks the hydrophobic COOH-terminal domain often found in Bcl-2 family proteins and which has a predominantly cytosolic localization (19). BID interacts with Bcl-2, Bcl-X_L, and Bax via its BH3 domain and can counteract the cytoprotective effects of Bcl-2 and Bcl-X_L (19). The murine BID amino acid sequence contains

* The costs of publication of this article were defrayed in part by the payment of page charges. This article must therefore be hereby marked "*advertisement*" in accordance with 18 U.S.C. Section 1734 solely to indicate this fact.

§ These two individuals contributed equally to the work described herein.

¶ Supported by a Postdoctoral Fellowship DAMD-17-981-8167 from United States Army Medical Research and Material Command.

** Present address: Institute of Physiology and Biophysics, Uzbek Academy of Science Nyazov St. 1Tashkent, Uzbekistan 700095.

‡‡ Both authors supported by National Institutes of Health GM-60049.

§§ Supported by National Institutes of Health Grant MH 01174 and by grants from the UCLA AIDS Institute, the UCLA Center on Aging, and the Stein-Oppenheimer fund.

¶¶ To whom correspondence should be addressed. Tel.: 619-646-3140; Fax: 619-646-3194; E-mail: jreed@burnham-inst.org.

[1] The abbreviations used are: BH, Bcl-2 homology domain; DOPC, 1,2-dioleoylphosphatidylcholine; DOPG, 1,2-dioleoylphosphatidylglycerol; GST, glutathione *S*-transferase; S, siemens; Casp, caspase; Cyt *c*, cytochrome *c*; POPE, 1-palmitoyl-2-oleoyl-*sn*-glycero-3-phosphatidylethanolamine; POPG, 1-pamitoyl-2-oleoyl-*sn*-glycero-3-rac-glycerol.

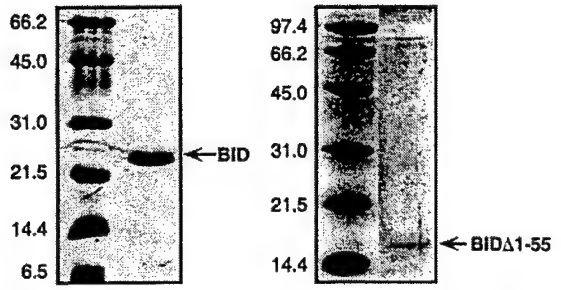

FIG. 1. **Analysis of recombinant BID and BIDΔ1–55 proteins.** Wild-type BID (*left*) and truncated BIDΔ1–55 (*right*) were purified using GST-Sepharose affinity chromatography. Molecular mass markers (kilodaltons) are indicated. Although similar amounts of each protein were loaded, the low intensity of the BIDΔ1–55 may be due to its low aromatic amino acid content.

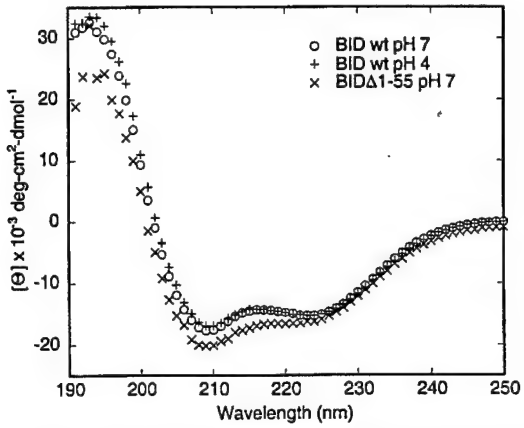

FIG. 2. **Far-UV circular dichroism spectra of BID and BIDΔ1–55.** BID (○, pH 7.0; +, pH 4.0) and truncated BIDΔ1–55 (×) were dialyzed into 20 mM potassium phosphate, pH 7.0, or 20 mM sodium acetate, pH 4.0, and the spectra scanned from 250 to 190 nm. Protein concentrations were 14 and 10 μM for wild-type and truncated BID, respectively. Spectra represent the average of three scans (5 s averaging time) corrected for background intensity by subtraction of the appropriate buffer blank.

a putative Casp-8 cleavage site (57-L-Q-T-D-G-61) within its NH_2 terminus and BID is indeed cleaved between residues 59 and 60 by Casp-8 both *in vivo* and *in vitro* (17, 18). The intact BID protein is found in the cytoplasm, but upon cleavage, truncated BID translocates to mitochondria (17, 18). *In vitro*, truncated, but not intact BID, is a potent inducer of Cyt *c* release from isolated mitochondria, prompting release of more than 80% of total Cyt *c* after treatment with nanogram amounts of Casp-8-cleaved BID (18). Thus, BID serves as a linker between the Fas receptor at the cytoplasmic membrane and the mitochondrial cell death machinery. The conversion from the cytosolic, soluble intact BID to the mitochondrial membrane-associated NH_2-terminal truncated BID and subsequent Cyt *c* release implies that truncated BID may play a role in priming the mitochondrial membrane to become more permeable, permitting Cyt *c* to escape. To explore this possibility, the membrane activity of both wild-type and truncated recombinant murine BID was examined using liposome and planar bilayer assays.

MATERIALS AND METHODS

Plasmid Preparation—A plasmid encoding a GST-BID fusion protein was constructed by liberating a *Eco*RI-*Xho*I cDNA encoding murine BID-(1–195) and subcloning into pGEX4Ti (Amersham Pharmacia Biotech). BIDΔ1–55 was constructed after introduction of an *Eco*RI site between the codons for residues 55 and 56 using forward (5′-CTCGAAGACGAATTCCAGACAGAC-3′; altered base pairs underlined) and reverse (5′-CCGGGAGCTGCATGTGTCAGAGG-3′) primers in a polymerase chain reaction reaction to amplify a ~0.5-kilobase pair fragment flanked by *Eco*RI-*Xho*I sites. Residue 55, rather than 59, was chosen to minimize the number of base pair changes necessary to introduce the *Eco*RI site. The fragment was then inserted into pGEX4Ti following *Eco*RI and *Xho*I digestion. The presence of the deletion was confirmed by DNA sequencing.

Protein Purification—Wild-type BID and BIDΔ1–55 were produced as GST fusion proteins from pGEX vectors using *Escherichia coli* BL21 (DE3) as the host strain. The purification method is identical for each protein. An overnight culture (5 ml) was used to inoculate 1 liter of LB medium that was incubated at 37 °C until an A_{600} of 0.8–1.0 was achieved. The cells were induced with 1 mM isopropyl-β-D-thiogalactopyranoside and incubated at 37 °C for an additional 4 h before harvesting by centrifugation. The cells were resuspended in 40 ml of lysis buffer (50 mM Tris-HCl, pH 8.0, 150 mM NaCl, 5 mM EDTA, 1% Triton X-100, 0.5 mg/ml lysozyme, Complete protease inhibitor tablet (Roche Molecular Biochemicals)) and incubated on ice for 30 min before brief sonication to reduce viscosity. The resulting lysate was centrifuged at (8000 × *g*) for 15 min to pellet cellular debris. Three ml GST-Sepharose beads (Amersham Pharmacia Biotech) were added to the supernatant and incubated at 4 °C with gentle rotation for 3 h. The beads were washed twice with 20 mM Tris-HCl, pH 8.0, 100 mM NaCl, 0.1% Tween 20, 1 mM EDTA followed by two washings with the same buffer lacking Tween 20. The beads were resuspended in 10 ml of the final wash buffer and incubated with 10 units thrombin (Roche Molecular Biochemicals) for 90 min at 4 °C. The supernatant was collected in fractions from the beads and passed over a benzamidine-agarose column (Sigma) to inactivate thrombin. For liposome and circular dichroism assays, the protein was dialyzed into 20 mM potassium phosphate buffer, pH 7.0. Purified proteins were characterized by SDS-polyacrylamide gel electrophoresis on 15% high Tris gels (20), followed by Coomassie staining. Concentrations were determined either by A_{280} using $\epsilon = 0.5$ and 0.1 for BID wild-type and BIDΔ1–55, respectively, or by Bradford assay (Bio-Rad).

Circular Dichroism—Circular dichroism (CD) measurements were carried out on an AVIV D60 spectropolarimeter equipped with a temperature control accessory and calibrated with d-10-camphor sulfonate. Measurements were taken using a 1-mm path length. All spectra were recorded in 1.0-nm wavelength increments with a 1-s time constant and a full-scale sensitivity of 10 millidegrees. Each spectrum is the average of three scans corrected for background solvent effects by subtraction of the appropriate buffer blank. BID and BIDΔ1–55 in either 20 mM potassium phosphate, pH 7.0, or 20 mM sodium acetate, pH 4.0, were diluted to a concentration of 0.3 and 0.1 mg/ml, respectively. Spectra were scanned in the far-UV from 250 to 190 nm. A value of 110 for the mean residue molecular weight was used in the calculation of the mean residue ellipticity (Θ).

Liposome Preparation and Cl^- Efflux Measurements—Large unilamellar vesicles composed of 70% dioleoylphosphatidylcholine (DOPC) and 30% dioleoylphosphatidylglycerol (DOPG) were produced as described previously (4). The liposomes were diluted to a final concentration of 0.05 mg/ml in 10 mM dimethyl glutaric acid, 100 mM choline nitrate, 2 mM $Ca(NO_3)_2$ at either pH 4.0 or pH 6.0. Valinomycin was added to a final concentration of 15 nM to generate an inside-negative potential. BID wild-type or BIDΔ1–55 was added at the indicated concentrations, and residual Cl^- was released following addition of Triton X-100 (0.1% v:v). The total amount of Cl^- released was compared against a calibration curve produced by successive additions of KCl. Electrode assembly is as described previously (4).

Molecular Modeling—Structure prediction for BID was attempted using a threading approach (21). The algorithm produced several possible predictions with similar significance scores. Out of the first four predictions, two were disqualified, because their sequence alignments failed to produce a three-dimensional model. The remaining predictions out of the first four were: apolipophorin III (PDB code 1aep, a four-helical bundle) and Bcl-X_L (1maz). The 1aep prediction was discarded because removal of the NH_2-terminal fragment up to Asp-59 (which is cleaved by caspase to produce an active protein) does not result in change of exposure of the BH3 domain in the model. The 1maz prediction was more consistent with experimental data, because removal of the NH_2-terminal fragment from the model results in a substantial change of BH3 domain accessible surface. Two models of BID, either the full-length or Δ1–59 based on the Bcl-X_L structure were then built using the MODELLER program (22).

Planar Bilayer Preparation and Single Channel Recording—Phospholipid bilayer membranes were formed as described previously (23). Solvent containing membranes were formed by placing a bubble of lipid onto the end of the Teflon tube approximately 300 microns in diameter.

The design of the chamber allowed rapid introduction of solution into immediate proximity with the membrane in a volume of only 50 microliters. Agar salt bridges were used to connect the electrodes to the solutions and voltage clamp conditions were employed in all experiments. Lipids were purchased from Avanti Polar Lipids (Birmingham, AL) and stored at −70 °C. In some cases, azolectin was used for membranes to increase sensitivity but this was unnecessary for BID (Δ1–55). Current was recorded with an Axopatch amplifier (Axon Instruments, Sunnyvale, CA) and stored on videotape for later playback and analysis. Membrane capacitance and resistance were monitored in order to assure the formation of reproducible membranes.

RESULTS AND DISCUSSION

To explore the possibility that BID interacts with membranes, recombinant BID and BIDΔ1–55 were expressed as GST fusion proteins in *E. coli*. BIDΔ1–55 represents a recombinant mimic of the ~15-kDa Casp-8 cleavage product of BID and was used to avoid any ambiguities associated with incomplete digestion of full-length BID or the possible confounding presence of Casp-8. The BID proteins were liberated from the GST moiety by thrombin digestion and determined to be >90% purity, as determined by SDS-polyacrylamide gel electrophoresis analysis with Coomassie staining (Fig. 1). The faintness of the BIDΔ1–55 band may be attributable to its lack of aromatic amino acids (one tyrosine and no tryptophans) required for Coomassie Blue binding (24).

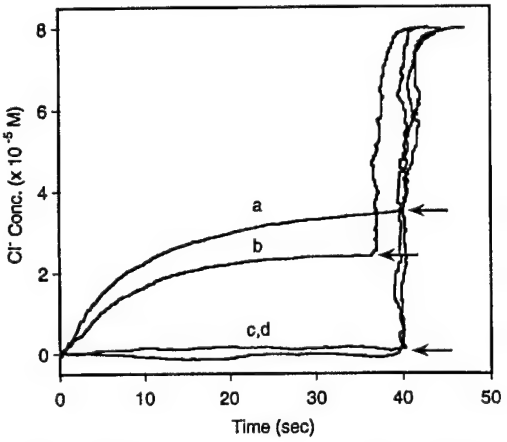

FIG. 3. **BIDΔ1–55 induced Cl^- efflux from KCl-loaded vesicles.** Either wild-type BID (*curve d*) or BIDΔ1–55 (*curves a, b,* and *c*) was added at $t = 0$ to 70% DOPC/30% DOPG vesicles suspended in 10 mM DMG buffer at pH 4.0 (*curves a, b,* and *d*) or pH 7.0 (*curve c*) in the presence (curves a, *c,* and *d*) or absence (*curve b*) of 15 nM valinomycin (added prior to protein addition). BID and BIDΔ1–55 were added to final concentrations of 1 μg/ml and 0.2 μg/ml, respectively. *Arrows* indicate the addition of 0.1% Triton X-100 to release residual chloride.

To assess whether the truncated form of BID possesses a significantly different structure, circular dichroism (CD) spectra were obtained for each protein. The far UV-CD spectrum (185–250 nm) is dominated by the amide bond absorption and is highly sensitive to the presence of ordered secondary structure. The far-UV spectrum for both wild-type and truncated forms of BID display minima at ~202 and 222 nm and are characteristic of proteins having at least 50–60% α-helical secondary structure (25) (Fig. 2). Little change was seen in the shape or amplitude of the far-UV spectrum between the wild-type and BIDΔ1–55, indicating that the α-helical nature of these two proteins remains intact despite the loss of the first 55 residues (Fig. 2). These CD data also demonstrate that BID and BIDΔ1–55 possess a high α-helical content. The high α-helical content of BID and BIDΔ1–55 is reminiscent of the channel-forming Bcl-X_L, Bcl-2, and Bax proteins as well as structurally related bacterial toxins such as the pore-forming colicins and diphtheria toxin.

When BID was added to KCl-loaded liposomes composed of 70% neutral (DOPC) and 30% acidic (DOPG), no chloride efflux could be observed, either at pH 4.0 or 7.0 (Fig. 3, *curve c*, and data not shown). In contrast, when BIDΔ1–55 was added in nanogram amounts to similar vesicles, the protein induced >50% release of encapsulated chloride at pH 4.0 (Fig. 3, *curve a*), but no ion release was detected at pH 7.0 (Fig. 3, *curve d*). The ion release induced by truncated BID displayed a partial

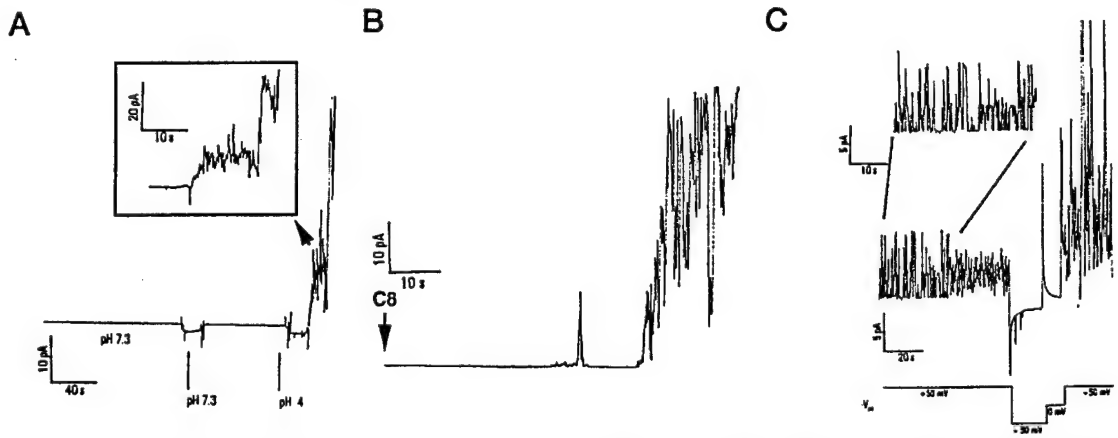

FIG. 4. **BID induces current only at acidic pH, while Casp-8-cleaved BID and BIDΔ1–55 form channels at neutral pH.** *A*, current is shown as a function of time through a membrane voltage-clamped at +50 mV. Wild-type BID (50 μg/ml) was added to the aqueous solution (100 mM KCl, 50 mM HEPES-Tris, pH 7.3). The flat current trace ($I = 0$) indicates that no channel activity was seen. At the *first arrow*, the chamber was perfused with BID-free solution, pH 7.3. A slight deflection was seen due to perfusion artifact. At the *second arrow*, the chamber was perfused with acidic BID-free solution (100 mM KCl, 50 mM citrate-Tris, pH 4.0). Membranes never showed activity in the absence of BID. The *inset* shows that individual "jumps" of current can be discerned at early times, perhaps representing single channel events. Membrane lipid was POPG:POPE (1:1). *B*, channel activity of Casp-8-activated BID. Current is shown as a function of time with voltage clamped at +50 mV. BID (60 μg/ml) was preincubated with Casp-8 (0.35 μM) in 100 mM KCl, 50 mM HEPES-Tris at 25 °C for 1 h prior to addition (*arrow*) to azolectin membrane. The increase in current indicates formation of channels by Casp-8-cleaved BID and was not observed either in the presence of uncleaved BID or Casp-8 alone at pH 7.3. Multiple simultaneous or overlapping channel openings are observed. *C*, current is shown as a function of time through a membrane to which BIDΔ1–55 had been added to a final concentration of 60 μg/ml. In the first half of the record, membrane voltage was held at + 50 mV, and the BIDΔ1–55 channels were seen to be frequently opening and closing (at least two to three channels appear to be present, see *inset*). When the voltage is changed to −50 mV, the channels close and only rarely reopen. When the membrane is returned to +50 mV, the channel opening resumed at somewhat higher frequency. This reflects the stochastic nature of single channel openings and the fact that new channels occasionally appear in the bilayers. Aqueous solution was 100 mM KCl, 50 HEPES-Tris, pH 7.3. Lipid was POPE:POPG (1:1). Aqueous solutions and lipid were the same as in *A*.

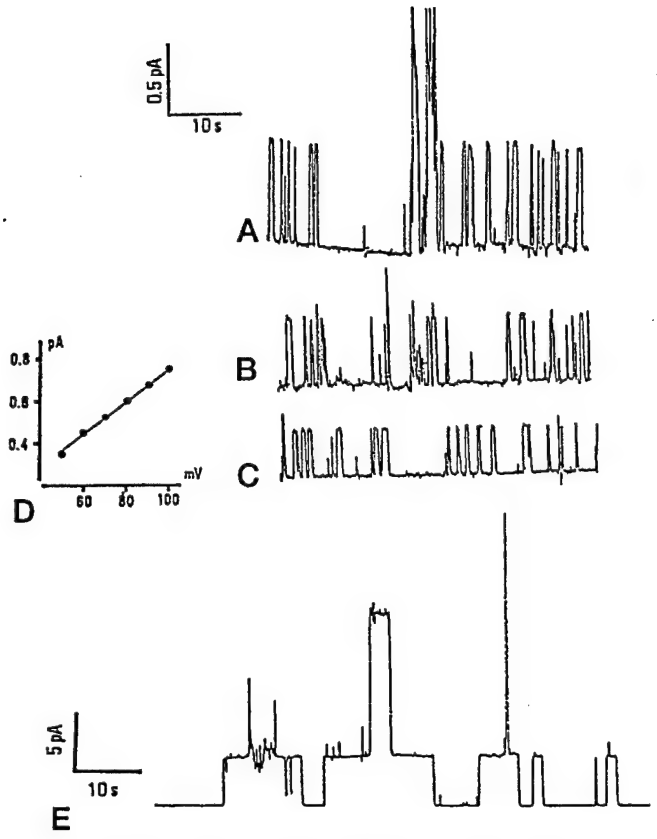

FIG. 5. **Single channel current induced by BIDΔ1–55.** The first three traces (*A*, *B*, *C*) show current as a function of time through a membrane to which BIDΔ1–55 has been added to a final concentration of 30 μg/ml. The membrane was held at voltages: +100 mV (*A*), +70 mV (*B*), +50 mV (*C*). Note the relatively consistent single channel conductance, 8 pS and lifetime (~0.5 s). *D* shows the ohmic I–V plot for the open channel at positive voltages. *E* shows larger single channels (90 pS) formed by BIDΔ1–55 at +100 mV. These tended to be seen at higher protein concentrations (60 μg/ml here). Aqueous solution was 100 mM KCl, 50 HEPES-Tris, pH 7.3, and voltage was clamped at +100 mV. Lipid was POPE:POPG (1:1).

dependence of an outside-positive voltage, as the amount of ion released in the absence of the K^+-specific ionophore valinomycin was reduced (Fig. 3, *curve b*). No BIDΔ1–55-induced ion release was detected at pH 4.0 when the vesicles lacked acidic lipids (100% DOPC) (not shown). The behavior of BIDΔ1–55 closely resembles that observed previously for Bcl-2 and Bcl-X_L in that the activity detected in this assay is pH and voltage-dependent and requires acidic lipids (2, 3). The chloride efflux assay detects channel activity on a macroscopic level and requires that the bulk of the protein molecules are participating in channel formation, excluding the possibility that a small subgroup of molecules are responsible for ion release.

To characterize the behavior of wild-type and truncated BID at a microscopic level, experiments were performed using planar bilayer membranes. This technique allows channels to be monitored at the single channel level and yields more specific information on pH, voltage dependence, and ion conductance. When wild-type BID was added to planar bilayers at pH 7.3 in the presence of a +50 mV membrane potential, no channel activity was observed (Fig. 4*A*). Yet when the chamber was flushed out and a pH 4.0 buffer solution was added, channel activity began immediately (Fig. 4*A*, expanded region), suggesting that the wild-type BID is able to associate with the membrane, but an acidic pH is necessary to achieve membrane insertion and channel activity. This channel activity does not appear to require that the protein undergo significant changes in secondary structure as the far-UV CD spectrum of wild-type

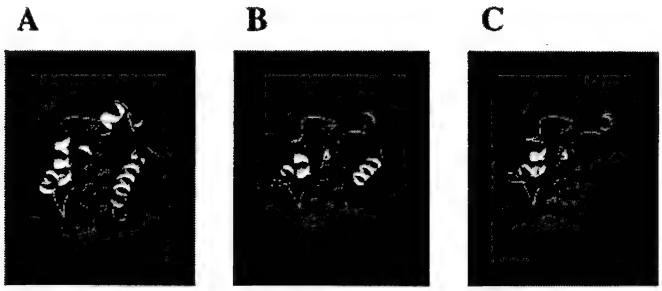

FIG. 6. **Predicted structures for BID and BIDΔ1–55.** *A*, Ribbon diagram for Bcl-X_L. *Red* helices represent α5 and α6 of the central hydrophobic hairpin, and the *blue* helix contains the BH3 domain. *B*, predicted structure for wild-type BID modeled on Bcl-X_L coordinates. *Red* helices correspond to helices α5 and α6 of Bcl-X_L and the *blue* helix to the BH3 domain. *C*, predicted structure for BIDΔ1–59. Removal of the first helix (*yellow*, compare with *B*) results in increased exposure of the hydrophobic central helices and the BH3 domain also has increased exposed surface area. Both predicted accessible surface changes are only lower estimates because for much of the BID NH_2-terminal region a model could not be built because of lack of similarity in this region to Bcl-X_L.

BID at pH 4.0 is indistinguishable from that at pH 7.0 (Fig. 2). However, the lack of a clear quantal size for these channels may reflect rapid transitions among multiple conformations of molecules undergoing tertiary structure changes as they interact with the membrane.

Since BID is a Casp-8 target *in vivo,* we explored whether Casp-8-cleaved BID also displays channel activity similar to the mutant mimic BIDΔ1–55. Incubation of BID with Casp-8 at a 10:1 (mole:mole) ratio produced a cleaved form of BID (not shown) that exhibited channel activity within 1 min after addition of the cleavage mixture to planar bilayers at pH 7 (Fig. 4*B*). Similar to Casp-8-cleaved BID, BIDΔ1–55 also demonstrated channel activity at neutral pH (Fig. 4*C*). Our ability to detect channels formed by BID Δ1–55 at neutral pH in planar bilayers but not in liposome-based ion efflux assays presumably reflects the greater sensitivity of the former method. Similar results were also obtained for Bcl-2 and Bcl-X_L (2, 3).

We used the BIDΔ1–55 protein as a recombinant mimic of Casp8-cleaved BID to further characterize BID channel activity in planar bilayers (Fig. 5). BIDΔ1–55 displayed a membrane potential dependence that was similar to that observed for the pore-forming colicins (26) and to that observed for truncated BID in liposomes, in that the channel was open when a positive voltage was applied on the side to which BID was added but converted to a nonconductive state when the voltage was reversed to a negative voltage. Several BIDΔ1–55 single channel conductances with clear quantal sizes were discerned in these experiments (Fig. 5), including smaller conductances of 7.4 pS and larger conductances of 40 and 100 pS in 150 mM KCl (Fig. 5).

Although the sequence similarity between BID and Bcl-X_L and other family members is confined to the BH3 domain, the high α-helical content of the protein and its ability to form ion channels *in vitro* prompted the consideration that BID may share structural similarity with Bcl-X_L or other pore-forming proteins. Accordingly, structure prediction for BID was attempted using a threading approach (21), revealing extensive predicted structural similarity with Bcl-X_L (Fig. 6). Using the MODELLER program, models for the full-length and truncated forms of BID were built using the Bcl-X_L coordinates as a guide. The COOH-terminal portion of both BID and BIDΔ1–55 are predicted to correspond to the last six of the seven α-helices observed for the Bcl-X_L structure. This includes a centrally located pair of hydrophobic α-helices previously implicated in pore formation by Bcl-2 and Bax (3, 14) and an α-helix corre-

sponding to the BH3 dimerization domain (Fig. 6). The NH_2-terminal region of full-length BID proximal to the caspase cleavage site does not model well on the Bcl-X_L structure, which corresponds to the BH4-containing first α-helix in Bcl-X_L. In contrast to BID, attempts to model other BH3-only proteins on the Bcl-X_L coordinates were unsuccessful, including BAD, Blk, Bik, Hrk, and Egl (not shown), thus suggesting that these members of the Bcl-2 family do not possess structures similar to Bcl-X_L and related pore-forming proteins.

Two observations related to the effects of cleavage of BID are predicted by comparisons of the models for full-length and truncated BID. First, removal of the NH_2-terminal segment (1–55) results in a 60 $Å^2$ increase of exposed hydrophobic surface area of the central pair of helices (α4-α5 in this model), which are candidate pore-forming regions of the protein. Consequently, removal of the NH_2-terminal region by proteolysis may promote the association of the cleaved BID protein with membranes. Second, excising the NH_2-terminal segment is predicted to result in increased accessibility of the BH3 dimerization domain by 90 $Å^2$. Since the hydrophobic surface of BH3 domains is known to be involved in dimerization among Bcl-2 family proteins (27), this suggests that cleavage of BID may also promote its heterodimerization with Bcl-2 family members (Fig. 6).

Taken together, the findings presented here argue that while BID shares very limited amino acid sequence similarity with Bcl-X_L and other documented pore-forming members of the Bcl-2 protein family, BID may nevertheless be a structurally similar protein that also shares pore-forming capability. Recent determination of the three-dimensional structure of BID, which was reported while this work was under review (28, 29), supports this view. The pore-forming activity of BID is unique in that it occurs primarily following proteolytic cleavage. Although full-length BID did display some channel activity on planar bilayers at acidic pH, this may reflect that the NH_2 terminus has become "unwrapped" from the protein at low pH in the same manner as previously documented for colicins (26). Thus, low pH may promote BID conformations that allow some of the uncleaved molecules to insert into membranes under conditions of nonphysiological pH. However, *in vivo*, where pH essentially never drops below pH 6.0, the NH_2-terminal domain of BID presumably requires physical removal by Casp-8 cleavage, although other mechanisms involving interactions with other proteins cannot be excluded.

Previously, BH3-only proteins have been viewed as transdominant inhibitors that relied exclusively on dimerization with other Bcl-2 family proteins to exert effects on cell life and death. The results presented here suggest that some BH3-only proteins may have intrinsic activities as membrane-integrating or channel proteins, necessitating re-evaluation of the role of this sub-branch of the Bcl-2 family.

Acknowledgments—We thank G. Salvesen for the gift of caspase-8, Z. Xie for advice on BID preparation, and E. Smith for manuscript preparation.

REFERENCES

1. Muchmore, S. W., Sattler, M., Liang, H., Meadow, R. P., Harlan, J. E., Yoon, H. S., Nettesheim, D., Chang, B. S., Thompson, C. B., Wong, S. L., Ng, S. L., and Fesik, S. W. (1996) *Nature* **381,** 335–341
2. Minn, A. J., Velez, P., Schendel, S. L., Liang, H., Muchmore, S. W., Fesik, S. W., and Fill, M. (1997) *Nature* **385,** 353–357
3. Schendel, S. L., Xie, Z., Montal, M. O., Matsuyama, S., Montal, M., and Reed, J. C. (1997) *Proc. Natl. Acad. Sci. U. S. A.* **93,** 5113–5118
4. Antonsson, B., Contin, F., Ciavatta, A., Montessuit, S., Lewis, S., Martinou, I., Bernasconi, L., Bernard, A., Mermod, J. J., Mazzei, G., Maundrell, K., Gambale, F., Sadoul, R., and Martinou, J. C. (1997) *Science* **277,** 370–372
5. Schendel, S. L., Montal, M., and Reed, J. C. (1998) *Cell Death Differ.* **5,** 372–380
6. Adams, J. M., and Cory, S. (1998) *Science* **281,** 1322–1325
7. Kelekar, A., and Thompson, C. B. (1998) *Trends Cell Biol.* **8,** 324–330
8. Green, D. R., and Reed, J. C. (1998) *Science* **281,** 1309–1312
9. Wolter, J. G., Hsu, Y. T., Smith, C. L., Nechushtan, A., Zi, X. G., and Youle, R. J. (1997) *J. Cell Biol.* **139,** 1281–1292
10. Gross, A., Jockel, J., Wei, M. C., and Korsmeyer, S. J. (1998) *J. Cell Biol.* **143,** 207–215
11. Liu, X., Kim, C. N., Yang, J., Jemmerson, R., and Wang, X. (1996) *Cell* **86,** 147–157
12. Li, P., Nijhawan, D., Budihardjo, I., Srinivasula, S. M., Ahmad, M., Alnemri, E. S., and Wang, X. (1997) *Cell* **91,** 479–489
13. Jürgensmeier, J. M., Xie, Z., Deveraux, Q., Ellerby, L., Bredesen, D., and Reed, J. C. (1998) *Proc. Natl. Acad. Sci. U. S. A.* **95,** 4997–5002
14. Marzo, I., Brenner, C., Zamzami, N., Jürgensmeier, J. M., Susin, S. A., Vieira, H. L., Prevost, M. C., Xie, Z., Matsuyama, S., Reed, J. C., and Kroemer, G. (1998) *Science* **281,** 2027–2031
15. Green, D. R. (1998) *Cell* **94,** 695–698
16. Srinivasula, S. M., Ahmad, M., Fernandes-Alnemri, T., Litwack, G., and Alnemri, E. S. (1996) *Proc. Natl. Acad. Sci. U. S. A.* **93,** 14486–14491
17. Li, H., Zhu, H., Xu, C.-J., and Yuan, J. (1998) *Cell* **94,** 491–501
18. Luo, X., Budihardjo, I., Zou, H., Slaughter, C., and Wang, X. (1998) *Cell* **94,** 481–490
19. Wang, K., Yin, X.-M., Chao, D. T., Milliman, C. L., and Korsmeyer, S. J. (1996) *Genes Dev.* **10,** 2859–2869
20. Fling, S. P, and Gregerson, D. S. (1986) *Anal. Biochem.* **155,** 83–88
21. Jaroszewski, L., Rychlewski, L., Zhang, B., and Godzik, A. (1998) *Protein Sci.* **7,** 1431–1440
22. Sali, A., and Blundell, T. L. (1993) *J. Mol. Biol.* **234,** 779–815
23. Mirzabekov, T. A., Silberstein, A. Y., and Kagan, B. L. (1999) *Methods Enzymol.* **294,** 661–674
24. Congdon, R. W., Muth, G. W., and Splittgerber, A. G. (1993) *Anal. Biochem.* **213,** 407–413
25. Johnson, W. C. (1990) *Proteins Struct. Func. Genet.* **7,** 205–214
26. Cramer, W. A., Heymann, J. B., Schendel, S. L., Deiry, B. N., Cohen, F. S., Elkins, P. A., and Stauffacher, C. V. (1995) *Annu. Rev. Biophys. Biomol. Struct.* **24,** 611–641
27. Sattler, M., Liang, H., Nettesheim, D., Meadow, R. P., Harlan, J. E., Eberstadt, M., Yoon, M. S., Shuker, S. B., Chang, B. S., Minn, A. J., Thompson, C. B., and Fesik, S. W. (1997) *Science* **275,** 983–986
28. Chou, J. J., Li, H., Salvesen, G. S., Yuan, J., and Wagner, G. (1999) *Cell* **96,** 615–624
29. McDonnell, J. M., Fushman, D., Milliman, C. L., Korsmeyer, S. J., and Cowburn, D. (1999) *Cell* **96,** 625–643

THE JOURNAL OF BIOLOGICAL CHEMISTRY

Vol. 273, No. 47, Issue of November 20, pp. 30995–31001, 1998
Printed in U.S.A.

Cytoprotection by Bcl-2 Requires the Pore-forming α5 and α6 Helices*

(Received for publication, July 31, 1998, and in revised form, September 4, 1998)

Shigemi Matsuyama, Sharon L. Schendel, Zhihua Xie, and John C. Reed‡

From the Burnham Institute, Program on Apoptosis & Cell Death Research, La Jolla, California 92037

We explored whether the putative channel-forming fifth and sixth α-helices of Bcl-2 and Bax account for Bcl-2-mediated cell survival and Bax-induced cell death in mammalian cells and in the yeast *Saccharomyces cerevisiae*. When α5-α6 were either deleted or swapped with each other, the Bcl-2Δα5α6 deletion mutant and Bcl-2-Bax(α5α6) chimeric protein failed to block apoptosis induced by either Bax or staurosporine in human cells and were unable to prevent Bax-induced cell death in yeast, implying that the α5-α6 region of Bcl-2 is essential for its cytoprotective function. Additional experiments indicated that, although α5-α6 is necessary, it is also insufficient for the anti-apoptotic activity of Bcl-2. In contrast, deletion or substitution of α5-α6 in Bax reduced but did not abrogate apoptosis induction in human cells, whereas it did completely nullify cytotoxic activity in yeast, implying that the pore-forming segments of Bax are critical for conferring a lethal phenotype in yeast but not necessarily in human cells. BaxΔα5α6 and Bax-Bcl-2(α5α6) also retained the ability to dimerize with Bcl-2. Bax therefore may have redundant mechanisms for inducing apoptosis in mammalian cells, based on its ability to form α5-α6-dependent channels in membranes and to dimerize with and antagonize anti-apoptotic proteins such as Bcl-2.

Bcl-2 family proteins play a pivotal role in the regulation of programmed cell death and apoptosis. Some members of this family such as Bcl-2 and Bcl-X_L function as cell death suppressors, whereas others such as Bax and Bak induce apoptosis (1–3). At least three biochemical characteristics have been ascribed to various Bcl-2 family proteins, including: (*a*) dimerization with themselves and each other; (*b*) interactions with other types of proteins, ranging from protein kinases and phosphatases to proteins that bind cell death proteases of the caspase family; and (*c*) formation of pores or ion channels in membranes (1). The relative significance of these different functions remains to be clarified, but may depend on the precise repertoire of Bcl-2 family proteins expressed in cells and the type of cell death stimuli applied.

The three-dimensional structure of one of the Bcl-2 family proteins, Bcl-X_L, has been determined, revealing seven α-helices separated by flexible loops (4). Some other members of the Bcl-2 family, including the anti-apoptotic protein Bcl-2 and the pro-apoptotic protein Bax, can be readily modeled on the Bcl-X_L crystallographic coordinates, implying that they share a similar fold despite having opposing effects on cell life and death (5). The C terminus of many Bcl-2 family proteins consists of a stretch of hydrophobic amino acids that serves the purpose of anchoring them within intracellular membranes, particularly the outer mitochondrial membrane, endoplasmic reticulum, and nuclear envelope, with the bulk of the protein oriented toward the cytosol (6, 7).

Comparisons with other proteins for which structures are available revealed striking structural similarity of Bcl-X_L to the pore-forming domains of certain bacterial toxins, including: (*a*) diphtheria toxin, which produces pores for transporting a polypeptide fragment of the toxin across lysosomal/endosomal membranes into the cytosol (8, 9); and (*b*) the colicins, which form ion channels that kill sensitive *Escherichia coli* by depolarizing their inner membranes (10). Moreover, Bcl-2, Bcl-X_L, and Bax have been reported to form ion channels in synthetic membranes *in vitro*, when tested under conditions similar to those required for channel formation by diphtheria toxin or the colicins (11–14). However, the characteristics of the channels formed *in vitro* by cytoprotective (Bcl-2, Bcl-X_L) and cytotoxic (Bax) members of the Bcl-2 family differ. In general, Bcl-2 and Bcl-X_L tend to form channels having low conductance, display modest cation selectivity, and exist in a mostly closed state, whereas Bax channels typically have 100–1000-fold larger conductances than Bcl-2 or Bcl-X_L channels, prefer anions, and dwell longer in an open state (reviewed in Ref. 5).

By analogy to structurally similar pore-forming domains from bacterial toxins, the predicted fifth and sixth α-helices of Bcl-2 and Bax are hypothesized to directly participate in channel formation. These α-helices are positioned in the core of these proteins (based on models derived from the Bcl-X_L structure) and are believed to be inserted into the membrane bilayer perpendicular to the membrane surface, with the loop connecting α5 and α6 presumably protruding from the other side of the membrane (5). Indeed, deletion of the α5-α6 regions from Bcl-2 abolishes its ability to form ion channels in synthetic membranes *in vitro* (12). The structural basis for differences in the channels formed *in vitro* by Bcl-2 and Bax is unknown, but could be due at least in part to differences between the polar residues of the fifth and sixth α-helices of these proteins. Two acidic amino acids are predicted to be on the hydrophilic face of α5 in Bcl-2 and Bcl-X_L, which would presumably line the lumen channel, compared with two basic amino acids in the corresponding position for the pro-apoptotic Bax and Bak proteins (reviewed in Ref. 5). These differences in α5 and α6 might account for the relative cation specificity of the Bcl-2 and Bcl-X_L channels (11, 12), and the anion selectivity of the Bax channel (13).

It remains to be determined whether channels are formed by Bcl-2 family proteins *in vivo* and whether this activity is critical for the biological functions of these proteins. However,

* This work was supported by California Breast Cancer Research Program Grant 1RB-0093, Department of Defense Breast Cancer Research Program Grant DAMD17-98-1-8167 (to S. L. S.), and CaP-CURE, Inc. The costs of publication of this article were defrayed in part by the payment of page charges. This article must therefore be hereby marked "*advertisement*" in accordance with 18 U.S.C. Section 1734 solely to indicate this fact.

‡ To whom correspondence should be addressed: Burnham Institute, 10901 N. Torrey Pines Rd., La Jolla, CA 92037. Tel.: 619-646-3140; Fax: 619-646-3194; E-mail: jreed@burnham-inst.org.

intrinsic bioactivities for the Bcl-2 and Bax proteins have been demonstrated in yeast, where no Bcl-2 homologs apparently exist based on sequence homology searches of the now completed genome of *Saccharomyces cerevisiae*. The Bax and Bak proteins, for example, confer a lethal phenotype when ectopically expressed in either the budding yeast *S. cerevisiae* or the fission yeast *Schizosaccharomyces pombe* (15–21). In contrast, mutants of Bax and Bak that lack the putative pore-forming α5 and α6 helices are devoid of cytotoxic activity in yeast. Bcl-2 and Bcl-X_L can rescue yeast from the lethal effects of Bax and Bak, without necessity for dimerization between these proteins (22). Moreover, ectopic expression of Bcl-2 in the absence of Bax or Bak in certain mutant strains of yeast has also been shown to preserve cell viability under some circumstances (23), providing further evidence of an intrinsic function for this anti-apoptotic protein.

In this report, we explored some of the structure-function relations of the Bcl-2 and Bax proteins that may be relevant to their similarity to pore-forming proteins, focusing specifically on the putative pore-forming α5 and α6 helices. The results provide further insights into the question of why Bcl-2 is cytoprotective and Bax is cytodestructive, and suggest that differences in the α5 and α6 helices of Bcl-2 and Bax are necessary but insufficient for determining the opposing phenotypes of these proteins.

MATERIALS AND METHODS

Plasmid Constructions—Human Bcl-2 and human Bax cDNAs were employed as the templates for the mutagenesis experiments. Mutations were created using a two-step polymerase chain reaction method (17, 24). All mutants were initially subcloned between *Eco*RI (5′ end) and *Xho*I (3′ end) sites in pEG202, pJG4–5, pcDNA3, or pcDNA3-HA plasmids. The following mutagenic primers were used in combination with the wild-type Bcl-2 forward (for pEG202, pJG4–5: 5′-GCGGAATTCATGGCGCACGCTGGGAGAACA-3; for pcDNA3: 5′-GCGGAATTCGCCACCATGGCGCACGCTGGGAGAACA-3′) and reverse (with C-terminal transmembrane domain (TM)[1]: 5′-ATTCTCGAGTCACTTGTGGCCCAGATAGGC-3′; without TM: 5′-CGCCTCGAGTCAAGTCTTCAGAGACAGCCAGGA-3′), for wild-type Bax forward (for pEG202, pJG4–5, or pcDNA3-HA: 5′-GCGGAATTCATGGACGGGTCCGGGGAGGAG-3′; for pcDNA3: 5′-GCGGAATTCGCCACCATGGACGGGTCCGGGGAGGAG-3′) and reverse (with TM: 5′-ATTCTCGAGTCAGCCCATCTTCTTCCAGAT-3′; without TM: 5′-ATTCTCGAGTCAGGGCGTCCCAAAGTAGGAGAG-3′), for Bcl-2Δα5α6, 5′-CTGCACACCTGGATCCAGGATAACGGA-3′ (forward) and 5′-CCAGGTGTGCAGCACCCCGTGCCTGAAGAGCTC-3′ (reverse), and for Bax2Δα5α6, 5′-GACGGCAACTTCGACCAGGGTGGTTGGGACGGC-3′ (forward) and 5′-GAAGTTGCCGTCAGAAAACATGTCAGC-3′ (reverse). For the construction of Bcl-2-Bax or Bax-Bcl-2 chimeras, first a *Sac*I site was introduced into the Bax cDNA by two-step polymerase chain reaction using 5′-GCAGCTGAGCTCTTTTCTGACGGCAACTTCAAC-3′ (forward) and 5′-AGAAAAGAGCTCAGCTGCCACTCGGAAAAAGAC-3′ (reverse) with the above primers for wild-type Bax. Then, the region of the Bcl-2 cDNA and Bax cDNAs between the *Sac*I and *Bam*HI sites was swapped. For the production of recombinant GST-Bax(ΔTM) and GST-BaxΔα5α6(ΔTM), cDNAs encoding Bax(ΔTM) and BaxΔα5α6(ΔTM) were subcloned between *Eco*RI (5′ end) and *Xho*I (3′ end) sites in pGEX-4T-1 vector.

Mammalian Cell Apoptosis Assays—293T cells were cultured for 12 h in 60-mm diameter dishes in 5 ml of Dulbecco's modified Eagle's medium containing 10% fetal calf serum. Fresh medium was exchanged, and 4 h later the cells were co-transfected with 0.5 μg of pEGFP (CLONTECH Laboratories, Inc.) and various plasmids encoding wild-type or mutants of Bcl-2 or Bax by a calcium phosphate precipitation method (total amount of DNA normalized to either 1.5 or 2.5 μg.). Four hours after transfections, fresh medium was exchanged and the cells were cultured for another 20 h before collecting both floating and adherent cells. Half of the recovered cells were used for immunoblot assays, and the remainder were stained with 4′,6-diamidino-2-phenylindole to determine the percentages of GFP-positive cells with apoptotic nuclei (25).

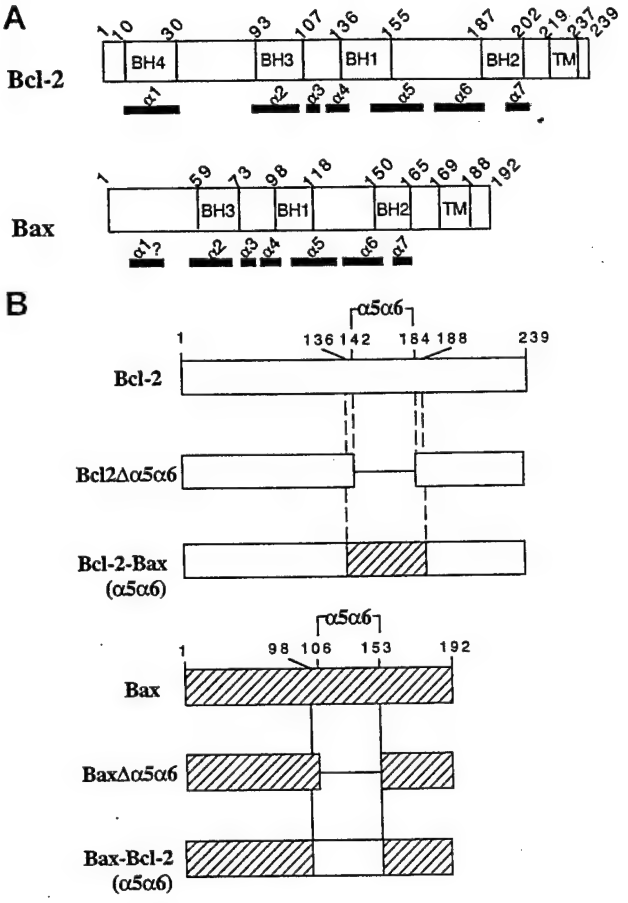

FIG. 1. **Bcl-2 and Bax mutants and chimeras.** The predicted positions of the α-helical regions within the human Bcl-2 and Bax proteins are depicted (*A*), and the α5-α6 region deletion mutants and chimeras of Bcl-2 and Bax are illustrated (*B*). The boundaries of the regions corresponding to the α5 and α6 helices were deduced from Ref. 4 and confirmed independently by modeling the human Bcl-2 and Bax proteins on the Bcl-X_L coordinates (5). *Numbers* indicate amino acid positions. The *open bars* refer to Bcl-2 and the *hatched bars* to Bax.

GM701 cells were grown in Dulbecco's modified Eagle's medium supplemented with 10% (v/v) calf serum. Cells were transfected with pRC/CMV-hBcl2, pcDNA3-Bcl-2Δα5α6, or pcDNA3-Bcl-2-Bax(α5α6) by a calcium-phosphate precipitation method and selected in 1.4 mg/ml (active) G418. Pools of stable transfectants were passaged and then were cultured in 96-well plates for 12 h at a density of 1×10^4 cells/0.1 ml/well. Fresh medium was exchanged, and 1 μM staurosporine (STS) was added to induce apoptosis. After 24 h, cell viability was determined by trypan blue dye exclusion assay.

Yeast Cytotoxicity Assays—EGY48 strain cells were transformed by the lithium acetate method, using 1 μg of plasmid DNA (25, 26). Cells were then plated on histidine-deficient glucose-based minimal medium supplemented with other essential amino acids. Colonies were counted after culturing at 30 °C for 3 days. For the examination of Bcl-2-mediated rescue of yeast from Bax-induced cell death, EGY48 cells were co-transformed with 1 μg of pGilda-Bax and 1 μg of pJG4–5-Bcl-2, pJG4–5-Bcl-2Δα5α6, pJG4–5-Bcl-2-Bax(α5α6), or pJG4–5-Bax-Bcl-2(α5α6), and plated on both histidine- and tryptophan-deficient glucose-based medium to select for the plasmids. Single colonies of transformed yeast cells were re-streaked on galactose-containing medium to induce the GAL-1 promoters in these plasmids and cultured for 4 days (25).

Yeast Two-hybrid Assays—Protein-protein interactions were evaluated by yeast two-hybrid assay as described previously, using EGY48 cells either for *LEU2* or *lacZ* reporter gene assays, in conjunction with pEG202 (LexA DNA-binding domain) and pJG4–5 (B42 transactivation domain) plasmids (15, 17, 27). Growth on leucine-deficient medium was scored 4 days after spotting on minimal medium plates containing 2% galactose and 1% raffinose to induce expression of the transactivation

[1] The abbreviations used are: TM, transmembrane; DOPC, 1,2-dioleoylphosphatidylcholine; DOPG, 1,2-dioleoylphosphatidylglycerol; GFP, green fluorescent protein; GST, glutathione *S*-transferase; HA, hemagglutinin; PAGE, polyacrylamide gel electrophoresis; STS, staurosporine.

domain-containing proteins from the GAL1 promoter in pJG4–5. Filter assays were similarly performed for β-galactosidase measurements, using cells plated on either galactose- or glucose-containing minimal medium supplemented with leucine. Blue color development was scored at 2 h after adding 5-bromo-4-chloro-3-indolyl-β-D-galactopyranoside (X-gal).

Immunoprecipitation and Immunoblotting Assays—For co-immunoprecipitation experiments, 293T cells (2×10^6) were cultured for 12 h in 10 ml of medium. Fresh medium was exchanged, and 4 h later the cells were co-transfected with 10 μg of pRC/CMV-Bcl-2 and 10 μg of pcDNA3-HA-Bax, pcDNA3-HA-BaxΔα5α6, or pcDNA3-HA-Bax-Bcl-2(α5α6), or with 10 μg of pcDNA3-Bax and 10 μg of pRc-CMV-Bcl-2, pcDNA3-Bcl-2Δα5α6, or pcDNA3-Bcl-2-Bax(α5α6), by a calcium phosphate precipitation method. Four hours after transfections, fresh medium was exchanged and the cells were cultured for another 4 h before lysing in 0.6 ml of Nonidet P-40 lysis buffer (10 mM Hepes (pH 7.5) 142.5 mM KCl, 5 mM $MgCl_2$, 1 mM EDTA, 0.2% Nonidet P-40), containing 1 mM phenylmethylsulfonyl fluoride, 5 μg/ml leupeptin, and 5 μg/ml aprotinin. After preclearing with 50 μl of Protein G-Sepharose at 4 °C for 1 h, immnoprecipitations were performed by incubating 0.2 ml of lysate with 20 μl of Protein G-Sepharose preabsorbed with 5 μg of anti-Bcl-2 mouse monoclonal antibody ascites (clone 4D7) or 10 μl of anti-Bax rabbit serum at 4 °C for 2 h (28, 29). After extensive washing in Nonidet P-40 lysis buffer, beads were boiled in 60 μl of Laemmli buffer and 20 μl of the eluted proteins were subjected to SDS-PAGE (12%) immunoblot analysis using anti-HA mouse monoclonal antibody conjugated with horseradish peroxidase (Boehringer Mannheim) or 4D7 anti-Bcl-2 mouse monoclonal antibody. For detection of Bcl-2, horseradish peroxidase-conjugated anti-mouse (Bio-Rad) antibody was employed. Immunodetection was achieved by using an enhanced chemiluminescence system (Amersham Pharmacia Biotech) with exposure to x-ray film.

For immunoblot assays, whole cell lysates were normalized for total protein content, and immunoblot assays were performed as described previously using 0.1% (v/v) anti-LexA rabbit serum or either anti-Bax or anti-Bcl-2 rabbit serum (21, 29).

Ion Channel Assays—Recombinant GST-Bax (ΔTM) and GST-BaxΔα5α6 (ΔTM) proteins were produced from pGEX-4T-1 in *E. coli* (BL21 (DE3) strain) bacteria and purified by glutathione-Sepharose affinity chromatography essentially as described (12, 30, 31). GST was removed by cleavage with thrombin, and the Bax(ΔTM) and BaxΔα5α6 (ΔTM) proteins were subsequently purified by ion-exchange chromatography (12, 30, 31) and dialyzed into 20 mM Tris-HCl, pH 8.0. Folding of the purified proteins was confirmed by circular dichroism measurements carried out on an AVIV 60DS spectropolarimeter. Proteins were assayed for channel activity on KCl-loaded unilammelar liposomes composed of 60% DOPC (1,2-dioleoylphosphatidylcholine) and 40% DOPG (1,2-dioleoylphosphatidylglycerol) at pH 4.0, measuring Cl^- ion efflux as described (12).

RESULTS

To examine the biological significance of the putative pore-forming α5 and α6 helices within Bcl-2 and Bax, mutants having α5 and α6 deleted were prepared. Alternatively, the α5 and α6 helices were swapped, thus generating chimeric proteins in which the α5 and α6 helices of Bax were replaced with those from Bcl-2 and *vice versa* (Fig. 1).

Previously, we demonstrated that deletion of the α5-α6 region from Bcl-2 abolishes the ability of the recombinant protein to form pH-dependent channels in liposomes *in vitro* (12). To explore the relevance of the α5-α6 region of Bax to its *in vitro* channel activity, recombinant Bax and BaxΔα5α6 proteins were produced in bacteria (without their C-terminal hydrophobic domains (ΔTM) for solubility purposes) and purified (data not shown). When applied at ~150 ng/ml to KCl-loaded unilammelar liposomes under conditions previously shown to be permissive for channel formation by Bcl-2 family proteins (11–14), Bax (ΔTM) induced striking ion efflux (Fig. 2). In contrast, the BaxΔα5α6 (ΔTM) protein exhibited little or no channel activity under the same conditions. Additional experiments revealed that Bax channel formation was dependent on acidic pH (optimal pH ~4.0) and the presence of acidic lipids within liposomes (DOPG), consistent with prior studies of Bax and other Bcl-2 family proteins (11–14). In contrast, the BaxΔα5α6

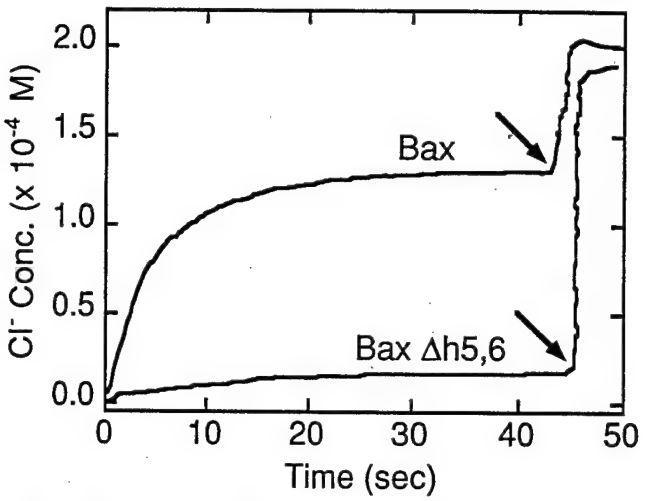

FIG. 2. **Bax channel activity requires α5-α6 region.** Bax (ΔTM) or BaxΔα5α6 (ΔTM) were added at 150 ng/ml to KCl-loaded unilammelar liposomes composed of 40:60 (mol/mol) DOPG:DOPC at pH 4.0 and ion efflux was monitored using a Cl^- electrode as described previously (12). Triton X-100 (0.1%) was added to release residual KCl at the point indicated by *arrow*.

(ΔTM) protein induced either negligible ion-efflux or (at higher concentrations) exhibited only nonspecific effects, producing similar amounts of Cl^- release at both neutral and acidic pH and regardless of whether lipsomes contained acidic lipids (DOPG) or were composed entirely of neutral lipids (DOPC) (data not shown). Although the absence of the C-terminal membrane anchoring domain may reduce the efficiency, these experiments nevertheless demonstrate α5-α6-dependent channel formation by Bax *in vitro*.

Studies of Bcl-2 and Bax Mutants in Mammalian Cells—When expressed in the human kidney epithelial cell line 293T by transient transfection, the wild-type Bax protein induced apoptosis in nearly half of the successfully transfected cells, as determined by 4′,6-diamidino-2-phenylindole staining of GFP-expressing cells (Fig. 3). Similarly, apoptosis was also induced by transfection with plasmids encoding either the BaxΔα5α6 or Bax-Bcl-2(α5α6) proteins into 293T cells. The BaxΔα5α6 and Bax-Bcl-2(α5α6) proteins consistently induced a lower percentage of the transiently transfected 293T cells to undergo apoptosis when compared with wild-type Bax in experiments where varying amounts of these plasmid DNAs were employed (1, 2, 4, and 8 μg). However, immunoblot analysis of lysates prepared from the transfected 293T cells suggested that these mutant proteins may be produced at somewhat lower levels than the wild-type Bax protein (Fig. 3*C*; data not shown). These results indicate that the α5 and α6 helices of Bax are not absolutely required for apoptosis induction in 293T cells. Furthermore, introduction of the α5 and α6 helices from Bcl-2 into the Bax protein is insufficient to convert Bax from a killer to a protector protein.

The bioactivities of Bcl-2 mutant proteins lacking either α5 and α6 (Bcl-2Δα5α6) or which contained the corresponding α5-α6 region from Bax (Bcl-2-Bax(α5α6)) were compared against the wild-type Bcl-2 protein in transient co-transfection assays to determine whether these proteins could suppress apoptosis induced by Bax. In contrast to wild-type Bcl-2, transfections performed with plasmids encoding the Bcl-2Δα5α6 or Bcl-2-Bax(α5α6) proteins failed to suppress Bax-induced apoptosis in 293T cells (Fig. 3*B*). Immunoblot analysis of lysates prepared from these transiently transfected cells revealed at least comparable levels of production of the Bcl-2Δα5α6 and Bcl-2-Bax(α5α6) proteins compared with wild-type Bcl-2 (Fig. 3*D*). Thus, removal of the α5-α6 region from Bcl-2 or replace-

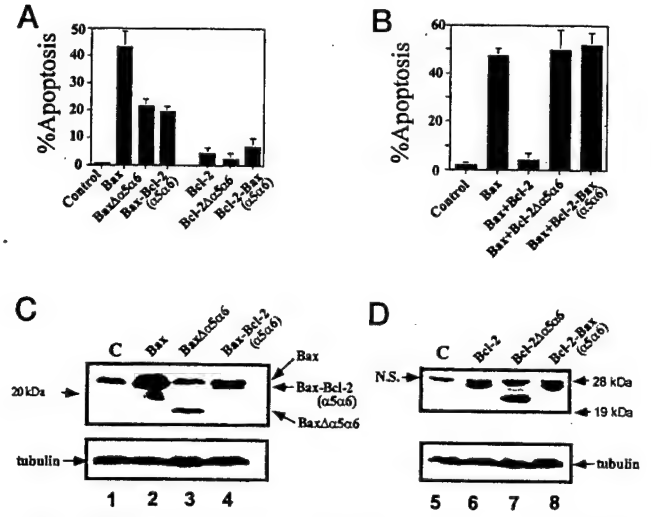

FIG. 3. **Function and expression of Bax and Bcl-2 mutant proteins in 293T cells.** *A*, 293T cells were transiently transfected with 0.5 μg of pEGFP and 1 μg each of plasmids encoding the indicated proteins. Cells were collected 24 h after transfection, and the percentage of GFP positive cells with apoptotic nuclei was determined by 4′,6-diamidino-2-phenylindole staining (mean ± S.D.; $n = 3$). *Control*, pcDNA3. *B*, 293T cells were transiently transfected with 0.5 μg of pEGFP and 2 μg total of the plasmids described below. *Control*, pcDNA3 (2 μg); *Bax*, pcDNA3-Bax (1 μg) and pcDNA3 (1 μg); *Bax+Bcl-2*, pcDNA3-Bax (1 μg) and pRC/CMV-Bcl-2 (1 μg); *Bax+Bcl-2Δα5α6*, pcDNA3-Bax (1 μg) and pcDNA3-Bcl-2Δα5α6 (1 μg); *Bax+Bcl-2-Bax(α5α6)*, pcDNA3-Bax (1 μg) + pcDNA3-Bax-Bcl-2(α5α6) (1 μg). The percentage of apoptotic GFP-expressing cells is indicated (mean ± S.D.; $n = 3$). *C* and *D*, immunoblot analysis of lysates prepared from 293T cells transfected as in *A* and *B*. All samples were normalized for total protein content (20 μg/lane). The blot in *C* (*lanes 1–4*) was probed with anti-Bax antiserum, whereas anti-Bcl-2 antiserum was employed for the blot in *D* (*lanes 5–8*). Blots were also incubated with anti-tubulin antibody to confirm loading of equivalent amounts of intact protein (*lower panel*). *N.S.* indicates nonspecific band.

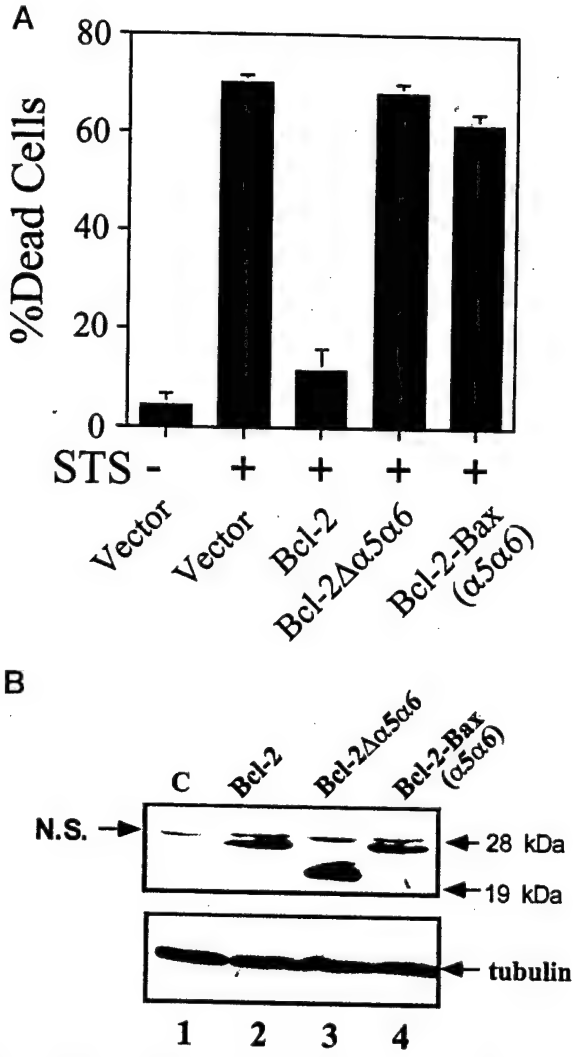

FIG. 4. **Functional analysis of Bcl-2 mutants in GM701 cells.** *A*, stable transfectants of GM701 cells were prepared by selection in G418 after transfection with the following plasmids: pcDNA3 (*Vector*), pRc-CMV-Bcl-2, pcDNA3-Bcl-2Δα5α6, and pcDNA3-Bcl-2-Bax(α5α6). Cells were cultured at 1×10^4 cells/0.1 ml/well in a 96-well dish and treated with or without STS (1 μM) for 24 h before assessing viability by trypan blue dye exclusion. *B*, immunoblot analysis of lysates prepared from stably transfected GM701 cells was performed, after normalization for total protein content (20 μg/lane). Blots were incubated with either anti-Bcl-2 antiserum (*top panel*) or anti-tubulin antibody (*lower panel*). *N.S.* indicates a nonspecific band.

ment of the corresponding region from Bax abolishes the ability of Bcl-2 to block Bax-mediated apoptosis. When expressed in 293T cells without co-transfection of Bax, neither the Bcl-2Δα5α6 nor the Bcl-2-Bax(α5α6) protein induced significant apoptosis (Fig. 3*A*), arguing that substitution of the α5-α6 region of Bax does not convert Bcl-2 into a killer protein.

To further explore the function of the Bcl-2Δα5α6 and Bcl-2-Bax(α5α6) proteins, their ability to inhibit STS-induced apoptosis in GM701 cells was compared with the wild-type Bcl-2 protein. Treatment with this broad-specificity kinase inhibitor induced apoptosis in ~70% of GM701 cells (Fig. 4). Wild-type Bcl-2 potently suppressed STS-induced apoptosis. In contrast, neither Bcl-2Δα5α6 nor Bcl-2-Bax(α5α6) interfered with STS-induced apoptosis (Fig. 4*A*), despite expression of these mutant proteins at levels equivalent to or greater than the wild-type Bcl-2 protein (Fig. 4*B*). Expression of Bcl-2Δα5α6 or Bcl-2-Bax(α5α6) in GM701 cells did not induce apoptosis in the absence of STS, indicating that these Bcl-2 mutant proteins are not intrinsically cytotoxic (data not shown). Taken together, these observations indicate that the α5-α6 region of Bcl-2 is essential for its anti-apoptotic activity in mammalian cells.

Studies of Bcl-2 and Bax Mutant Proteins in Yeast—Ectopic expression of Bax in *S. cerevisiae* has been shown to induce cell death through a Bcl-2-suppressible mechanism (15, 17, 21). The behavior of the Bcl-2 and Bax mutants was therefore tested in budding yeast. As in our prior reports (15, 17, 21, 25), wild-type and mutant versions of Bcl-2 and Bax were expressed as LexA fusion proteins, using the LexA sequences as an epitope tag for monitoring expression levels.

In contrast to the results obtained in mammalian cells, deletion of the α5-α6 region from Bax or substitution of the corresponding region from Bcl-2 abolished the cell death-inducing activity of Bax in yeast, as determined by a colony-forming assay, which measures relative numbers of viable clonigenic cells (15, 17, 21). As shown in Fig. 5*A*, yeast transformed with the plasmid encoding wild-type Bax formed very few colonies due to the lethal effect of Bax expression, whereas numerous colonies (typically >1000/μg of plasmid DNA) were formed when yeast were transformed with plasmids encoding BaxΔα5α6 or Bax-Bcl-2(α5α6). The failure of BaxΔα5α6 and Bax-Bcl-2(α5α6) to kill yeast was not attributable to poor expression of these proteins, as revealed by immunoblot assays performed using cells that had been cotransformed with Bcl-2 to nullify the cytotoxic actions of the wild-type Bax protein (Fig. 5*B*). Thus, the α5-α6 region of Bax is required for its cytotoxic activity in *S. cerevisiae*.

Although necessary for inducing yeast cell death, the α5-α6 helices of Bax are insufficient for mediating the lethal effects of Bax because the chimeric Bcl-2-Bax(α5α6) protein, in which the α5-α6 of Bax had been substituted for the corresponding

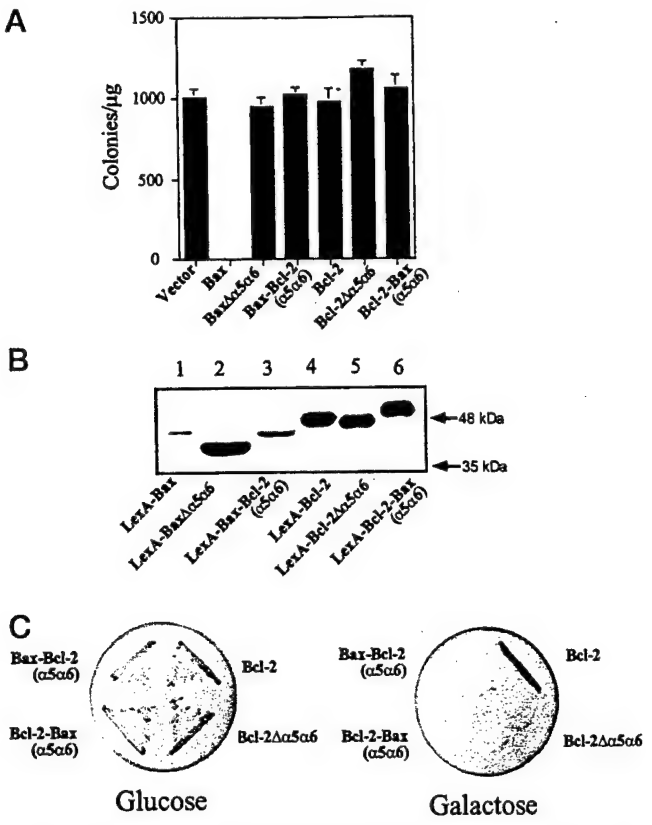

FIG. 5. **Functional analysis of Bax and Bcl-2 mutants in yeast.** *A*, EGY48 strain yeast were transformed with 1 μg of either pEG202 parental DNA (*Vector*) or pEG202 plasmids containing cDNAs encoding the indicated proteins. Cells were plated on plasmid-selective medium (histidine-deficient). The number of independent colonies was counted after 3 days (mean ± S.D.; $n = 3$). *B*, lysates were prepared from EGY48 cells transformed as in *A*, normalized for total protein content (20 μg), and then subjected to SDS-PAGE (7.5%) immunoblot assay using anti-LexA antiserum for detection of either the LexA DNA fragment encoded in the pEG202 parental vector or LexA fusion proteins containing Bcl-2, Bax, or various Bax mutants as indicated. *C*, yeast cells were co-transformed with 1 μg of pGilda-Bax and 1 μg of pJG4–5 plasmids encoding wild-type Bcl-2, Bcl-2Δα5α6, Bcl-2-Bax(α5α6), or Bax-Bcl-2(α5α6). These plasmid utilize the GAL1 promoter to drive gene expression, resulting in repression of expression when cells are grown on glucose plates and gene induction on galactose. Transformants were first allowed to grow on histidine-deficient glucose plates (*left*) and then restreaked on galactose plates (*right*). Photographs represent growth obtained after culture at 30 °C for 4 days.

region within the Bcl-2 protein, failed to display a lethal phenotype in yeast (Fig. 5*A*). Immunoblot analysis again confirmed production of this protein at levels equivalent to or greater than wild-type Bax (Fig. 5*B*), discounting poor expression as an explanation of the findings. Taken together, these observations indicate that the putative pore-forming α5 and α6 helices of Bax are necessary but insufficient for conferring a lethal phenotype in *S. cerevisiae*.

Bcl-2 can rescue yeast from the lethal effects of the wild-type Bax protein (15, 17, 21). To explore the role of the α5-α6 region of Bcl-2 for abrogation of Bax-induced cell death in yeast, cDNAs encoding wild-type or mutant Bcl-2 proteins were subcloned into a plasmid pJG4–5 in which expression is driven from a conditional GAL1 promoter. These galactose-inducible plasmids were then co-transformed into yeast with pGilda-Bax, which also expresses wild-type Bax by GAL1 promoter, and the cells were plated initially on glucose to repress the GAL1 promoter. The resulting transformants were then streaked onto either glucose (control) or galactose (test) plates. As shown in Fig. 5*C*, wild-type Bcl-2 effectively rescued yeast from the lethal effects of Bax, allowing growth of cells on galactose plates,

TABLE I
Summary of two-hybrid assay results

Binding results were deduced from yeast two-hybrid assays performed in both directions. Each cDNA was subcloned into pEG202 (for LexA-fusion) and pJG4–5 (for B42-fusion) vectors. Interactions were designated as "+" only if both directions showed positive binding signals (both β-galactose activity and Leu(−) assay) in comparison with negative control based on LexA-Fas and B42-Ras.

	Bcl-2	Bcl-2Δα5α6	Bcl-2-Bax(α5α6)	Bax	BaxΔα5α6	Bax-Bcl-2(α5α6)
Bcl-2	+	+	+	+	+	+
Bcl-2Δα5α6	+	−	−	−	−	−
Bcl-2-Bax(α5α6)	+	−	−	±	+	+
Bax	+	−	±	+	+	+
BaxΔα5α6	+	−	+	+	−[a]	+
Bax-Bcl-2(α5α6)	+	−	+	+	+	+

[a] LexA-BaxΔα5α6 showed relatively high background and the signal of LexA-BaxΔα5α6 and B42-BaxΔα5α6 was similar to the negative control of LexA-Bax Δα5α6 and B42-Ras, thus resulting in a "−" score.

whereas the Bcl-2Δα5α6 mutant lacking the putative pore-forming α5 and α6 helices and the Bcl-2-Bax(α5α6) chimera containing the α5-α6 region from Bax failed to nullify Bax-induced yeast cell death. Immunoblot analysis confirmed expression of these Bcl-2 mutant proteins at levels comparable to the normal Bcl-2 protein (data not shown). Thus, the α5-α6 region of Bcl-2 appears to be necessary for rescuing yeast from the cytotoxic actions of Bax. However, the putative pore-forming α-helices of Bcl-2 are evidently insufficient for rescue, as expression of the Bax-Bcl-2(α5α6) in which the α5-α6 region of Bcl-2 was inserted in place of the corresponding segment of Bax also failed to protect yeast from Bax-induced cell death (Fig. 5*C*). Thus, similar to the results obtained in mammalian cells, the α5-α6 region of Bcl-2 appears to be necessary but insufficient for the cytoprotective effect of Bcl-2.

Analysis of Dimerization Capabilities of Bcl-2 and Bax Mutants—Bcl-2 and Bax are known to both homodimerize with themselves and heterodimerize with each other (1–3). We explored the effects of deleting the α5-α6 regions of Bcl-2 and Bax or swapping them on homo- and heterodimerization, using a yeast two-hybrid approach (Table I). For these assays, mutant and wild-type Bcl-2 and Bax proteins were expressed with appended N-terminal LexA DNA binding or B42 transactivation domains, but without their C-terminal membrane anchoring regions which could interfere with nuclear import. Removal of the membrane anchoring domain from the C terminus of Bax also abolishes its insertion into mitochondrial membranes, abolishing entirely or greatly reducing its cytotoxicity in yeast (11–13).

The BaxΔα5α6, Bax-Bcl-2(α5α6), and wild-type Bax proteins retained the ability to interact with both Bcl-2 and Bax in yeast two-hybrid assays, consistent with reports indicating the ability of the second α-helix (BH3 domain) within this protein to bind to pockets found on the surface of other Bcl-2 family proteins (32). Thus, the α5-α6 region of Bax is not required for dimerization with the wild-type Bcl-2 or Bax proteins. The Bax-Bcl-2(α5α6) chimeric protein also retained the ability to interact with itself (Table I), implying that its lack of cell death inducing activity in yeast cannot be attributed to defective homodimerization. In contrast, the BaxΔα5α6 protein failed to interact with itself, consistent with structural studies that have implicated portions of the α5 and α6 helices in forming the base of the pocket into which the BH3 domain inserts (32).

Analysis of the α5-α6 region mutants of Bcl-2 revealed that all retained the ability to interact with Bcl-2 in yeast two-hybrid assays, implying that they were not grossly misfolded despite their apparent lack of bioactivity in both yeast and

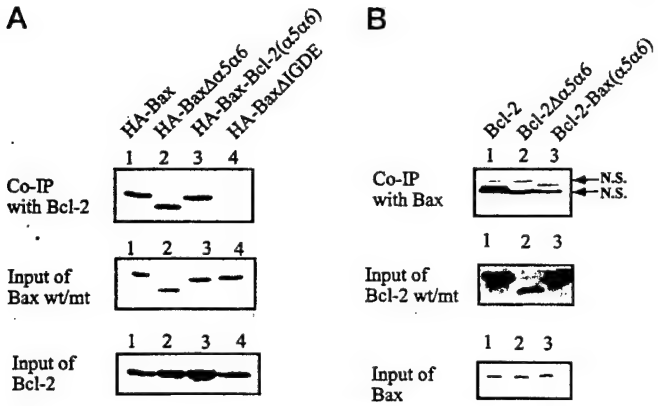

FIG. 6. **Analysis of dimerization of Bax and Bcl-2 mutant proteins by co-immunoprecipitation.** *A*, 293T cells were transfected with pRc-CMV-Bcl2 (*lanes 1–4*) and pcDNA3-HA-Bax (*lane 1*), pcDNA3-HA-BaxΔα5α6 (*lane 2*), pcDNA3-HA-Bax-Bcl-2(α5α6) (*lane 3*), or pcDNA3-HA-BaxΔIGDE (*lane 4*). Two days after transfection, cell lysates were prepared and subjected to immunoprecipitation using anti-Bcl-2 monoclonal antibody. Immune complexes were analyzed by SDS-PAGE (12%) immunoblot assay, using anti-HA antibody (*upper panel*) or anti-Bcl-2 antiserum for immunodetection (*bottom panel*). *Middle panel* represents lysates from the same cells that were normalized for total protein content (20 μg/lane) and analyzed for relative levels of Bax protein by immunoblotting using anti-Bax antiserum, confirming production of wild-type Bax and all Bax mutants in the transfected cells. *B*, 293T cells were transiently transfected with pcDNA3-Bax (*lanes 1–3*) and pRc/CMV-h Bcl-2 (*lane 1*), pcDNA3-Bcl-2Δα5α6 (*lane 2*), or pcDNA3-Bcl-2-Bax(α5α6) (*lane 3*). Immunoprecipitations were performed using anti-Bax antiserum, followed by SDS-PAGE (12%) immunoblot analysis using anti-Bcl-2 monoclonal antibody (*upper panel*) or anti-Bax antiserum (*bottom panel*) for detection. In the *middle panel*, lysates were normalized for total protein content (20 μg) and subjected to immunoblot assay using anti-Bcl-2 antiserum, confirming production of wild-type Bcl2 and all Bcl-2 mutant proteins. Negative controls to confirm the specificity of these protein interactions included immunoprecipitations performed with HA-BaxΔIGDE and anti-HA antibodies and blotting with anti-Bcl-2 antibody (data not shown).

mammalian cells. However, neither Bcl-2Δα5α6 nor Bcl-2-Bax(α5α6) homodimerized. The Bcl-2Δα5α6 deletion mutant also entirely failed to interact with Bax, and the Bcl-2-Bax(α5α6) chimera displayed reduced interaction with Bax in two-hybrid assays compared with the wild-type Bcl-2 protein (Table I).

To further explore the dimerization capabilities of the α5-α6 region mutants of Bcl-2 and Bax, co-immunoprecipitation experiments were performed using lysates from 293T cells that had been transiently transfected with plasmids encoding these proteins (Fig. 6). Consistent with the results of yeast two-hybrid experiments, HA-epitope tagged versions of the wild-type and α5-α6 region mutants of Bax retained the ability to co-immunoprecipitate with Bcl-2, and were recovered in anti-Bcl-2 immune complexes with approximately equivalent efficiency relative to each other (Fig. 6). As a control, experiments were also performed with a mutant of Bax in which a well conserved I-G-D-E amino acid sequence found within the BH3 domain had been deleted. Consistent with our previous studies of this mutant, no co-immunoprecipitation with Bcl-2 was detected, thus confirming the specificity of the results (24).

Analysis of the Bcl-2 mutants also reinforced the findings of yeast two-hybrid assays. When expressed in 293T cells, the Bcl-2Δα5α6 deletion mutant failed to co-immunoprecipitate with Bax and the Bcl-2-Bax(α5α6) chimeric protein displayed reduced co-immunoprecipitation relative to the wild-type Bcl-2 proteins. Immunoblot analysis of the same lysates indicated that the wild-type Bcl-2 and Bcl-2-Bax(α5α6) proteins were produced at comparable levels in transiently transfected 293T cells, excluding differences in the relative amounts of these proteins as a likely explanation for the reduced ability of Bcl-2-Bax(α5α6) to co-immunoprecipitate with Bax (Fig. 6). A variety of control co-immunoprecipitations using HA-tagged or untagged irrelevant proteins were performed, confirming the specificity of the results presented in Fig. 6 (data not shown).

DISCUSSION

Bcl-2 and Bax are known to form ion channels in synthetic membranes *in vitro*, and it has been speculated that the regions predicted to coincide with the α5 and α6 helices of the homologous protein Bcl-X_L are directly involved in this process (5). Here, we report the results of experiments in which the predicted α5 and α6 region of Bcl-2 and Bax were either deleted or swapped with each other. Our data provide evidence that: (*a*) α5 and α6 of Bcl-2 are required for its cytoprotective activity in both mammalian cells and yeast, (*b*) α5 and α6 of Bax are necessary for its cytodestructive activity in yeast but not in mammalian cells, and (*c*) swapping the α5-α6 regions of Bcl-2 and Bax is insufficient for converting the phenotype of Bcl-2 to a killer and Bax to a protector. These results imply that, although necessary, these α-helices are apparently insufficient to explain why Bcl-2 is anti-apoptotic and Bax is pro-apoptotic in most cellular contexts.

The observation that the α5-α6 region is not required for Bax-induced apoptosis in mammalian cells can presumably be explained by the ability of its BH3 domain (predicted second α-helix) to bind to and antagonize anti-apoptotic Bcl-2 family proteins (27). As shown here, the α5-α6 mutants of Bax retained the ability to co-immunoprecipitate with Bcl-2 and to interact with Bcl-2 in yeast two-hybrid assays. Previous studies have shown that overexpressing fragments of Bax or Bak that retain little more than their BH3 domain are sufficient to bind Bcl-2 or Bcl-X_L and to induce apoptosis in mammalian cells (33). Similarly, a Bcl-2 family subgroup comprising pro-apoptotic proteins such as Bik, Bid, Bim, and Hrk has sequence similarity with other family members that is limited to the BH3 domain. Predicted structures for these proteins cannot be modeled on the Bcl-X_L coordinates, implying that do not share structural similarity with the ion channel-forming proteins such as Bcl-2, Bcl-X_L, and Bax (11–13). This BH3-mediated cell death mechanism may be relevant only in cells that express anti-apoptotic members of the Bcl-2 family, accounting for why α5-α6 region mutants of Bax were inactive in yeast that lack an identifiable Bcl-2 family protein. However, the observation that deletion of the α5-α6 region of Bax abrogates its cytotoxic function in yeast raises the possibility that Bax has two mechanisms for inducing apoptosis in mammalian cells: one that relies on BH3-mediated antagonism of proteins such as Bcl-2 and Bcl-X_L and another that maps to the α5 and α6 helices required for its channel-forming activity. Support for a second, BH3-independent mechanism of cell killing has been obtained through experiments involving BH3 domain mutants of Bax that failed to dimerize with Bcl-2 or Bcl-X_L, and yet retained their pro-apoptotic function in mammalian cells (22, 34). A major question now is which of these two mechanisms for promoting apoptosis is quantitatively more important under physiological conditions where Bax is not artificially overexpressed.

In contrast to Bax, deletion or substitution of the putative channel forming α5 and α6 helices of Bcl-2 abolished its cytoprotective function in both mammalian cells and yeast, indicating that this region is indispensable for function of the Bcl-2 protein. Previously, we reported that deletion of α5 and α6 from Bcl-2 abrogates its ability to form ion channels in lipsomes and planar bilayers *in vitro* (12). Thus, it is possible that channel activity is required for Bcl-2 to promote cell survival and diminish Bax-induced cell death. Unfortunately, multiple at-

tempts to produce the Bcl-2-Bax(α5α6) chimeric protein in bacteria for ion channel studies were unsuccessful due to protein instability and insolubility, thus precluding a comparison with the wild-type Bcl-2 protein *in vitro* channel activity.[2] Although we cannot exclude the possibility that substitution the α5-α6 region of Bcl-2 for the corresponding region of Bax caused a gross misfolding of the protein when expressed in mammalian cells or yeast, the Bcl-2-Bax(α5α6) chimeric protein appeared to be stable, accumulating to levels comparable to the wild-type Bcl-2 protein. Bcl-2-Bax(α5α6) also retained its ability to dimerize with Bax, albeit with reduced efficiency compared with wild-type Bcl-2. Moreover, the Bcl-2-Bax(α5α6) chimera retained the ability to interact with Bcl-2 in yeast two-hybrid assays. Thus, dimerization with Bax or Bcl-2 appears to be insufficient for maintaining the cytoprotective function of the Bcl-2 protein in either mammalian cells or yeast. It will be of interest to identify other proteins with which this Bcl-2-Bax(α5α6) chimera and the wild-type Bcl-2 protein interact. In this regard, Bcl-2 has been reported to bind directly or at least participate in protein complexes containing several types of non-homologous proteins in mammalian cells, including the kinase Raf-1 (35), the phosphatase calcineurin (36), the Hsp70/Hsc70-regulator BAG-1 (37), the caspase-binding protein Bap31 (38), the spinal muscular atrophy protein (SMN) (39), and others (1). Although the CED-4 homolog Apaf-1 (without WD domain) has recently received much attention for its ability to bind both caspases and Bcl-X_L (40, 41), we have been unable to detect interactions between Bcl-2 and Apaf-1 using numerous experimental approaches,[2] making it unlikely that differential binding of wild-type and chimeric Bcl-2 to Apaf-1 accounts for the ability of the former and failure of the latter to promote cell survival in mammalian cells. Moreover, as the completed genome of *S. cerevisiae* reveals no Apaf-1 homologs or caspases, it is highly unlikely that the cytoprotective function of Bcl-2 observed in yeast is involved in such protein interactions.

Although necessary for function of Bcl-2, the α5-α6 region appears to be insufficient for promoting cell survival, as replacing the α5-α6 region of Bax with this segment of Bcl-2 did not convert Bax to a cytoprotective protein. Likewise, although the α5-α6 region of Bax was necessary for its cytotoxic activity in yeast, engineering these predicted α-helices into the Bcl-2 protein was insufficient for switching its phenotype. Several previous reports have suggested that the BH3 domain (second α-helix) is an important determinant of the functions of pro-apoptotic Bcl-2 family proteins in mammalian cells and yeast (1, 24, 27). The BH4 domain (first α-helix in Bcl-X_L structure) of anti-apoptotic Bcl-2 family proteins has also been shown to be important for their cytoprotective function in both yeast and mammalian cells (1, 17, 35). Therefore, the opposing phenotypes of Bcl-2 and Bax presumably require both the α5-α6 region and additional domains such as BH3 or BH4. Determination of the topology of the Bcl-2 and Bax proteins when integrated into membranes in channel-forming conformation will help to reveal whether these other domains such as BH3 and BH4 directly contribute to channel formation by integrating perpendicularly through membranes as proposed for α5 and α6, *versus* regulating cell death through their contributions to dimerization among Bcl-2 family proteins or interactions with other types of non-homologous proteins such as those involved in caspase regulation.

Acknowledgments—We thank T. Brown for manuscript preparation and S. Fuess for technical assistance.

[2] S. Matsuyama, S. L. Schendel, Z. Xie, and J. C. Reed, unpublished observations.

REFERENCES

1. Reed, J. C. (1997) *Nature* **387,** 773–776
2. Nuñuz, G., and Clarke, M. F. (1994) *Trends Cell Biol.* **4,** 399–403
3. Reed, J. C. (1994) *J. Cell Biol.* **124,** 1–6
4. Muchmore, S. W., Sattler, M., Liang, H., Meadows, R. P., Harlan, J. E., Yoon, H. S., Nettesheim, D., Changs, B. S., Thompson, C. B., Wong, S., Ng, S., and Fesik, S. W. (1996) *Nature* **381,** 335–341
5. Schendel, S., Montal, M., and Reed, J. C. (1998) *Cell Death Differ.* **5,** 372–380
6. Krajewski, S., Tanaka, S., Takayama, S., Schibler, M. J., Fenton, W., and Reed, J. C. (1993) *Cancer Res.* **53,** 4701–4714
7. Lithgow, T., van Driel, R., Bertram, J. F., and Strasser, A. (1994) *Cell Growth Differ.* **3,** 411–417
8. Kagan, B. L., Finkelstein, A., and Colombini, M. (1981) *Proc. Natl. Acad. Sci. U. S. A.* **78,** 4950–4954
9. Donovan, J. J., Simon, M. I., and Montal, M. (1985) *J. Biol. Chem.* **260,** 8817–8823
10. Cramer, W. A., Heymann, J. B., Schendel, S. L., Deriy, B. N., Cohen, F. S., Elkins, P. A., and Stauffacher, C. V. (1995) *Annu. Rev. Biophys. Biomol. Struct.* **24,** 611–641
11. Minn, A. J., Velez, P., Schendel, S. L., Liang, H., Muchmore, S. W., Fesik, S. W., Fill, M., and Thompson, C. B. (1997) *Nature* **385,** 353–357
12. Schendel, S. L., Xie, Z., Montal, M. O., Matsuyama, S., Montal, M., and Reed, J. C. (1997) *Proc. Natl. Acad. Sci. U. S. A.* **94,** 5113–5118
13. Schlesinger, P., Gross, A., Yin, X.-M., Yamamoto, K., Saito, M., Waksman, G., and Korsmeyer, S. (1997) *Proc. Natl. Acad. Sci. U. S. A.* **94,** 11357–11362
14. Antonsson, B., Conti, F., Ciavatta, A., Montessuit, S., Lewis, S., Martinou, I., Bernasconi, L., Bernard, A., Mermod, J.-J., Mazzei, G., Maundrell, K., Gambale, F., Sadoul, R., and Martinou, J.-C. (1997) *Science* **277,** 370–372
15. Sato, T., Hanada, M., Bodrug, S., Irie, S., Iwama, N., Boise, L. H., Thompson, C. B., Golemis, E., Fong, L., Wang, H.-G., and Reed, J. C. (1994) *Proc. Natl. Acad. Sci. U. S. A.* **91,** 9238–9242
16. Bodrug, S. E., Aimé-Sempé, C., Sato, T., Krajewski, S., Hanada, M., and Reed, J. C. (1995) *Cell Death Differ.* **2,** 173–182
17. Hanada, M., Aimé-Sempé, C., Sato, T., and Reed, J. C. (1995) *J. Biol. Chem.* **270,** 11962–11968
18. Greenhalf, W., Stephan, C., and Chaudhuri, B. (1996) *FEBS Lett.* **380,** 169–175
19. Ink, B., Zornig, M., Baum, B., Hajibagheri, N., James, C., Chittenden, T., and Evan, G. (1997) *Mol. Cell. Biol.* **17,** 2468–2474
20. Jürgensmeier, J. M., Krajewski, S., Armstrong, R., Wilson, G. M., Oltersdorf, T., Fritz, L. C., Reed, J. C., and Ottilie, S. (1997) *Mol. Biol. Cell* **8,** 325–229
21. Zha, H., Fisk, H. A., Yaffe, M. P., Mahajan, N., Herman, B., and Reed, J. C. (1996) *Mol. Cell. Biol.* **16,** 6494–6508
22. Zha, H., and Reed, J. C. (1997) *J. Biol. Chem.* **272,** 31482–31488
23. Longo, V. D., Ellerby, L. M., Bredesen, D. E., Valentine, J. S., and Gralla, E. B. (1997) *J. Cell Biol.* **137,** 1581–1588
24. Zha, H., Fisk, H. A., Yaffe, M. P., and Reed, J. C. (1996) *Mol. Cell. Biol.* **16,** 6494–6508
25. Matsuyama, S., Xu, Q., Velours, J., and Reed, J. C. (1998) *Mol. Cell* **1,** 327–336
26. Schiestl, R. H., and Giest, R. D. (1989) *Curr. Genet.* **16,** 339–346
27. Zha, H., Aime-Sempe, C., Sato, T., and Reed, J. C. (1996) *J. Biol. Chem.* **271,** 7440–7444
28. Reed, J. C., Tanaka, S., Cuddy, M., Cho, D., Smith, J., Kallen, R., Saragovi, H. U., and Torigoe, T. (1992) *Anal. Biochem.* **205,** 70–76
29. Krajewski, S., Blomvqvist, C., Franssila, K., Krajewska, M., Wasenius, V.-M., Niskanen, E., and Reed, J. C. (1995) *Cancer Res.* **55,** 4471–4478
30. Marzo, I., Brenner, C., Zamzami, N., Susin, S., Beutner, G., Brdiczka, D., Xie, Z., Reed, J., and Kroemer, G. (1998) *J. Exp. Med.* **187,** 1261–1271
31. Zamzami, N., Marzo, I., Susin, S., Brenner, C., Larochette, N., Marchetti, P., Reed, J. C., Reinhard, K., and Kroemer, G. (1998) *Oncogene* **16,** 1055–1063
32. Sattler, M., Liang, H., Nettesheim, D., Meadows, R. P., Harlan, J. E., Eberstadt, M., Yoon, H. S., Shuker, S. B., Chang, B. S., Minn, A. J., Thompson, C. B., and Fesik, S. W. (1997) *Science* **275,** 983–986
33. Simonen, M., Keller, H., and Heim, J. (1997) *Eur. J. Biochem.* **249,** 85–91
34. Simonian, P. L., Grillot, D. A. M., Merino, R., and Nunez, G. (1996) *J. Biol. Chem.* **271,** 22764–22772
35. Wang, H. G., Rapp, U. R., and Reed, J. C. (1996) *Cell* **87,** 629–638
36. Shibasaki, F., Kondo, E., Akagi, T., and McKeon, F. (1997) *Nature* **386,** 728–731
37. Takayama, S., Sato, T., Krajewski, S., Kochel, K., Irie, S., Millan, J. A., and Reed, J. C. (1995) *Cell* **80,** 279–284
38. Ng, F. W. H., Nguyen, M., Kwan, T., Branton, P. E., Nicholson, D. W., Cromlish, J. A., and Shore, G. C. (1997) *J. Cell Biol.* **39,** 327–338
39. Iwahashi, H., Eguchi, Y., Yasuhara, N., Hanafusa, T., Matsuzawa, Y., and Tsujimoto, Y. (1997) *Nature* **390,** 413–417
40. Pan, G., O'Rourke, K., and Dixit, V. M. (1998) *J. Biol. Chem.* **273,** 5841–5845
41. Hu, Y., Benedict, M., Wu, D., Inohara, N., and Nunez, G. (1998) *Proc. Natl. Acad. Sci. U. S. A.* **95,** 4386–4391

Biochemistry **1998,** *37,* 6410−6418

Acidic pH Promotes Dimerization of Bcl-2 Family Proteins

Zhihua Xie, Sharon Schendel, Shigemi Matsuyama, and John C. Reed*

The Burnham Institute, Program of Apoptosis & Cell Death Research, 10901 N. Torrey Pines Rd., La Jolla, California 92037

Received December 12, 1997; Revised Manuscript Received March 9, 1998

ABSTRACT: Several members of the apoptosis-regulating Bcl-2 family of proteins can homo- or heterodimerize with each other at neutral pH and can also form ion channels in synthetic membranes at low pH. The effects of low pH on dimerization among these proteins, however, have not heretofore been examined. Surface plasmon resonance was used to examine the kinetics of dimerization as a function of pH between the anti-apoptotic protein Bcl-X_L (applied in the mobile phase) and three other members of the Bcl-2 family: Bcl-2, Bax, and Bid (immobilized on biosensor chips). In all cases, the relative affinity of dimerization was substantially increased at pH 4.0 compared to pH 7.0−7.4, ranging from a ~10-fold enhancement for Bcl-X_L/Bcl-X_L homodimers to >60-fold for Bcl-X_L/Bid heterodimers. Comparison of the apparent association (k_a) and dissociation (k_d) rates at neutral and acidic pH revealed that the major contributor to increased affinity at low pH was a decreased rate of dimer dissociation. Thus, low pH stabilizes homo- and heterodimeric complexes comprised of Bcl-X_L and these other Bcl-2 family proteins. At pH 4.0, the circular dichroism spectra of Bcl-X_L and Bax were essentially unchanged relative to pH 7.0−7.4, indicating a complete retention of α-helical secondary structure at low pH and excluding gross denaturation of the proteins. Size-exclusion chromatography and bisANS (4,4′-dianilino-1,1′-binaphthyl-5,5′-disulfonic acid) labeling studies provided indirect evidence that Bcl-X_L may undergo conformational changes at low pH. The findings are discussed with respect to the mechanisms of ion-channel formation by Bcl-2 family proteins and the putative molten globule state that has been proposed for these and structurally similar proteins.

Bcl-2 family proteins are important regulators of programmed cell death and apoptosis (*1*−*3*). These proteins either inhibit or induce cell death, with the ratios of anti-apoptotic relative to pro-apoptotic members of the Bcl-2 family representing a critical determinant of the ultimate sensitivity or resistance of mammalian cells to various apoptotic stimuli. Many Bcl-2 family proteins can physically interact with themselves and each other, forming homo- and heterodimers (*1, 2*). In some instances, these dimerization events appear to play important roles in the regulation or effector functions of these proteins (*4*−*6*). Thus, a need exists to understand more about how dimerization among the Bcl-2 family proteins is controlled.

The domains within Bcl-2 and its homologues that are required for dimerization have been determined by deletional and mutational analysis, and these results were recently corroborated by X-ray crystallographic and NMR-based structural studies (*4, 5, 7*−*15*). The 3-dimensional structure of the Bcl-X_L protein consists of seven α-helices joined by flexible loops of variable length (*14*). Amino acid sequence alignments of Bcl-2 family proteins have demonstrated up to four evolutionarily conserved domains, termed Bcl-2 homology (BH) domains: BH1, BH2, BH3, and BH4. The BH4 and BH3 domains correspond to the first and second amphipathic α-helices in these proteins, as predicted from the 3-dimensional structure of Bcl-X_L (*14*). The BH1 domain begins within a loop located upstream of the fifth α-helix in Bcl-X_L and extends partially into this α-helix. The BH2 domain corresponds to the latter portion of the sixth α-helix and loop which follows.

The BH1, BH2, and BH3 domains in combination form the borders of a hydrophobic pocket located on the surface of the Bcl-X_L protein. Mutation of particular residues lining this pocket has been shown to abolish dimerization (*7, 12*). Thus, this surface pocket appears to function analogous to a receptor, binding regions located on partner proteins that dimerize with Bcl-2 and Bcl-X_L. In contrast, the BH3 domain by itself is sufficient to insert into the surface pocket created by the combination of BH1, BH2, and BH3, perhaps serving as a peptide-ligand that mediates dimerization among Bcl-2 family proteins (*5, 11, 13, 15*−*18*). This finding implies that at least some Bcl-2 family proteins could exist in two states: one in which the protein creates a receptor-like pocket and the other in which the amphipathic α-helix that comprises BH3 rotates outward to expose its hydrophobic surface which then buries into the receptor-like pocket on dimerization partner proteins (*15*).

Some pro-apoptotic members of the Bcl-2 family, including Bid, Hrk, and Bik, contain only a BH3 domain (*4, 5, 13*). Deletion of the BH3 domains from these proteins uniformly abolishes dimerization with other members of the family and nullifies their function as inducers of cell death. Thus, the BH3 domain is apparently sufficient to modulate the functions of anti-apoptotic Bcl-2 proteins such as Bcl-2

† This work was supported by CaP-CURE and the California Breast Cancer Research Program (1RB-0093).

* Address correspondence at 619-646-3140 (phone), 619-646-3194 (fax), jreed@burnham-institute.org (e-mail).

S0006-2960(97)03052-3 CCC: $15.00
Published on Web 04/15/1998

and Bcl-X_L. It has not been determined whether these "BH3-only" members of the Bcl-2 family must undergo conformational changes to expose the hydrophobic face of their BH3 domains for insertion into the pockets on Bcl-2 and Bcl-X_L.

An intriguing characteristic of many Bcl-2 family proteins is their predicted structural similarity to the pore-forming domains of bacterial toxins such as diphtheria toxin (DT) and the colicins (*14*). Though the 3-dimensional structure has been determined thus far only for Bcl-X_L, both anti-apoptotic proteins such as Bcl-2 and pro-apoptotic proteins such as Bax can be modeled easily on the same crystallographic coordinates, suggesting they share overall structural similarity (*19*). Consistent with these ideas, recombinant Bcl-2, Bcl-X_L, and Bax proteins have been shown to form ion-conducting channels in vitro in both liposomes and planar bilayers (*20*−*23*). In contrast, most of the BH3-only subgroup of Bcl-2 family proteins do not appear to share the same fold with Bcl-X_L, implying that they lack pore-forming capability (unpublished observations).

By analogy to the bacterial toxins, it has been speculated that the process of pore formation by Bcl-2 family proteins involves the membrane insertion of two α-helices normally buried in the interior of the compact folded protein. Indeed, deletion of these two hydrophobic core α-helices (α5 and α6) abolishes channel formation by Bcl-2 in vitro and destroys its ability to block cell death induced by Bax in mammalian cells and yeast (*21*). The process of channel formation in vitro by Bcl-2 family protein and the pore-forming domains of their structurally related bacterial toxins is highly pH dependent, with optima typically of pH ~4.0 (*20*−*23*). Thus, acidic pH has been speculated to facilitate a conformational change in Bcl-2 family proteins which allows them to insert the putative pore-forming α5 and α6 helices perpendicularly into the lipid bilayer.

How the process of channel formation may be related to the ability of many Bcl-2 family proteins to homo- or heterodimerize remains unknown. The structure of Bcl-X_L reveals only two α-helices of sufficient length and hydrophobicity to span the lipid bilayer (α5 and α6). Consequently, it has been proposed that the minimum stoichiometry for a Bcl-X_L or Bcl-2 channel is a dimer of membrane-integrated proteins with each contributing a pair of α-helices to the channel (*21*). This reasoning derives from previous attempts to create channels in vitro using synthetic amphiphatic peptides, which revealed a four α-helix bundle as the minimum structure necessary to create an ion channel in vitro (*24*, *25*). Since in vitro channel formation in liposomes is dependent on low pH, it is important to understand how pH might influence dimerization among Bcl-2 family proteins.

In this report, we employed surface plasmon resonance (SPR)[1] (*26*−*30*) to characterize the kinetics of interactions of Bcl-X_L with several other members of the Bcl-2 family, including the anti-apoptotic protein Bcl-2, the pro-apoptotic protein Bax, and the pro-apoptotic BH3-only protein Bid. The findings suggest the existence of different conformational states which can markedly affect the dimerization properties of these proteins and show that acidic pH favors dimerization among these proteins primarily by slowing their rates of dissociation.

MATERIALS AND METHODS

Production and Purification of Recombinant Bcl-2 Family Proteins. The construction of most plasmids used for expression of Bcl-2 family proteins in bacteria has been described (*10*, *21*, *31*). For production of a mutant of Bcl-2 lacking the BH3 domain (Δ93−107), a two-step PCR approach was employed using pET-21a-Bcl-2 (ΔTM) (*21*) as the DNA template and two pairs of primers: (1) 5′-GCGGAATTCATGGCGCACGCTGGGAGAACA-3′ with 5′-CACAGGTGGCACCGGGCTGAGCGCAGG-3′; and (2) 5′-GTGCCACCTGTGTACCGCCGCGACTTCGCCGA-GATG-3′ with 5′-CGCCTCGAGTCACTTCAGAGACAGC-CAGGAGAAATC-3′. The two resulting PCR products were gel purified and mixed, and PCR was performed again using the outer primers, followed by digestion with *Eco*RI and *Xho*I. The resulting fragment was subcloned into pET-21a. All protein preparations were >95% pure, as determined by Coumassie staining of SDS−PAGE gels.

His_6-Tagged Proteins. His_6-human Bcl-2 (1−218), Bcl-2 (ΔBH3), and human Bcl-X_L (1−211) were expressed with an N-terminal His_6-tag using a modified pET vector (Novagen, Inc.) that removed the T7 protein 10 sequences (*32*), thus excluding any additional amino acids between the His_6 and first methionine of Bcl-2 and Bcl-X_L. Both proteins were expressed in BL21(DE3) cells. Briefly, a single colony was inoculated into 1 L of LB media containing 50 μg/mL ampicillin and grown at 37 °C overnight. The culture was then diluted by half with fresh LB/ampicillin and cooled to room temperature for an hour, before inducing with 1 mM IPTG for 6 h at ~25 °C.

For purification of His_6−Bcl-2 and His_6−Bcl-2 (ΔBH3), cells from 1 L of culture were resuspended into 50 mL of 50 mM phosphate buffer (pH 6.8), 150 mM NaCl, and 1% (v/v) Tween 20 and then incubated with 0.5 mg/mL lysozyme at 25 °C for 0.5 h, followed by sonication to reduce viscosity. After centrifugation at 27500*g* for 10 min, the resulting pellets were washed twice with the same buffer and solubilized in 50 mM phosphate-buffered (pH 6.8) 6 M guanidinium-hydrochloride (GuHCl). Supernatants were collected and incubated with 10−20 mL of nickel resin (Qiagen, Inc.) at 4 °C for 3 h. The resin was washed with 50 mM phosphate-buffered (pH 6.8) 25 mM imidazole, 4 M GuHCl, and 0.1% Tween until the OD_{280} reached ≤0.01, followed by continued washing with 5 vol of 50 mM phosphate-buffered (pH 6.8) 25 mM imidazole and 4 M GuHCl. Proteins were eluted in 0.2 M acetic acid and 4 M GuHCl. Eluted His_6−Bcl-2 and His_6−Bcl-2 (ΔBH3) proteins were dialyzed against 25 mM acetic acid at 4 °C overnight, passed through 0.22 μm Whatmann filters and stored at −20 °C.

His_6−Bcl-X_L was purified under native conditions. Briefly, after sonication, the supernatant was incubated with 20 mL of nickel resin in 50 mM phosphate-buffered (pH 6.8) 150 mM NaCl, 1% Tween, and 25 mM imidazole at 4 °C for 3 h. The resin was washed with 50 mM phosphate-buffered (pH 6.8) 150 mM NaCl, 0.1% Tween, and 25 mM imidazole until the OD_{280} reached ≤0.01. His_6−Bcl-X_L was eluted with 250 mM imidazole in same buffer, followed by further purification by FPLC on a Mono Q (HR 10/10) column

[1] Abbreviations: RU, response units; TM, transmembrane; SPR, surface plasmon resonance.

(Pharmacia) using a linear gradient of 0.5 M NaCl at pH 8.0.

GST-Fusion Proteins. The GST-Bcl-X_L (1−211), GST-mouse Bax (1−171), and GST-mouse BID proteins were expressed in XL-1 Blue cells (Stratagene, Inc.) from the plasmids pGEX-4T-1 (*10, 31, 33*). Briefly, cells were grown in 2 L of LB with 50 μg/mL ampicillin at 37 °C to an OD_{600nm} of 1.0. IPTG (0.4 M) was then added, and cultures were incubated at 25 °C for 6 h. Cells were then recovered and incubated with 0.5 mg/mL lysozyme in 50 mM Tris (pH 8.0), 150 mM NaCl, 1% Tween, 0.1%, 2-mercaptoethanol, 5 mM EDTA, 1 mM PMSF, and a mixture of other protease inhibitors (Boehringer 1697498) at room temperature for 0.5 h, followed by sonication (*21*). Cellular debris was pelleted by centrifugation at 27500*g* for 10 min, and the resulting supernatants were incubated with 30 mL of glutathionine-Sepharose (Pharmacia) at 4 °C for 4 h. The resin was washed with 20 mM Tris (pH 8.0), 150 mM NaCl, 0.1% Tween, and 0.1% 2-mercaptoethanol until the OD_{280nm} reached ≤0.01. For removal of GST, the resin containing bound GST-fusion proteins was incubated with 10 units of thrombin (Boehringer, Inc.) at 4 °C in 20 mM Tris (pH 8.0), 150 mM NaCl, 0.1% 2-mercaptoethanol, 0.1% Tween 20, and 2.5 mM $CaCl_2$ overnight, and the released Bcl-X_L and Bax were then purified on Mono Q (HR 10/10) by FPLC using a linear gradient of 0.5 M NaCl at pH 8.0. BID was purified on Mono S (HR 10/10) using a linear gradient of 0.5 M NaCl at pH 5.0.

Gel-Filtration Chromatography. Purified protein samples (20−50 μg in 50 μL) were injected into a Superdex 200 column (HR 10/30) (Pharmacia) which had been equilibrated with various buffers as described in the text. Chromatography was performed using a flow rate of 0.8 mL/min by FPLC, monitoring absorbance at OD_{280nm}. A mixture of proteins that served as molecular weight markers (Bio-Rad) was used for column calibration.

Surface Plasmon Resonance. Kinetic measurements were performed using a BIAcore-II instrument with CM5 sensor chips and an Amine Coupling Kit (Pharmacia Biosensor AB, Sweden). For immobilization of proteins, the sensor chip was equilibrated with HB flow buffer [10 mM Hepes (pH 7.4), 150 mM NaCl, and 3.4 mM EDTA] at 5 μL/min, then activated by injecting 17 μL of 0.2 M *N*-ethyl-*N*′-(3-diethylaminopropyl)-carbodiimide and 0.05 M *N*-hydroxysuccinimide (NHS/EDC) followed by a 35 μL injection of Bcl-2 family or control proteins at 50−100 ug/mL in 10 mM acetate, pH 3.5−4.8. Excess NHS-esters on the surface were deactivated with 17 μL of 1 M ethanolamine-hydrochloride (pH 8.5). After immobilization, 10 μL of regeneration buffer [50 mM phosphate (pH 6.8) and 4 M GuHCl] was injected to remove noncovalently bound dimers.

For studying protein−protein interactions, kinetic data were obtained by diluting the samples in interaction buffer [HB buffer for neutral pH experiments, AB buffer consisting of 50 mM acetate (pH 4.0), 150 mM NaCl, and 3.4 mM EDTA, for low pH experiments] and injecting 20 μL at 10 μL/min across the prepared surface. The surface was regenerated after each injection with 5 μL of 50 mM phosphate (pH 6.8) and 4 M GuHCl. The rate constants k_{ass} and k_{diss} were calculated from the association and dissociation phases of the sensorgrams. The apparent affinity constants K_D were calculated directly from the kinetic parameters (k_{diss}/k_{ass}), while K_D(eq) was determined by Scatchard analysis, using the BIAcore software package (Pharmacia).

Peptides. A synthetic peptide corresponding to the BH3 domain of murine Bax (residues 57−72) with a Cys → Ser substitution (NH_2-KKLSESLKRIGDELDS-amide) or various control peptides were purchased from Chiron, Inc. and purified by C18 reverse phase HPLC to >90% purity.

BisANS Fluorescence. BisANS (4,4′-dianilino-1,1′-binaphthyl-5,5′-disulfonic acid) (Sigma, D4162) was diluted into 40 mM buffer (Tris-HCl, pH 8.0; Sodium phosphate, pH 7.0 or pH 6.0; Sodium acetate, pH 5.0, 4.0, or 3.0; or Gly-HCl, pH 2.5), 150 mM NaCl, and 3.4 mM EDTA to final concentration of 9.5 μM, without or with ~0.2 μM Bcl-X_L. Samples were incubated at room temperature for 0.5 h. Fluorescence intensity was measured at 490 nm following excitation at 294 nm using a 5 nm slit width in a luminescence spectrometer (Perkin-Elmer LS50B). Recorded data were plotted against pH (*34*). Fluorescence intensities were corrected for buffer effects by subtraction of the appropriate blank.

Circular Dichroism. Circular dichroism measurements were carried out using a JASCO-J600 spectropolarimeter equipped with a temperature control accessory and calibrated with d_{10}-camphor sulfonate. Spectra were taken using cells of 1 mm path length, and recorded in 0.5 nm wavelength increments with a 2 s time constant and a full-scale sensitivity of 50 mdeg. Each spectrum is the average of four scans corrected for background solvent effects by subtraction of the appropriate blank. Bcl-X_L was dissolved in 20 mM DMG (dimethyl glutaric acid) and 150 mM NaCl, pH 4.0 or 7.0. To monitor changes in secondary structure, spectra were scanned in the far-UV from 200 to 250 nm. A value of 110 Da for the mean residue molecular weight was used in the calculation of the mean residue ellipticity, [Θ].

RESULTS

SPR Analysis of Bcl-2 Family Protein Interactions at Neutral pH. Using SPR, we evaluated the kinetics of interactions among recombinant purified His_6−Bcl-2, His_6−Bcl-X_L, Bax, and Bid. Most Bcl-2 family protein are anchored in intracellular membranes via a stretch of hydrophobic amino acids that constitutes a transmembrane (TM) domain (reviewed in ref *35*). For solubility purposes, these proteins were produced without their C-terminal ~20 amino acids and purified to homogeneity (Figure 1).

Attempts to flow each of these proteins across dextran chips demonstrated that all but Bcl-X_L exhibited nonspecific interactions with the chip surface at low pH (data not shown). Therefore, Bcl-X_L was employed in the mobile phase for all SPR experiments, with Bcl-2, Bax, and Bid each immobilized on the chip surface. Bcl-X_L exhibited specific interactions with all Bcl-2 family proteins tested. Figure 2A, for example, shows typical sensorgrams obtained for interaction of immobilized Bcl-2 with various concentrations of Bcl-X_L in the mobile phase. When flowed over immobilized Bcl-2 chips in 150 mM NaCl solution at neutral pH, Bcl-X_L exhibited rapid binding until a steady-state equilibrium was reached, followed by rapid dissociation when the Bcl-X_L-containing mobile phase was replaced with flow buffer. The RU plateau obtained increased in a concentration-dependent

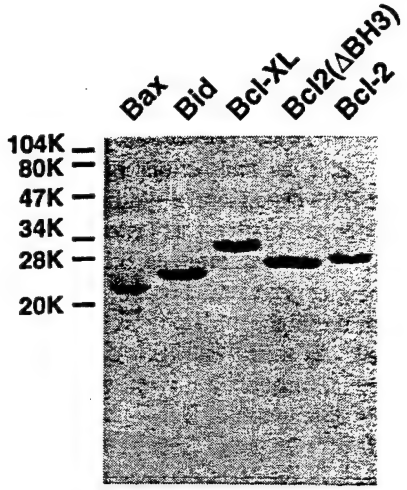

FIGURE 1: SDS−PAGE analysis of purified proteins. The purified human Bcl-2 (1−218), human Bcl-X_L (1−213), mouse Bax (1−171), and mouse Bid proteins were analyzed by SDS−PAGE (10 μg/lane in 12% gels) and stained with Coomassie. Molecular weight markers are indicated.

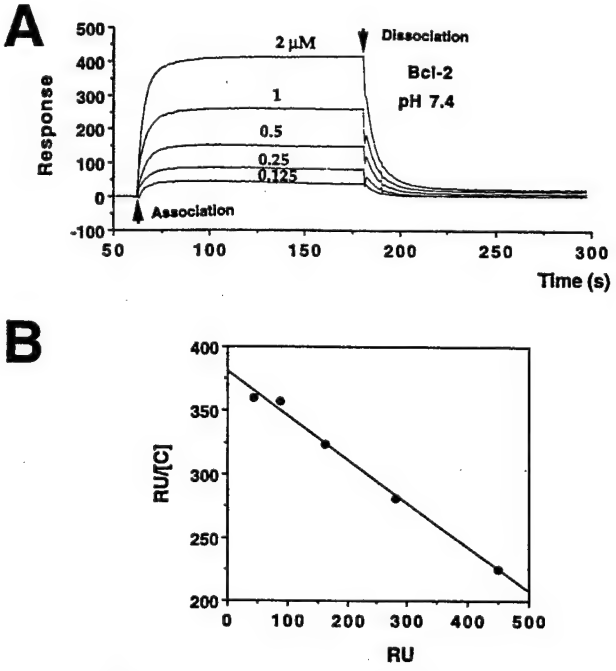

FIGURE 2: SPR analysis of Bcl-X_L interaction with Bcl-2. In panel A, typical sensorgrams are presented where various concentrations of Bcl-X_L (0.125, 0.25, 0.5, 1.0, and 2.0 μM, bottom to top) were flowed over a chip containing immobilized Bcl-2 protein (~5000 RU) at pH 7.4 in 150 mM NaCl and 3.4 mM EDTA. Bcl-X_L containing solution was applied at 10 μL/min. The binding and subsequent dissociation upon switching to flow buffer without Bcl-X_L were recorded. The chip was regenerated with 5 μL of 4 M GuHCl buffered with 50 mM sodium phosphate (pH 6.8). In panel B, a Scatchard plot of the equilibrium binding results is presented, using the plateau phase of the sensorgrams (RU) produced by flowing various concentrations [C] of Bcl-X_L over the Bcl-2-containing chip. The dissociation constant was estimated to be 2.8 μM ($1/K_a$) for this interaction.

manner. Essentially no binding of Bcl-X_L was detected by SPR when using dextran-control chips or certain mutants of Bcl-2 (see below).

Scatchard analysis of the data was performed by plotting RU/[C] versus RU for each concentration of Bcl-X_L used in the mobile phase (Figure 2B). A linear relationship between concentration and RU was observed for each of the immobilized Bcl-2 family proteins tested, including Bcl-2, Bax, and Bid, consistent with pseudo-first-order kinetic interactions. Figure 2B provides an example, showing the results obtained for Bcl-2/Bcl-X_L. The slopes of these plots were derived to obtain an apparent K_D for each protein−protein interaction at pH 7.4 in 150 mM NaCl (Table 1). On the basis of this analysis, the highest affinity interaction was obtained when using Bid in combination with Bcl-X_L, but all the apparent K_D values were within ~3-fold of each other (1.9−5.7 uM). Similar results were obtained using mobile-phase solutions containing nonionic detergents (0.1% Tween 20) and divalent cations (10 mM $MgCl_2$) (not shown). The rapid rate of dissociation made it difficult to accurately estimate K_D from kinetic data (k_d/k_a).

Table 1: Characteristics of Bcl-X_L Interactions with Bcl-2 Family Proteins

	K_D (μM)			kinetics (pH 4.0)		
	pH 7.4	pH 4.0	ΔK_D	k_a (μM^{-1} s^{-1})	k_d (s^{-1})	K_D (μM)
Bcl-XL/Bcl-2	2.8	0.16	18	0.32	0.05	0.16
Bcl-XL/Bax	4.6	0.11	42	0.34	0.04	0.12
Bcl-XL/Bid	1.9	0.03	63	0.32	0.009	0.03
Bcl-XL/Bcl-XL	5.7	0.42	14	0.27	0.12	0.44

Low pH Enhances Interactions among Bcl-2 Family Proteins. Under acidic conditions in vitro, the Bcl-2, Bcl-X_L, and Bax proteins can insert into lipid membranes, forming ion channels (*20*−*22*). Presumably, the dependence on low pH for this phenomenon reflects the need for a conformational change that allows the putative pore-forming fifth and sixth α-helices of these proteins to penetrate the lipid bilayer. To determine how low pH affects heterodimerization among Bcl-2 family proteins, we examined the kinetics and magnitude of binding of Bcl-X_L with immobilized Bcl-2, Bax, Bid, and Bcl-X_L by SPR over a range of pH values (2.5−8.0). The amount of Bcl-X_L interacting with chips containing immobilized Bcl-2 family proteins (as determined by RU) increased as the pH of the flow solution was lowered to pH 4.0, beyond which reduced interactions were observed. Figure 3A shows an example of sensorgrams obtained for the interaction of Bcl-X_L with immobilized Bcl-2 at various pHs, using fixed concentrations of Bcl-X_L in the flow solution and constant amounts of Bcl-2 on the chip. Maximum binding was obtained at pH 4.0 (Figure 3). The paucity of binding at neutral pH in this experiment can be attributed to the usage of 5-fold less Bcl-X_L compared to the previous experiments shown in Figure 2, where the binding was conducted at pH 7.4. The specificity of the enhanced interactions detected at lower pH between Bcl-X_L and immobilized Bcl-2 family proteins was confirmed by use of control proteins such as Bcl-2 (ΔBH3) in which the BH3 domain has been deleted, thus preventing its dimerization with other Bcl-2 family proteins (Figure 4).

Kinetic Analysis of Bcl-2 Family Interactions at Low pH Reveals a Slower Rate of Dissociation. The kinetics of Bcl-X_L binding to chips containing immobilized Bcl-2 family proteins were studied by SPR in experiments where various concentrations of Bcl-X_L were flowed over chips at pH 4.0. Figure 4 presents typical sensorgrams for chips coated with Bcl-2, Bax, Bid, and Bcl-X_L, as well as for control chips lacking an immobilized protein or containing Bcl-2 (ΔBH3) protein. In all cases, concentration-dependent binding of Bcl-

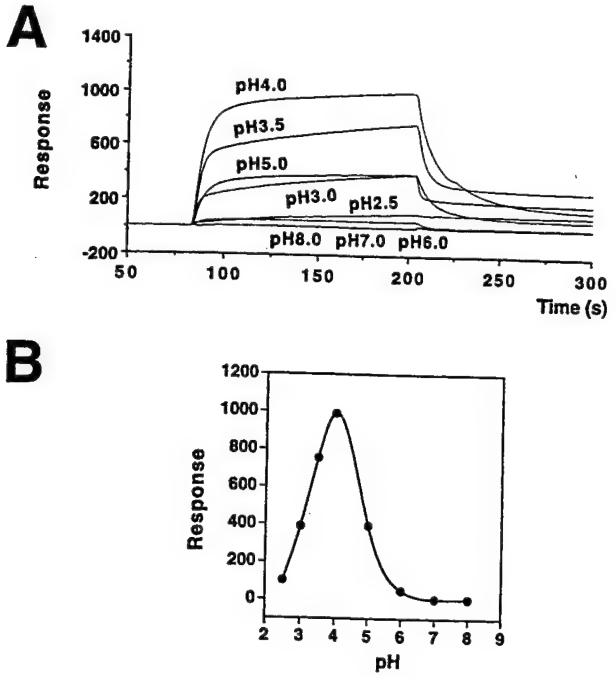

FIGURE 3: pH dependence of Bcl-X_L interactions with Bcl-2. In panel A, representative sensorgrams are presented for Bcl-X_L (soluble phase) binding to immobilized Bcl-2 at various pHs as indicated (2.5−8.0). The Bcl-2 containing chip (~5000 RU) was equilibrated with various interaction buffers, all containing 150 mM NaCl and 3.4 mM EDTA, with 50 mM of either Tris [pH 8.0], sodium phosphate (pH 6.0, 7.0), sodium acetate (pH 3.0, 3.5, 4.0, 5.0), or Gly-HCl (pH 2.5). Bcl-X_L (~0.4 uM) was injected at 10 μL/min and the binding recorded. After reaching steady state, flow over the chip was continued without Bcl-X_L. In panel B, the maximum RU obtained for binding of Bcl-X_L to the Bcl-2 chip at each pH was plotted, arbitarily normalized relative to the results obtained for pH 8.0.

X_L was observed, with rapid initial binding, which then gradually slowed until a plateau or near plateau steady-state equilibrium was reached. Comparisons with measurements performed at pH 4.0 revealed that the association-phase kinetics for these binding events were not substantially different from those obtained at pH 7.4. In all cases, however, the dissociation rates appeared to be markedly slower at pH 4.0. The binding of Bcl-X_L to Bid-containing chips was the most stable of the protein−protein interactions tested, exhibiting a very slow rate of dissociation at pH 4.0 (Figure 4).

To directly compare the relative dissociation rates at pH 4.0 with 7.4, Bcl-X_L was flowed over either a Bid or a Bcl-2 chip at pH 4.0, and binding was allowed to proceed until equilibrium was reached, then the mobile phase was switched to either pH 4.0 or 7.4 without Bcl-X_L protein. As shown in Figure 5, dissociation of Bcl-X_L from either immobilized Bcl-2 or Bid was considerably slower at pH 4.0 compared to pH 7.4. Though the rapid rate of dissociation at pH 7.4 precluded accurate determination, the estimated k_d values were roughly 15-fold lower for Bcl-2/Bcl-X_L (0.05 μM/s versus 0.74 μM/s) and ~60-fold lower for Bcl-X_L/Bid (0.009 μM/s versus 0.55 μM/s).

Table 1 contrasts the apparent equilibrium dissociation constants for Bcl-X_L binding to Bcl-2, Bax, Bid, and Bcl-X_L at pH 4.0 and 7.4. The apparent K_D for Bcl-X_L dimerization with all proteins tested was ~14 to ~63 times lower at pH 4.0 compared to pH 7.4, indicating a substantially higher affinity interaction at lower pH.

BH3 Domain Dependence of Interactions of Bcl-X_L with Other Bcl-2 Family Proteins. Previous studies have demonstrated that dimerization among Bcl-2 family proteins depends on insertion of the BH3 domain of one partner into a surface hydrophobic pocket on the other (*15*). To determine whether the interactions measured here by SPR at low pH are BH3 dependent, a synthetic peptide representing the BH3 domain of Bax was tested for ability to inhibit binding of Bcl-X_L to immobilized Bid at pH 4.0. Bid was chosen for these experiments because its binding to Bcl-X_L occurred with the highest affinity among the Bcl-2 family proteins tested. As shown in Figure 6, addition of a 16 mer BH3 Bax peptide produced a concentration-dependent inhibition of the interaction of Bcl-X_L with immobilized Bid, with an IC50 of ~25 μM. Similar results were obtained when the effects of the BH3 domain peptide were tested on interactions of Bcl-X_L with Bcl-2 and Bax (data not presented). A variety of unrelated non-BH3 peptides however had little or no effect (Figure 6 and data not shown).

Size-Exclusion Chromatography Analysis of Bcl-X_L Suggests Induction of a Conformational Change at Low pH. Size-exclusion chromatography was used to compare the state of the Bcl-X_L protein at neutral and low pH, making comparisons with the BH3-only protein Bid. When chromatographed on Superdex 200 at either pH 7.4 or 4.0, Bcl-X_L eluted as a single peak corresponding to monomeric protein (Figure 7A and data not shown). Similar results were obtained with Bid at pH 7.4 and 4.0, which also was present as a monomer. Thus, low pH does not promote oligomerization of Bcl-X_L or Bid.

When nonionic detergent (0.1% Tween 20) was included during chromatographic analysis of Bcl-X_L on Superdex 200 at pH 7.4, some Bcl-X_L eluted at higher molecular weight (Figure 7B), in addition to the monomeric Bcl-X_L seen previously at neutral pH in the absence of detergent. At pH 4.0 in the presence of detergent, the majority of the Bcl-X_L eluted from the column as a larger complex (Figure 7C). In contrast, the Bid protein continued to behave as a monomer when analyzed by gel-sieve chromatography even at low pH and in the presence of detergent. Since the large complexes of Bcl-X_L were not observed when the detergent was absent (not shown), we interpret this pH and detergent-dependent alteration in the chromatographic behavior of Bcl-X_L as evidence either that Bcl-X_L associates with detergent vesicles at pH 4.0 or that the combination of low pH and detergent promotes conformational changes in Bcl-X_L that allow it to oligomerize. The observation that Bid does not exhibit this altered behavior is consistent both with its predicted lack of structural similarity to pore-forming proteins and its reported inability to homodimerize (*5*). Interestingly, it has recently been reported that nonionic detergents can induce dimerization among members of the Bcl-2 family as a post-cell-lysis event (*36*).

BisANS Fluorescence Studies Indicate Exposure of Hydrophobic Regions of Bcl-X_L at Low pH. The fluorochrome BisANS associates with hydrophobic regions on proteins, such that the extent of emissions at 490 nm is an indication of the relative hydrophobicity of a protein (*34*). We therefore compared the BisANS labeling of Bcl-X_L over the pH range of 2.5−8.0. As shown in Figure 8, the relative amount of BisANS association with the Bcl-X_L protein increased at pH <6.0, reaching a maximum at pH 3.0−4.0. Over the same

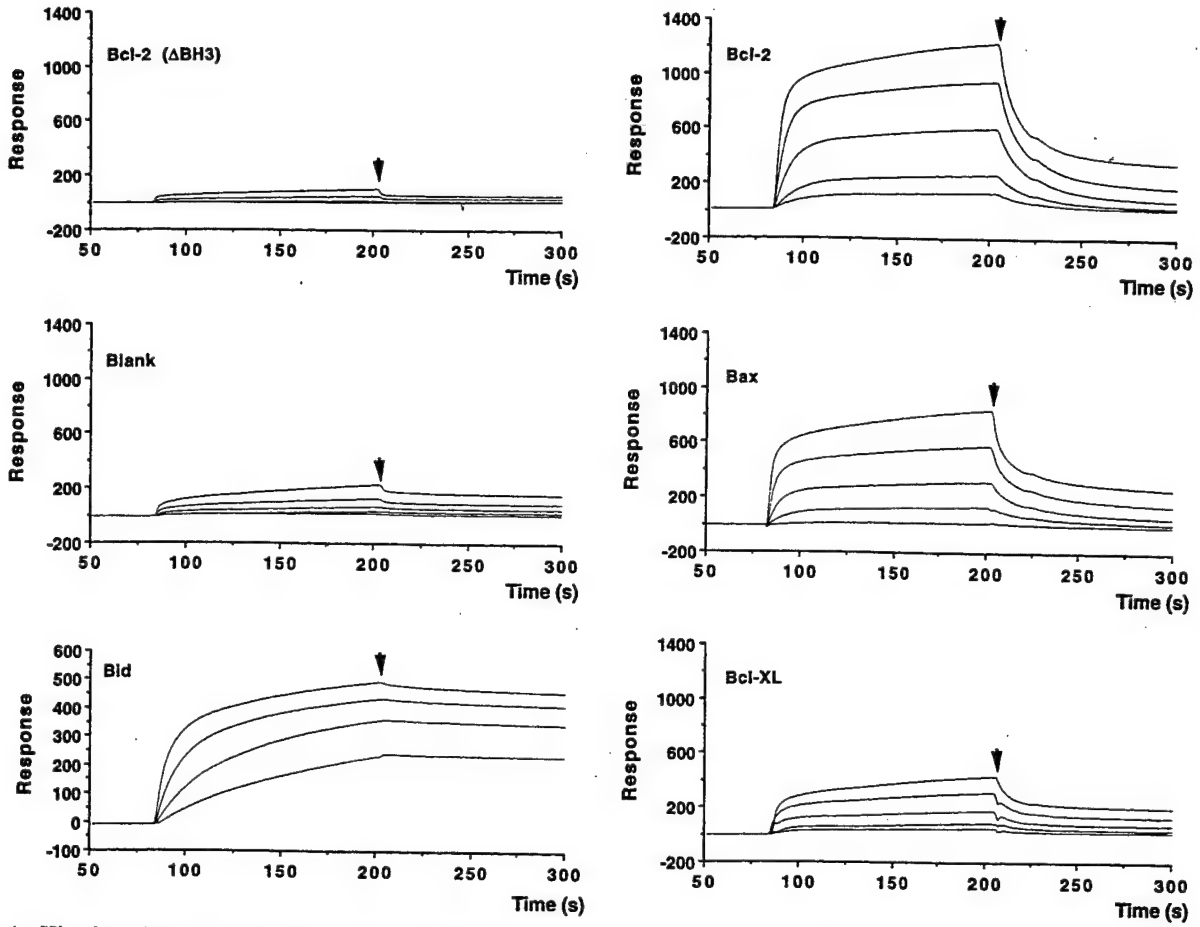

FIGURE 4: Kinetics of Bcl-X_L interactions with other Bcl-2 family proteins at acidic pH. SPR analysis was conducted at pH 4.0, flowing Bcl-X_L at various concentrations over chips containing immobilized Bcl-2, Bax, Bid, Bcl-X_L, or Bcl-2 (ΔBH3) (~5000 RU). Alternatively, the chip was inactivated with ethanolamine to block reactive groups and Bcl-X_L was flowed over the blank chip. Bcl-X_L at ~50−750 nM was injected (20 μL) at a flow rate of 10 μL/min. The binding and dissociation were recorded. The chip was regenerated using 5 μL of 4 M GuHCl containing 50 mM Sodium phosphate (pH 6.8) after each injection.

pH range, the basal fluorescence from BisANS was stable. Thus, acidic pH in the 3.0−4.0 range appears to induce the Bcl-X_L protein to undergo conformational changes which result in exposure of hydrophobic surfaces of this protein.

Circular Dichroism Analysis of Bcl-X_L and Bax Proteins Indicates Retention of Overall Secondary Structure at Low pH. One concern with studies of Bcl-2 family proteins performed at pH 4.0 is whether they become denatured and thus nonspecifically adsorb to each other or expose hydrophobic regions. To address this concern, circular dichroism (CD) analysis was performed for Bcl-X_L and Bax at pH 4.0 and 7.0, using the far-UV region which is sensitive to secondary structure. The far-UV CD spectra for these proteins were nearly superimposable at pH 4.0 and 7.0, indicating retention of their overall α-helical content and secondary structure. Figure 9, for example, shows the far-UV spectra for Bcl-X_L at pH 4.0 and 7.0. Note the retention of the absorption minima at 208 and 222 nm at pH 4.0, which is characteristic of α-helical proteins. These data therefore argue that the secondary structure of this protein is preserved at low pH, implying that acidic pH does not denature Bcl-2 family proteins.

DISCUSSION

The data presented here provide the first kinetic analysis of dimerization among Bcl-2 family proteins. Consistent with previous studies, the protein−protein interactions detected by SPR analysis appear to be dependent on the BH3 domain, based on the observations that: (a) deletion of the BH3 domain from Bcl-2 abolished its interactions with Bcl-X_L and (b) a BH3 peptide abrogated binding in SPR experiments. Interestingly, at acidic pH, the relative affinity of interactions among Bcl-2 family proteins was increased. The basis for this increased affinity was attributable primarily to a markedly reduced dissociation rate. Thus, Bcl-X_L complexes with Bcl-2, Bax, or Bid were considerably more stable at pH 4.0 than at pH 7.0−7.4.

The molecular basis for the increased stability of Bcl-X_L complexes with Bcl-2, Bax, and Bid could have several explanations. First, protonation of specific residues directly involved in binding could increase the stability of these protein complexes, perhaps by reducing electrostatic repulsions or increasing hydrophobicity and thus promoting hydrophobic interactions. Second, low pH could promote or stabilize a conformational change in these proteins which then indirectly affects binding. Third, acidic pH could help to decrease the rigidity of Bcl-X_L and other Bcl-2 family proteins, loosening their α-helical segments from intramolecular interactions with each other and creating more flexibility for dimerization. In this regard, Bcl-X_L and the structurally similar pore-forming domains of the colicins and diphtheria toxin are proposed to assume a molten globule state which allows them the flexibility to transition back and forth from tight compact α-helical bundle structures in

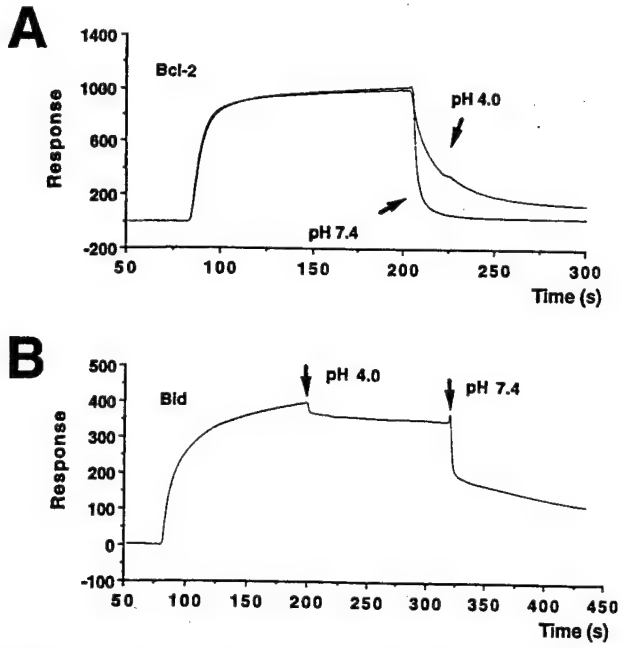

FIGURE 5: Acidic pH decreases rate of dissociation of Bcl-X_L from Bcl-2 family proteins. Bcl-X_L protein (~0.4 uM) in Sodium acetate (pH 4.0), 150 mM NaCl, and 3.4 mM EDTA was flowed across chips containing either immobilized (A) Bcl-2 or (B) Bid protein (~5000 RU) and binding was allow to proceed until steady state was reached. Dissociation was then monitored at pH 4.0 by continuing flow of the same solution or at pH 7.4 by switching to phosphate-buffered (pH 7.4) saline/EDTA solution. In panel B, dissociation was initiated at pH 4.0, and then the buffer was switched to pH 7.4 at the indicated time (arrow).

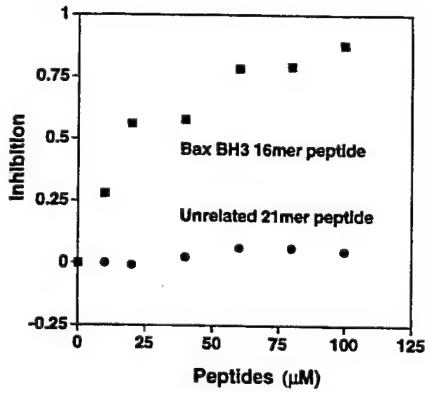

FIGURE 6: BH3 domain dependence of Bcl-X_L dimerization with other Bcl-2 family proteins. Bcl-X_L (~0.3 μM) alone or in combination with various concentrations of either 16 mer Bax BH3 peptide or unrelated 21 mer was flowed over a Bid-containing chip (~1500 RU) at pH 4.0. Injections were performed using 20 μL of Bcl-X_L solution at 10 μL/min, with regeneration in 4 M GuHCl (pH 6.8) between injections.

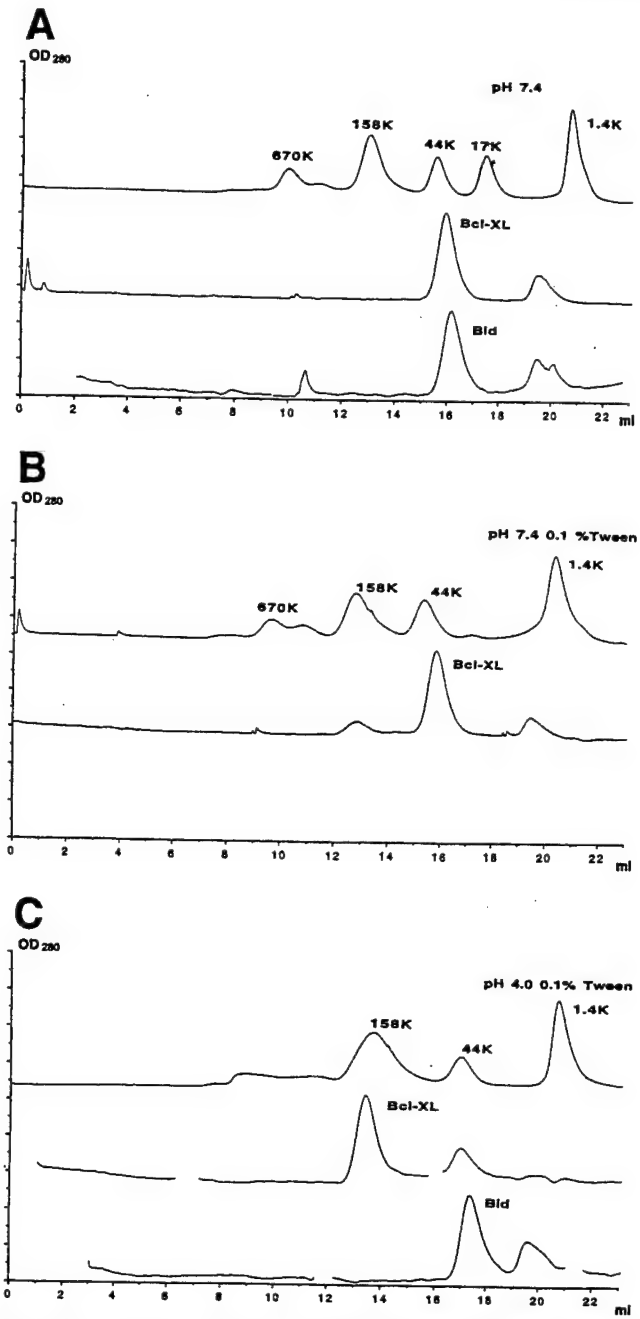

FIGURE 7: Analysis of Bcl-X_L and Bid at acidic and neutral pH by gel-filtration chromatography. Bcl-X_L or Bid protein (25 μg in 50 μL) was applied to a Superdex 200 (10/30) column previously equilibrated with 10 mM HEPES (pH 7.4), 150 mM NaCl, and 3.4 mM EDTA without (A) or with 0.1% (v/v) Tween 20 (B). Alternatively, chromatography was performed in 50 mM Sodium acetate [pH 4.0], 150 mM NaCl, and 3.4 mM EDTA with 0.1% Tween 20 (C). The locations of the protein standards are indicated at the top of each panel.

aqueous environments to membrane inserted molecules with much looser packing of their α-helices (*37*, *38*). Consistent with the requirement of the molten globule state, our CD analysis suggested no changes in overall α-helical content of Bcl-X_L when compared at pH 4.0 and 7.0–7.4, implying a preservation of secondary structure.

It should be emphasized that the affinities (K_D) and kinetic constants (k_a, k_d) obtained here by SPR are merely apparent values (*28*). For the purpose of these studies, the importance of the determined K_D and rate constants permits comparisons of the *relative* changes in K_D and in association and dissociation rates at acidic versus neutral pH. For example, the relative affinity of Bcl-X_L/Bid heterodimerization at pH 4.0 compared to pH 7.0 was estimated by SPR to be ~63-fold greater (ΔK_D), whereas Bcl-X_L/Bcl-X_L homodimerization was only ~14-fold greater at pH 4.0. Hence, acidic pH has a greater impact on stabilizing Bcl-X_L/Bid complexes than Bcl-X_L/Bcl-X_L complexes. Consistent with these data, Bcl-X_L migrated predominantly as a monomer in gel-sieve chromatography experiments even at pH 4.0.

Several lines of evidence support the idea that acidic pH either induces a specific conformational change in Bcl-2 family proteins or loosens the packing of their α-helices,

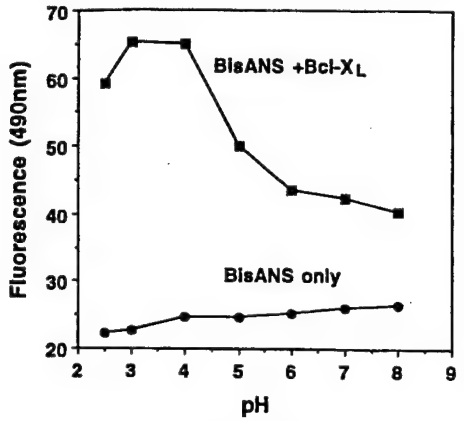

FIGURE 8: pH effects on bisANS binding to Bcl-X_L. BisANS (4,4′-dianilino-1,1′-binaphthyl-5,5′-disulfonic acid) (~10 μM) was mixed with ~0.2 μM Bcl-XL at various pH conditions (50 mM buffer, Tris-HCl, pH 8.0, Sodium phosphate, pH 7.0, pH 6.0, Sodium acetate, pH 5.0, pH 4.0, pH 3.0, Gly-HCl, pH 2.5) in 150 mM NaCl, and 3.4 mM EDTA. Samples were incubated at 25 °C for 0.5 h, and excited at 294 nm. Emission at 490 nm were recorded and plotted against pH.

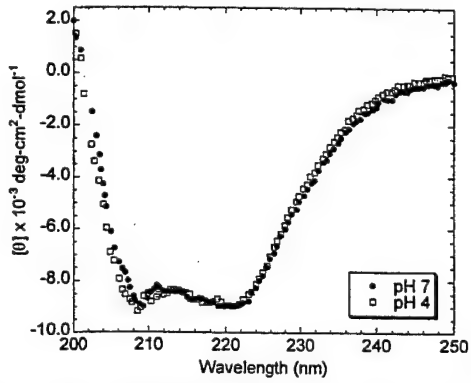

FIGURE 9: Circular dichroism (CD) analysis of Bcl-X_L at pH 4.0 and 7.0. The secondary structure at pH 4.0 and 7.0 was monitored by scanning from 200 to 250 nm in a 1 mm path length cell. Bcl-X_L was dissolved in 20 mM DMG and 100 mM NaCl, pH 4.0 (squares) or 7.0 (circles). Each spectrum represents the average of five scans corrected for background intensity by subtraction of the buffer blank.

thus providing greater flexibility for dimerization. First, recent structural analysis by NMR of BH3 peptides bound to the hydrophobic surface pocket of Bcl-X_L implies a need for a conformation among Bcl-2 family proteins in which the amphipathic α-helix that comprises the BH3 domain is rotated outward to expose its hydrophobic surface for interactions with the hydrophobic pocket on Bcl-X_L (*15*). Second, studies of ion-channel formation by Bcl-X_L, Bcl-2, and Bax using synthetic liposomes have shown that low pH (~4.0) markedly enhances channel activity and indeed is required for converting the bulk of the molecules into a state that is competent to form ion channels in vitro (*20, 21, 23*). By analogy to structurally similar pore-forming domains of bacterial toxins (*39*), channel formation by Bcl-2 and Bcl-X_L is predicted to require insertion of the hydrophobic α5 and α6 helical hairpin perpendicularly into the lipid bilayer, with the surrounding amphipathic α-helices (which include BH3) folding away from the core hydrophobic helices analogous to the opening of an umbrella. This membrane-insertion competent conformation of the protein ("open conformation") is presumably favored by low pH and would presumably extricate the BH3 domain from its normal docking site against the core hydrophobic α5 and α6 helices, freeing it for dimerization with other Bcl-2 molecules that retain the compact α-helical bundle structure ("closed conformation") that creates a hydrophobic pocket on the surface of the protein. Third, comparisons of Bcl-X_L by gel chromatography at neutral and acidic pH in the presence of detergents suggest that low pH induces a conformation which promotes Bcl-X_L association with detergent vesicles or induces its oligomerization. Fourth, labeling with BisANS suggests greater exposure of hydrophobic regions within Bcl-X_L at low pH. Fifth, CD studies indicate no overall change in secondary structure of Bcl-X_L at pH 4.0 compared to pH 7.0, implying that the α-helical regions of the protein remain intact and that a denaturation of the protein cannot account for increased exposure of hydrophobic regions at acidic pH.

The relevance of the enhanced affinity of dimerization seen at acidic pH to the pore-forming activity of Bcl-2 family proteins remains to be determined. When applied to liposomes, the ability of Bcl-2, Bcl-X_L, and Bax to form ion-conducting channels is greatly enhanced by low pH, with optimal pH typically ~4.0 (*20*−*22*). Because dimerization among Bcl-2 family proteins is preserved and even enhanced at low pH, it could be speculated that homodimerization facilitates the process of membrane insertion. In contrast, certain heterodimerization events might impair integration and channel formation at low pH, such as those involving pore-forming Bcl-X_L-like proteins with BH3-only proteins such as Bid. Alternatively, if not altering the actual process of insertion, homodimerization might enhance channel formation by placing two protein molecules in contact with each other once in the membrane. This is because Bcl-X_L contains only two α-helices which are sufficiently long to span the planar bilayer (α5 and α6) (*14*), and yet a minimum of four α-helices integrated into the membrane has been shown to be required for creating ion-conducting channels in vitro (*24, 25*). This implies that at least two Bcl-X_L, Bcl-2, or Bax molecules must collaborate in membranes to create a channel.

Though acidic pH can evidently alter the binding behavior and presumably the conformation of Bcl-X_L and other Bcl-2 family proteins in vitro, the question is what controls these events in vivo? Acidic pH of ~4.0 does not occur within the cytosol of cells, probably not even under pathological situations. However, it may be relevant that many Bcl-2 family proteins are anchored in the outer membrane of mitochondria (*40*). A proton gradient exists across the inner membrane of these organelles, creating an acidic pH environment of ~6.0−6.5 in the space between the inner and outer mitochondria membranes (*41*). The influence of this pH gradient on Bcl-2 family proteins might be most pronounced at the contact sites where the inner and outer membranes abut and where various transport phenomena occur. Interestingly, previous immuno-electron microscopy studies have localized Bcl-2 predominantly to these contact sites (*42*). Thus, while insufficient by itself, the lower pH environment of the mitochondrial intermembrane space may facilitate dimerization among Bcl-2 family proteins.

In addition to local pH effects, interactions with other proteins may also influence dimerization among Bcl-2 family proteins in vivo. In this regard, evidence that Bcl-2 may interact with components of the Hsp70-family of chaperones has been obtained. Specifically, a Hsp70/Hsc70-binding

protein BAG-1 (also known as HAP-1 and RAP46) has been identified which can interact with Bcl-2 and enhance its anti-apoptotic function (*43*−*45*). The implication of these findings is that Bcl-2 can be recognized by Hsc70/BAG-1 complexes, thus providing a potential mechanism for modulating the conformation of Bcl-2 in cells. Other protein interactions with Bcl-2 could also conceivably alter its conformation in ways that might impact on dimerization with Bcl-2 family proteins (reviewed in refs *3* and *35*). Regardless of the in vivo mechanisms involved, the data reported here showing that acidic pH stabilizes dimerization among Bcl-2 family proteins provide insights into the biophysical properties of these proteins which may be relevant to their mechanisms of ion-channel formation.

ACKNOWLEDGMENT

We thank H. Gallant for manuscript preparation, K. Ely, J. Stewart, J. Smith, and D. Hu for helpful discussions.

REFERENCES

1. Reed, J. C. (1994) *J. Cell Biol. 124*, 1−6.
2. Yang, E., and Korsmeyer, S. J. (1996) *Blood 88*, 386-401.
3. Kroemer, G. (1997) *Nat. Med. 3*, 614−20.
4. Boyd, J. M., Gallo, G. J., Elangovan, B., Houghton, A. B., Malstrom, S., Avery, B. J., Ebb, R. G., Subramanian, T., Chittenden, T., Lutz, R. J., and Chinnadurai, G. (1995) *Oncogene 11*, 1921−1928.
5. Wang, K., Yin, W.-M., Chao, D. T., Milliman, C. L., and Korsmeyer, S. J. (1996) *Genes Dev. 10*, 2859−2869.
6. O'Connor, L., Strasser, A., O'Reilly, L. A., Adams, J. M., Cory, S., and Huang, D. C. S. (1997) *EMBO J.* (In press).
7. Yin, X. M., Oltvai, Z. N., and Korsmeyer, S. J. (1994) *Nature 369*, 321−333.
8. Hanada, M., Aimé-Sempé, C., Sato, T., and Reed, J. C. (1995) *J. Biol. Chem. 270*, 11962−11968.
9. Bodrug, S. E., Aimé-Sempé, C., Sato, T., Krajewski, S., Hanada, M., and Reed, J. C. (1995) *Cell Death Differ. 2*, 173−182.
10. Zha, H., Aime-Sempe, C., Sato, T., and Reed, J. C. (1996) *J. Biol. Chem. 271*, 7440−7444.
11. Chittenden, T., Flemington, C., Houghton, A. B., Ebb, R. G., Gallo, G. J., Elangovan, B., Chinnadurai, G., and Lutz, R. J. (1995) *EMBO J. 14*, 5589−5596.
12. Sedlak, T. W., Oltvai, Z. N., Yang, E., Wang, K., Boise, L. H., Thompson, C. B., and Korsmeyer, S. J. (1995) *Proc. Natl. Acad. Sci. U.S.A. 92*, 7834−7838.
13. Inohara, N., Ding, L., Chen, S., and Nunez, G. (1997) *EMBO J. 16*, 1686−1694.
14. Muchmore, S. W., Sattler, M., Liang, H., Meadows, R. P., Harlan, J. E., Yoon, H. S., Nettesheim, D., Changs, B. S., Thompson, C. B., Wong, S., Ng, S., and Fesik, S. W. (1996) *Nature 381*, 335−341.
15. Sattler, M., Liang, H., Nettesheim, D., Meadows, R. P., Harlan, J. E., Eberstadt, M., Yoon, H. S., Shuker, S. B., Chang, B. S., Minn, A. J., Thompson, C. B., and Fesik, S. W. (1997) *Science 275*, 983−986.
16. Zha, H., Aime-Sempe, C., Sato, T., and Reed, J. C. (1996) *J. Biol. Chem. 271*, 7440−7444.
17. Zha, H., Fisk, H. A., Yaffe, M. P., Mahajan, N., Herman, B., and Reed, J. C. (1996) *Mol. Cell. Biol. 16*, 6494−6508.
18. Diaz, J.-L., Oltersdorf, T., Horne, W., McConnell, M., Wilson, G., Weeks, S., Garcia, T., and Fritz, L. C. (1997) *J. Biol. Chem. 272*, 11350−11355.
19. Schendel, S., Montal, M., and Reed, J. C. (1997) *Cell Death Differ.* (In press).
20. Minn, A. J., Velez, P., Schendel, S. L., Liang, H., Muchmore, S. W., Fesik, S. W., Fill, M., and Thompson, C. B. (1997) *Nature 385*, 353−357.
21. Schendel, S. L., Xie, Z., Montal, M. O., Matsuyama, S., Montal, M., and Reed, J. C. (1997) *Proc. Natl. Acad. Sci. U.S.A. 94*, 5113−5118.
22. Antonsson, B., Conti, F., Ciavatta, A., Montessuit, S., Lewis, S., Martinou, I., Bernasconi, L., Bernard, A., Mermod, J.-J., Mazzei, G., Maundrell, K., Gambale, F., Sadoul, R., and Martinou, J.-C. (1997) *Science 277*, 370−372.
23. Schlesinger, P., Gross, A., Yin, X.-M., Yamamoto, K., Saito, M., Waksman, G., and Korsmeyer, S. (1997) *Proc. Natl. Acad. Sci. U.S.A. 94*, 11357−11362.
24. Oblatt-Montal, M., Buhler, L. K., Iwamoto, T., Tomich, J. M., and Montal, M. (1993) *J Biol Chem 268*, 14601−14607.
25. Reddy, L. G., Iwamoto, T., Tomich, J. M., and Montal, M. (1993) *J. Biol. Chem. 268*, 14608−14615.
26. Raghavan, M., and Bjorkman, P. J. (1995) *Curr. Biol. 3*, 331−333.
27. Fisher, R. J., and Fivash, M. (1994) *Curr. Opin. Biotech. 5*, 389−395.
28. Schuck, P. (1997) in *Annu. Rev. Biophys. Struct.* (Stroud, R. M., Ed.) pp 541−566, Annual Reviews Inc., Palo Alto, CA.
29. Fägerstam, L. G., Frostell-Karlsson, Å., Karlsson, R., Persson, B., and Rönnberg, I. (1992) *J. Chromatogr. A 597*, 397−410.
30. Chaiken, I., Rosé, S., and Karlsson, R. (1992) *Anal. Biochem. 201*, 197−210.
31. Zha, H., and Reed, J. C. (1997) *J. Biol. Chem. 272*, 31482−31488.
32. Wang, H.-G., Takayama, S., Rapp, U. R., and Reed, J. C. (1996) *Proc. Natl. Acad. Sci. U.S.A. 93*, 7063−7068.
33. Wang, H. G., Rapp, U. R., and Reed, J. C. (1996) *Cell 87*, 629−638.
34. Rosen, C. G., and Weber, G. (1969) *Biochemistry 8*, 3915−3920.
35. Reed, J. C. (1997) *Nature 387*, 773−776.
36. Hsu, Y. T., and Youle, R. J. (1997) *J. Biol. Chem. 272*, 13829−13834.
37. van der Goot, F. G., Gonzalez-Manas, J. M., Lakey, J. H., and Pattus, F. (1991) *Nature 354*, 408−410.
38. Ramsay, G., Montgomery, D., Berger, D., and Freire, E. (1989) *Biochemistry 28*, 529−533.
39. Cramer, W. A., Heymann, J. B., Schendel, S. L., Deriy, B. N., Cohen, F. S., Elkins, P. A., and Stauffacher, C. V. (1995) *Annu. Rev. Biophys. Biomol. Struct. 24*, 611−641.
40. Krajewski, S., Tanaka, S., Takayama, S., Schibler, M. J., Fenton, W., and Reed, J. C. (1993) *Cancer Res 53*, 4701−4714.
41. Alberts, B., Bray, D., Lewis, J., Raff, M., Roberts, K., and Watson, J. D. (1994) in *Molecular Biology of the Cell* (Robertson, M., Ed.) pp 653−720, Garland Publishing, Inc., New York.
42. de Jong, D., Prins, F. A., Mason, D. Y., Reed, J. C., van Ommen, G. B., and Kluin, P. M. (1994) *Cancer Res. 54*, 256−260.
43. Takayama, S., Sato, T., Krajewski, S., Kochel, K., Irie, S., Millan, J. A., and Reed, J. C. (1995) *Cell 80*, 279−284.
44. Takayama, S., Bimston, D. N., Matsuzawa, S., Freeman, B. C., Aime-Sempe, C., Xie, Z., Morimoto, R. J., and Reed, J. C. (1997) *EMBO J. 16*, 4887−4896.
45. Zeiner, M., Gebauer, M., and Gehring, U. (1997) *EMBO J. 16*, 5483−5490.

BI973052I

Cell Death and Differentiation (1998) 5, 372–380

http://www.stockton-press.co.uk/cdd

Review

Bcl-2 family proteins as ion-channels

Sharon L. Schendel[1], Mauricio Montal[2] and John C. Reed[1,3]

[1] The Burnham Institute, Program on Apoptosis and Cell Death Research, 10901 North Torrey Pines Road, La Jolla, California 92037, USA
[2] The University of California at San Diego, Department of Biology, 9500 Gilman Drive, La Jolla, California 92093-0366, USA
[3] corresponding author: Dr Reed, tel: 619-646-3140; fax: 619-646-3194; email: jreed@burnham-institute.org

Received 30.9.97; revised 9.12.97; accepted 11.12.97
Edited by G. Melino

Abstract

The Bcl-2 protein family function(s) as important regulators of cellular decisions to heed or ignore death signals. The three-dimensional structure of the Bcl-2 homolog, Bcl-X_L, bears a strong resemblance to some pore-forming bacterial toxins. This similarity suggested that the Bcl-2 family proteins may also possess channel-forming capability. This review summarizes the recent initial studies on the *in vitro* channel activity of Bcl-2, Bcl-X_L and Bax and offers some speculation as to the physiological role that these channels may play in the cell death pathway.

Keywords: apoptosis: membrane: colicin

Abbreviations: BH, Bcl-2 homology; DT, diptheria toxin; $\Delta\Psi_m$, mitochondrial membrane potential; PCD, programmed cell death; pS, picosiemen; PT, mitochondrial permeability transition

Introduction

Akin to a spy who carries a cyanide capsule with which to commit suicide upon capture, each cell in an animal species carries within it a program to direct its own death. An attenuated rate of programmed cell death (PCD) can result in disorders ranging from autoimmune disease to cancer, while an increased rate of PCD occurs in diseases such as AIDS or neurodegenerative disorders (e.g. Parkinson's disease) (Reed, 1994; Thompson, 1995). The gene encoding Bcl-2 (*B-cell lymphoma/leukemia-2*) was first identified on the basis of its involvement in B-cell malignancies where chromosomal translocations activate *bcl-2* in ~85% of follicular non-Hodgkin's B-cell lymphomas (Tsujimoto *et al*, 1985). Bcl-2 extends cell survival against apoptotic signals induced by a variety of treatments including: growth factor deprivation; ultraviolet and γ-radiation; heat shock; some cytotoxic lymphokines (i.e., tumor necrosis factor); calcium ionophores; viral infection; and agents that promote formation of free-radicals (Reed, 1994). The ability of Bcl-2 to protect cells from such an assortment of insults, and the differing biochemical pathways which they utilize, suggests that Bcl-2 must control one or more of the distal steps in the cell death pathway.

Immunoprecipitation and yeast-two hybrid assays have aided in the expansion of the Bcl-2 family which now includes 16 cellular members and five viral homologs, among which are: Bcl-X_L, Bcl-X_s (Boise *et al*, 1993), Bax (Oltvai *et al*, 1993), Bak (Chittenden *et al*, 1995). The Bcl-2 family members are at cross-purposes; Bcl-2 and Bcl-X_L promote cell survival, while Bcl-X_s, Bax and Bak encourage cell demise. While Bcl-X_L shows the greatest degree of sequence identity with Bcl-2 (~45%), the pro-apoptotic proteins Bcl-X_s, Bax and Bak have pockets of sequence similarity, denoted BH1, 2, 3 and 4. The BH3 domain is present within all family members, while BH4 is found at the extreme N-terminus of primarily only anti-apoptotic proteins. Deletion mutagenesis has suggested that it is these regions of sequence similarity that govern protein-protein interactions between the family members to form either homo- or heterodimers (Yin *et al*, 1994; Sedlak *et al*, 1995; Zha *et al*, 1996a). The fate of the cell appears to rest with the relative amounts of these proteins, and the identity of the predominate protein complexes (Korsmeyer *et al*, 1993).

Cellular localization of Bcl-2, Bcl-X_L, Bax

With no readily identifiable sequence motifs, the biochemical mechanism by which the Bcl-2 family of proteins modulates apoptosis has remained elusive. Bcl-2, Bcl-X_L, and Bax are localized to the outer mitochondrial membrane via a C-terminal ~20-residue hydrophobic tail. (Krajewski *et al*, 1993; Gonzalez-Garcia *et al*, 1994; Zha *et al*, 1996b), although Bcl-2 and Bcl-X_L can be found in other sites as well, including the nuclear envelope and the ER. Immuno-electron microscopy revealed a non-uniform distribution of Bcl-2 in mitochondrial membranes, suggesting that it may be preferentially localized to zones of adhesion (ZOA) which join the outer and inner mitochondrial membrane (Krajewski *et al*, 1993; de Jong *et al*, 1994). Association of Bcl-2 with ZOAs, which are predicted to be sites of protein and ion import (Schatz, 1993), implies that Bcl-2 may be involved in regulating these activities.

Previously, Bcl-2 was predicted to have the ability to influence intracellular Ca^{2+} distribution (Baffy *et al*, 1993; Lam *et al*, 1994) and play a role in an antioxidant pathway (Hockenberry *et al*, 1993; Kane *et al*, 1993). However, the importance of these possibilities are questioned by studies which showed that the apoptotic pathway can proceed in an anaerobic environment and with decreased Ca^{2+} levels (Jacobson and Raff, 1995; Reynolds and Eastman, 1996; Shimizu *et al*, 1996). Alternatively, Bcl-2 is able to

counteract a decrease in mitochondrial membrane potential ($\Delta\Psi_m$), an early event in the apoptotic process, suggesting that Bcl-2 can perhaps balance perturbations in normal $\Delta\Psi_m$ (Zamzani *et al*, 1995). The mitochondrial membrane localization would thus place Bcl-2 at an advantageous site to participate in all of the above functions.

Bcl-X_L structure and implications for function

A new possibility for the biochemical function of the Bcl-2 family proteins is suggested by the recently determined 3-dimensional structure of Bcl-X_L (Muchmore *et al*, 1996). Bcl-X_L is comprised of 7 α-helices arranged in three layers. The outer two layers of amphipathic helices sandwich between them two long central α-helices (each approximately 20 residues) with a bias toward hydrophobic residues. A long loop devoid of secondary structure intervenes between the first and second helices. Interestingly, the sequence corresponding to this proline-rich 'loop' region of Bcl-X_L is absent in the pro-apoptotic members of the Bcl-2 family and poorly conserved among anti-apoptotic proteins such as Bcl-2 and Bcl-X_L. Although this loop is dispensable for the anti-apoptotic function of Bcl-X_L and Bcl-2, this region may be vulnerable to protease digestion (Strack *et al*, 1996) and contains phosphorylation sites (Chang *et al*, 1997). Post-translational modifications or conformational changes mediated via this domain may serve as a means for modulating the anti-apoptotic activity of Bcl-2 and Bcl-X_L (Minn *et al*, 1997).

The BH1, 2 and 3 domains fold together to give one face of the Bcl-X_L molecule a pronounced hydrophobicity. This structural feature, coupled with site-directed mutagenesis studies, suggests that hydrophobic protein-protein interactions may be the 'glue' that holds the Bcl-2 family homo- and heterodimers together. Indeed, a peptide corresponding to the BH3 region of Bak was found to be able to nestle into a crevice formed by the apposition of the BH1, BH2 and BH3 regions of Bcl-X_L (Sattler *et al*, 1997). This crevice is just wide enough to accommodate an α-helix and the Bak BH3 peptide obliges this structural constraint by undergoing a transition from random coil to α-helix upon binding to Bcl-X_L *in vitro*. This interaction is governed by both hydrophobic and electrostatic forces, and disruption of either by introduction of alanine at several sites along the Bak peptide's length was sufficient to abolish binding. BH3 peptides also disrupt dimerization among other members of the family, including Bcl-2 and Bax (Diaz *et al*, 1997)

A bacterial connection?

The Bcl-X_L structure bears a striking resemblance to the previously solved structures of the diphtheria toxin membrane-translocation domain (Choe *et al*, 1992) and the pore-forming domains of colicins A and E1 (Parker *et al*, 1992; Elkins *et al*, 1997). The diphtheria toxin, produced by *Corynebacterium diphtheriae*, is composed of two parts: the A and B fragments, which possess ADP-ribosylation and pore-forming activity, respectively (London, 1992). The diphtheria toxin gains access to the cell by receptor-mediated endocytosis and upon encountering the acidic pH inside the endosome, the B fragment forms a channel in the endosomal membrane through which the A-fragment passes.

Colicins are plasmid-encoded protein antibiotics that are produced by and active against *Escherichia coli* and related strains. The ability to produce colicin is not a rare trait among *E. coli* inhabiting the human gut. Out of a survey of 234 *E. coli* strains isolated from healthy or diseased humans, more than 60% of the strains had the ability to produce at least one form of colicin (Achtman *et al*, 1983). Within populations of colicinogenic bacteria, a small fraction of the cells are producing colicin. Colicin expression is strongly repressed under normal conditions, but this repression can be relieved when the cell's DNA is irretrievably damaged (Pugsley and Oudega, 1987). Colicin producing cells are non-viable and thus colicin production is assumed to be a lethal event wherein some cells are sacrificed so that the community may survive, not unlike the clearing of aged or defective cells by apoptosis in animal species.

The pore-forming colicins kill sensitive cells via the formation of a highly conductive voltage-gated ion channel in the target cell's cytoplasmic membrane. This channel is non-specific and conducts monovalent ions with diffusion rates ($>10^6$ ions-channel^{-1}-sec^{-1}) that exceed the rate of cellular proton extrusion and results in depolarization of the cytoplasmic membrane. There are several consequences of this depolarization: inhibition of active transport; and depletion of intracellular K^+, phosphate, and ATP stores either through hydrolysis or leakage through the colicin pore (Cramer *et al*, 1995).

Although colicins and diphtheria target very different organisms, the structures of both these bacterial toxins share a similar 'cloak and dagger' strategy in which the hydrophobic 'dagger' is shielded within a shell of amphipathic helices, allowing these proteins to lead 'dual lives' in that they may exist in a soluble state, but under certain conditions, will insert into membranes to form a channel (Oh *et al*, 1996; Shin *et al*, 1993; Donovan *et al*, 1982). This characteristic has made them the subject of numerous studies having the goal of determining how proteins insert into a membrane bilayer.

The structural similarity between BclX_L and the pore-forming domains of bacterial toxins suggests that the Bcl-2 family of proteins should have pore-forming potential. The features of the Bcl-X_L structure should be applicable to the other Bcl-2 family members, an inference supported by the example of the pore-forming domains of colicins A, E1, and Ia, which share at most 30% sequence identity (Cramer *et al*, 1995), yet have highly similar 3-dimensional structures. Figure 1 shows the predicted structures of Bcl-2 and Bax which were modeled using the coordinates of Bcl-X_L.

Bcl-X_L, Bcl-2, and Bax pore formation *in vitro*

For the Bcl-2 protein family members to form pores they must contain helices that are long enough to span the membrane bilayer and these helices must be largely devoid of charged residues. Each residue of an α-helix contributes ~1.5 Å to its overall length. If an average lipid bilayer has a hydrophobic cross-section of ~30 Å (Montal and Mueller, 1972), then for an α-helix to span a membrane bilayer and participate in channel

formation, it must be ~20 residues long. Bcl-X_L has two helices that meet these criteria, and they are the two central helices (i.e., α5 and α6; Figure 1, as indicated). Although two helices are insufficient to enclose an aqueous lumen, the propensity for the Bcl-2 protein family members to form dimers suggests that two or more molecules could come together, each contributing their hydrophobic helices to create a pore.

To explore the pore-forming capability of the Bcl-2 protein family, several groups have undertaken studies of Bcl-2, Bcl-X_L, and Bax effects on planar lipid bilayers and lipid vesicles. Large, unilamellar vesicles that encapsulate either ions or fluorescent dyes are useful for observing channel formation. This technique monitors channel formation on a macroscopic level, in that for solute efflux from these vesicles to be detected, (particularly measurement of ion efflux) a majority of protein molecules must participate in channel formation. Demonstration of channel activity in vesicles discounts the possibility that only a very small fraction of molecules are inserting into the membrane bilayer. However, this method lacks the sensitivity to yield specific information concerning channel conductance, voltage-gating, or ion selectivity. These specific channel characteristics are best studied using the planar lipid bilayer configuration. In the planar bilayer approach, two chambers are divided by a septum having a small (50–200 μM diameter) aperture in which the membrane bilayer is formed (for reviews see Montal and Mueller, 1972; Kagan and Sokolov, 1994). Consistent with the structural prediction, Bcl-2, Bcl-X_L, and most recently, Bax, have demonstrated avid pore-forming capability *in vitro* when assayed under conditions similar to those employed previously for assessing DT and colicin channel activity *in vitro*.

In vitro channel formation by the pore forming domains of both colicins and diphtheria toxin requires that several requirements be met: (i) the pH must be less than 4.0; (ii) the membrane must contain at least 10% negatively charged lipids; and (iii) a *trans*-negative membrane potential (i.e. the side of the membrane opposite to which the protein is added has an excess negative charge) must be present. With these requirements in mind, an assay used to measure *in vitro* colicin channel activity was carried out, except with the substitution of Bcl-X_L or Bcl-2 for colicin E1. Bcl-X_L and Bcl-2 induce solute efflux from KCl-loaded vesicles composed of 70% and 30% neutral and anionic lipid, respectively. Interestingly, Bcl-2 induced Cl^--efflux from KCl-loaded vesicles required sixfold less protein compared to Bcl-X_L (300 *vs* 1800 ng/mL). This variation could be attributable to the fact that the Bcl-2 protein preparation used for these studies was soluble only at acidic (pH 3.3) pH, while Bcl-X_L was soluble at pH 7. In the case of colicin E1, incubation of the protein at acidic pH prior to addition to liposomes results in a dramatically increased activity, as if the protein were 'primed' to interact with the membrane (S.L. Schendel and W.A. Cramer, unpublished observations). A similar situation could occur for Bcl-2 as well. Side-by-side comparison of colicin E1 channel peptide activity and that of Bcl-2 showed that only ~5-fold more Bcl-2 was necessary to induce an efflux rate similar to that of colicin E1, highlighting the pore-forming capability of Bcl-2. As with colicin E1, Bcl-X_L-induced significant ion efflux only when the pH was lower than 4.0. Channel activity was improved in the presence of the K^+-specific ionophore valinomycin, which transports K^+ ions out of the liposome, creating a *trans*-negative membrane

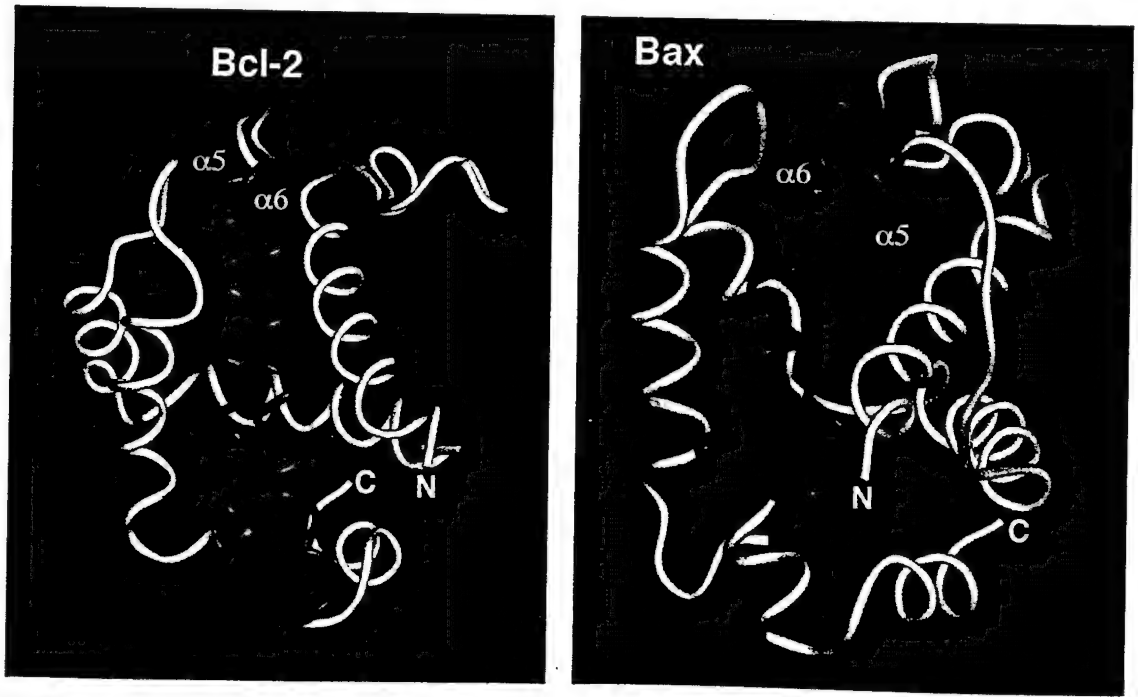

Figure 1 Ribbon diagrams of Bcl-2 and Bax modeled on the coordinates of Bcl-X_L using the QUANTA software package (Molecular Simulations, San Diego, CA). The putative membrane-spanning helices, α5 and α6, are the darker ones. The predicted loop of Bcl-2 is not shown

potential. When the same assay was performed with liposomes composed solely of neutral lipids, both Bcl-X_L and Bcl-2 lost all channel-forming activity.

Most studies of colicin and DT channel formation utilized the fragments of the toxins containing the pore-forming region which lacks domains required for binding to the integral membrane protein receptors on the surface of the target cells. The removal of these other regions from the toxin adds additional constraints for channel activity which are probably irrelevant *in vivo*. In the case of the colicin pore-forming domain, the low pH and acidic lipid requirements for *in vitro* channel activity can be explained in terms of lipid-protein interactions. The colicin E1 pore-forming domain has a number of lysine residues which are vital in docking the protein at the negatively charged membrane surface (Zakharov *et al*, 1996). The low pH also may induce a conformational change in the colicin molecule, presumably a loosening of the outer amphipathic shell that would expose the central hydrophobic helical hairpin, freeing it to insert into the membrane bilayer (van der Goot *et al*, 1991; Schendel and Cramer, 1994). Analogously, the Bcl-X_L and Bcl-2 proteins used in all studies to date lack the hydrophobic C-terminal anchor, which facilitates purification, but also relieves the protein of its normal means of membrane tethering. Therefore *in vitro*, it may be necessary to have acidic pH to increase the likelihood that the protein will 'find' the membrane surface. Bcl-X_L and Bcl-2 have a slightly net negative charge at neutral pH and therefore the acidic pH could be necessary to protonate these negatively charged residues and the resultant charge neutralization could increase the hydrophobicity of the protein, making it more likely to insert into the membrane bilayer.

To gain information about the details of Bcl-X_L and Bcl-2 channel formation, their activities on planar bilayers were examined (Minn *et al*, 1997; Schendel *et al*, 1997). Upon addition of the proteins to one side of the planar bilayer apparatus, a voltage can be applied at a constant value. Any resultant current can be plotted as a function of the applied voltage which yields the channel conductance. The channel conductance is expressed in terms of siemens (S), and the channel conductances observed for the Bcl-2 protein family are in the picosiemen (pS) range. The conductance (g) is readily obtained using Ohm's law from a plot of current *vs* voltage (I-V plot) by dividing the current (expressed in Ampere, A) by the voltage difference across the membrane (V) (I=gV) (Hille, 1984) (Box 1).

At pH 4.0, after imposition of 20 mV potential, Bcl-X_L rapidly (<5 min) incorporated into the lipid bilayer to give a conductance that increased in a step-wise fashion, eventually to levels where resolution of single-channel conductance was difficult. In contrast to the liposome measurements, channel formation by Bcl-X_L could be detected at neutral pH. Channel formation at this pH was a much rarer event, with a lag time between addition of protein to observation of channel formation increasing to ~30 min. At both pH 7.2 and pH 4.0, the relationship between voltage and current was Ohmic in that a plot of current *vs* applied voltage is linear. The Bcl-X_L channel displayed multiple conductance states with the most common conductance value being 276 pS for Bcl-X_L and three other conductance states of 80, 134, and 179 pS in 0.15 M KCl (Table 1).

Box 1: Definitions of channel parameters obtained from single channel recordings using planar lipid bilayers.

* Channel conductance is expressed in units of siemens: the reciprocal of an ohm.
* Channel conductance (g) is given by g=I/V where I is the current flowing through an open channel in response to an applied voltage V (the membrane potential).
* In the case of a channel having a 20 pS conductance: a current of 2 pA (picoamperes) would flow across the lipid bilayer at a membrane potential of 100 mV. Since an ampere is the flow of 6.24×10^{18} charges/sec. it follows that about 10 million ions flow through the open 20 pS channel.

Table 1 Single channel characteristics of Bcl-2 family proteins reconstituted in planer lipid bilayers

Protein	pH	Voltage (mV)	Salt (mM)	Conductance States (pS)	Ion Selectivity	Reference
Bcl-2	7.4	100	500 KCl	20 40 90	Cation	Schendel *et al*, 1997
Bcl-X_L	7.2	20	150/50 KCl (cis:trans)	276 179 134	Cation	Minn *et al*, 1997
Bax	7.0	100	125 NaCl	80 26 80 180 250	Cation	Antonsson *et al*, 1997
Bax	7.0	40	450/150 KCl (cis:trans)	2000 329	Anion	Schlesinger *et al*, 1997

When assayed in planar bilayers, Bcl-2 also displayed a linear relationship between current and voltage, in that the current conducted at +100 and −100 mV was identical except for opposite direction of current flow. However, the Bcl-2 channel's conductance states were much different than those detected for Bcl-X_L. The primary conductance levels for Bcl-2 were ~1/10 that of Bcl-X_L, with the most common channel events having conductance of 20 and 40 pS in 0.5 M KCl (Table 1). A larger conductance of 90 pS was also observed, albeit only rarely. Each of these conductance levels was a unique channel activity and not representative of several simultaneous openings of 20 pS channels (Schendel *et al*, 1997). The conductances of Bcl-2 channels were nearly the same at neutral and low pH, but at lower pH the Bcl-2 channels opened more frequently, suggesting that channel insertion increases markedly.

Structural implications of conductance measurements

The 20 pS conductance level of Bcl-2 is highly similar to that observed for colicin E1 in planar lipid bilayers (Bullock *et al*, 1983). The colicin E1 channel is predicted to consist of a bundle of four α-helices, two hydrophobic, and two amphipathic, which penetrate the membrane bilayer spontaneously and upon imposition of a *trans*-negative membrane potential, respectively (Elkins *et al*, 1997). Although Bcl-2 would be predicted to possess only two helices of sufficient length to span a membrane bilayer, two Bcl-2 monomers could come together to form a four helix bundle, with each contributing two α-helices to the channel. Alternatively, studies employing synthetic peptides which insert into membranes to form pentameric helical bundles gave rise to ~40 pS channel conductances (Montal *et al*, 1993). For this situation to occur, additional helices of Bcl-2 could insert into the membrane, although the other predicted helices, while possibly long enough, contain residues which would entail significant energy costs to insert into the hydrophobic membrane bilayer (e.g. Lys, Arg) or residues traditionally considered to disrupt helices (e.g. Pro, Gly). Although these studies were performed with Bcl-2 lacking its C-terminal anchoring region, it is conceivable that this region of the protein, while dispensable for function *in vivo* (Borner *et al*, 1994), could contribute to channel formation. More likely, however, the larger conductances measured for Bcl-2 and particularly for Bcl-X_L could result from oligomerization of three or more molecules integrated into the lipid bilayer.

Ion selectivity of Bcl-2 and Bcl-X_L channels

Ion selectivity of a channel can also be determined using planar bilayer measurements. The selectivity is a preferential ability of a channel to conduct a given ionic species more efficiently than others and can be expressed in terms of the ratio of permeability or conductance values for the ions under comparison. The pore selectivity can be affected by the residues lining the mouth and lumen of the pore, e.g., the presence of negatively charged residues in the lumen of the pore would be expected to impede the passage of anions through the pore. When channel activity is measured in a planar bilayer apparatus in which the ion concentration of the *cis*-compartment differs from that in the *trans*-, there occurs a potential at which the current is zero, which appears as the y-intercept on a current *vs* voltage plot.

This zero-current potential can be related to the permeability ratios of the ions under consideration by the following equation:

$$E_{rev} = 59.1 \frac{\log P_A [A]}{P_B [B]}$$

where E_{rev} is the zero-current potential and P_A and P_B represent the permeabilities of the ion A and B, where both ions have identical valences. Using a variety of solutes and concentration gradients, and measuring the point at which no net current flows, it is possible to determine the ion selectivity.

The ion selectivity of the Bcl-X_L channel varied as a function of pH, having a permeability ratio between K^+ and Cl^- (P_K/P_{Cl}) of 1.05 and 4.31 at pH 4.0 and 7.2, respectively. This indicates that at pH 4.0 there exists no barrier within the lumen that would impede the passage of either cations or anions, but at pH 7.2, cations pass

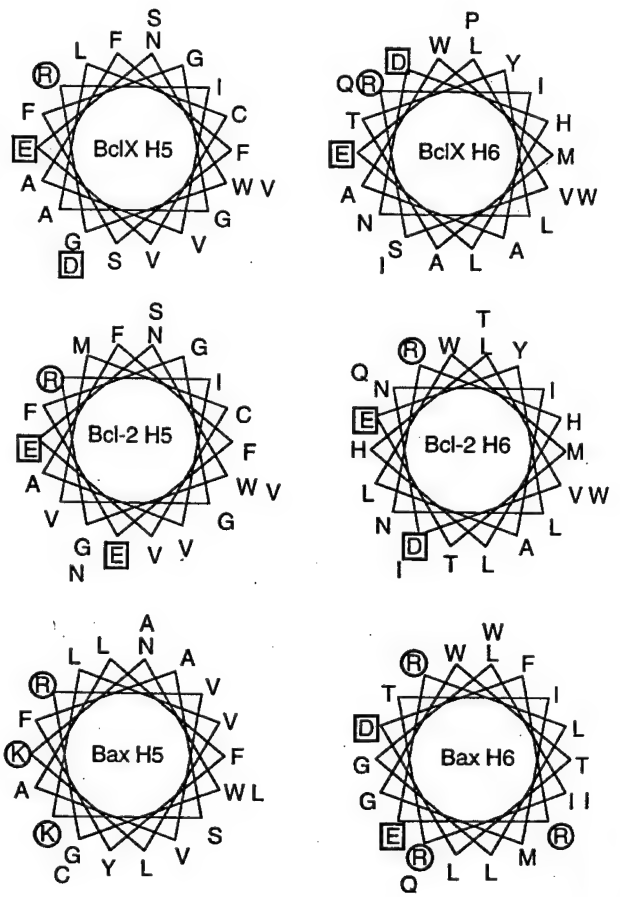

Figure 2 Helical wheel analysis of predicted α-helices 5 and 6 of Bcl-2, Bcl-X_L, and Bax. Residues for Bcl-2 and Bax were selected on the basis of sequence alignment with Bcl-X_L. The plots were constructed based on the helical periodicity of *i*...*i*+4. Positive and negative residues are highlighted with a circle and square, respectively. The charged face of the helix would be predicted to line the channel lumen

through the channel with much greater ease. This result supports the prediction that Bcl-X_L should prefer to pass cations, as a α-helical wheel analysis of the putative membrane insertion domain shows a bias toward acidic residues on one face of the helices (Figure 2). Presumably at pH 4.0, these residues would be protonated and would not interfere with the passage of either cations or anions, but at pH 7.2 the negative charge on these residues should discourage anion passage. At pH 5.4, Bcl-2 was also 90% cation selective (Schendel *et al*, 1997). Again, this agrees well with a α-helical wheel analysis of the putative fifth and sixth helices of Bcl-2, which suggested that the faces of these helices predicted to line the channel lumen have residues with acidic side chains (Figure 2).

To explore whether the predicted 5th and 6th helices of Bcl-2 were indeed responsible for its observed ion channel activity, this region was deleted resulting in a protein that is highly similar to the alternatively spliced variant of Bcl-X_L, Bcl-X_S. The loss of this region converted Bcl-2(Δh5,6) to a pro-apoptotic protein, similar to Bcl-X_S. Bcl-2(Δh5,6) promiscuously promoted low-level ion efflux from KCl-loaded vesicles in that identical amounts of ion flux were detected under all conditions tested, even those where Bcl-2 failed to display activity, such as on 100% neutral lipid vesicles and at pH values above pH 4.5 (Schendel *et al*, 1997). This non-specific behavior may be due to the amphipathic nature of this shortened Bcl-2 molecule, in that it may be interacting with the membrane surface in much the same way an amphipathic detergent would.

In planar bilayers, Bcl-2(Δh5,6) failed to form discrete channels, but produced only random stray conductances. These results suggest that pore formation of Bcl-2, and presumably Bcl-X_L, absolutely requires the presence of the hydrophobic central 5th and 6th helices.

Bax *in vitro* channel formation

The most recent member of the Bcl-2 protein family documented to display pore-forming activity is the pro-apoptotic protein Bax (Antonsson *et al*, 1997). As with Bcl-X_L and Bcl-2, Bax lacking its C-terminal hydrophobic anchor was used. As with Bcl-2, only nanomolar concentrations of Bax were necessary to induce a healthy efflux of liposome-encapsulated fluorescent dye carboxyfluorescein at pH 4.0. But in contrast to Bcl-2 and Bcl-X_L, detectable levels of dye efflux from liposomes were noted even up to pH 7.4, although at ~8-fold lower amounts. Whether or not this result indicates that the channel properties of Bax differ from that of Bcl-2 and Bcl-X_L is unclear, as the inactivity of Bcl-2 at pH 7.4 could be attributable to its low solubility in the absence of detergents at this pH. Moreover, it should be noted that the colicin E1 pore-forming domain has detectable activity using a similar dye-encapsulation method, although it shows no appreciable activity with measurements of ion-efflux at neutral pH using electrodes. Thus, the capability of this fluorescence-based assay to detect much lower amounts of solute loss prevents a direct comparison with the findings obtained by other groups who employed methods relying on electrodes to detect ion-efflux.

In planar bilayer measurements, Bax was able to increase membrane conductance at both pH 4 and 7 within 10–60 min after Bax addition (Antonsson *et al*, 1997). At pH 4.0, unitary conductance steps similar to those detected for Bcl-2 were seen: 27 and 77 pS in 125 mM NaCl (Table 1). These conductances were transient, consistent with the behavior of Bcl-2 and Bcl-X_L. The conductances increased as the pH was raised to 7.0 and sub-populations of channels having conductances at 26, 80, 180 and 250 pS were detected. As the measurement progressed with time, larger conductances occurred in steps of 450 pS resulting in a final conductance near 2 nS. Recent studies of Bax channel activity in planar bilayers were in agreement with these results in that a predominant conductance state of 300 pS was detected at pH 7.0 (Schlesinger *et al, 1997).*

Unlike the channels observed for Bcl-2 and Bcl-X_L, the Bax channel did not display a linear relationship between current and voltage (Antonsson *et al*, 1997; Schlesinger *et*

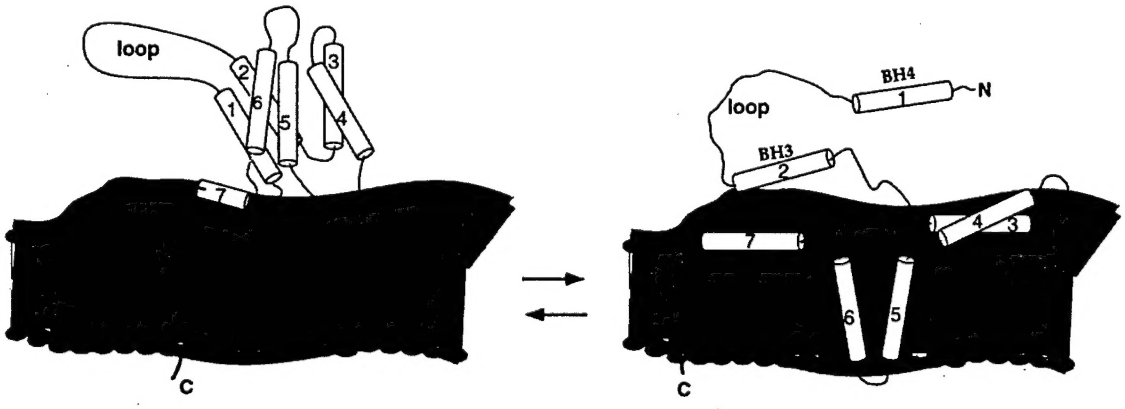

Figure 3 Schematic representation of Bcl-2 tethered to a membrane via its hydrophobic C-terminal region. The BH4 and BH3 domains involve α-helices 1 and 2, respectively. The loop connecting α-helices 1 and 2 is shown devoid of secondary structure, as suggested by the Bcl-X_L structure (Muchmore *et al*, 1996). Upon membrane integration, α-helices 5 and 6 are postulated to insert into the membrane bilayer. This insertion could be accompanied by a conformational change which could free the BH4 and BH3 domains for interactions with other proteins. Presumably, at least two Bcl-2 molecules would participate to form a conductive channel consistent with a four-helix bundle

al, 1997). Application of a *cis*-negative voltage enhanced channel formation, suggesting that channel formation by Bax is voltage-dependent. It must be borne in mind that this voltage dependence could reflect either the steps of Bax protein insertion into membranes or opening/formation of channels after insertion. The membrane potential dependence is opposite that observed for the colicins, which insert into planar bilayers upon imposition of a *cis*-positive voltage (Cramer *et al*, 1995). Bax channels were more weakly ion selective at pH 7.0 than were either Bcl-2 or Bcl-X_L having a permeability ratio of Na^+ to Cl^- of 2.1, nearly half that of Bcl-X_L. This result differs from a recent study of Bax channel characteristics wherein Bax channels were anion-selective at pH 7.0 (P_K/P_{Cl}=0.5) (Schlesinger *et al*, 1997). The actual ion preference of the Bax channel thus remains unsettled, however the bias towards positively charged side chains in the predicted 5th and 6th helices of Bax (Figure 1) would appear to support the latter study's findings.

Though highly controversial, it is tempting to speculate that the presence of a proton gradient and membrane potential across the inner mitochondrial membrane may somehow impact on the processes of protein insertion or channel formation/opening, particularly at the contact sites where the inner and outer membranes come together and where Bcl-2 family proteins tend to be concentrated.

Antonsson *et al* (1997), reported that in lipid vesicles at neutral pH Bcl-2 was able to prevent Bax-channel formation. When Bcl-2 was incubated with carboxyfluorescein-loaded vesicles at pH 7.0 (where Bcl-2 would have no activity) prior to the addition of Bax at a 1:10 Bax-Bcl-2 ratio, Bax channel activity was abolished (Antonsson *et al*, 1997). This antagonism of Bax channel activity was specific to Bcl-2 as control proteins had no effect on channel formation. It is unclear as to the nature of the interaction between Bcl-2 and Bax that impedes channel formation, and at what point the interaction occurs. For example, Bcl-2 might interfere with Bax by binding to it in solution before it contacts membranes or inserts into membranes. Assays of Bcl-2 vesicle association done in this laboratory indicate that at pH 7.0, Bcl-2 has an affinity for the membrane surface. This result would suggest that Bcl-2 would be bound to the membrane surface, but unable to insert into the membrane bilayer at pH 7.0. Bax-Bcl-2 interactions at the membrane surface could prohibit Bax from undergoing the transition from the soluble to membrane-inserted state (Figure 3). At pH 4.0, however, where Bcl-2 displays its own channel-forming capability, the addition of Bcl-2 and Bax together to a vesicle suspension causes an enhanced rate of efflux, presumably due to an additive effect (our unpublished results). Thus, further investigations of the interactions between Bax and Bcl-2 channels are required to gain better understanding of how Bcl-2 might antagonize Bax channel formation in some cases and not others. In particular, studies of interactions of Bcl-2 and Bax channels in planar bilayers should be very informative.

In vivo significance of pore formation

The idea of the Bcl-2 family proteins functioning as pore-forming proteins is still in its infancy and explanations of a physiological role for pore formation by these proteins are at best highly speculative. Although pore forming propensity appears to be a trait that is shared by several of the Bcl-2 family members, it remains to be demonstrated whether these proteins actually form pores *in vivo*, and if they indeed do, what is the functional significance of the resultant pore. It is also unclear why both pro- and anti-apoptotic proteins should share pore forming capability, although the recent demonstration that under certain conditions Bcl-2 can block Bax pore formation partially relieves this dilemma. Other than what can be indirectly gleaned from ion conductance measurements, there is as yet no information regarding the *in vivo* channel lumen diameters of the Bcl-2 family channels and this characteristic will be important in defining just what sorts of molecules these channels can accommodate in their lumens. Also, it is unclear what the molecularity of the channels are, although it seems clear that the channels must be formed by more than one molecule, as the two central hydrophobic helices are insufficient to completely line a channel lumen. Several possibilities for how Bcl-2, Bcl-X_L, and Bax can regulate apoptosis through pore formation can be envisioned.

Bcl-2 regulation of mitochondrial permeability transition

One early event associated with apoptosis is a decrease in the mitochondrial membrane potential (Zamzani *et al*, 1995), and this increase involves the so-called mitochondrial 'permeability transition'. This phenomenon is characterized by an increased permeability of the inner mitochondrial membrane to solutes $\leqslant$1500 Da (Zoratti and Szabo, 1995) which is caused by the opening of pores formed by multiprotein complexes situated at mitochondrial membrane contact sites. The PT may play an important role in regulation of Ca^{2+} homeostasis, as recently demonstrated (Schinder *et al*, 1996; Ichas *et al*, 1997). One important feature of the PT is its voltage dependence and its openings and closing are highly dependent on the mitochondrial membrane potential ($\Delta\Psi_m$). Therefore, a drop in $\Delta\Psi_m$ such as that which occurs early during apoptosis could result in PT opening. The overexpression of Bcl-2 prevents this early perturbation of $\Delta\Psi_m$ and the subsequent PT opening. Bcl-2 pore formation could serve to offset ion imbalances that may result in a lowered $\Delta\Psi_m$, and thus restore $\Delta\Psi_m$ to normal levels, preventing PT opening. Interestingly, patch clamp measurement of channel conductances present in a mitochondrial fraction enriched in contact sites yielded evidence for a variety of channels, some in the 10–80 pS range, others conducting at 475 and 550 pS (Moran and Sorgato, 1992), which corresponds to channel conductances observed for Bcl-2, Bax, and Bcl-X_L, respectively. A new method to study intracellular ion channels *in situ* using double-barreled patch clamp electrodes may provide access to record directly the PT channels and their regulation by Bcl-2 family proteins (Jonas *et al*, 1997).

Another possibility for the function of the Bcl-2 family pores is as conduits for proteins. The role of cytochrome (Cyt *c*) release from mitochondria during apoptosis has taken on an increased importance. Cyt *c*, which normally skitters across the mitochondrial inner membrane as part of the electron transport chain is somehow freed from the confines of the

ochondrial inter-membrane space and after gaining ccess to the cytosol, plays a role in the activation of spases, a family of proteases involved in the ultimate egradation of the cellular framework (Kluck *et al*, 1997). Bcl- was able to block the release of Cyt *c* from the mitochondria intact cells and in a cell-free extract, and it did so at the evel of the mitochondria, as addition of exogenous Cyt *c* circumvented this blockage. Perhaps Cyt *c* is escaping the mitochondria using the PT pore as its portal, and Bcl-2 with its ability to block PT is shutting this escape hatch. Alternatively, Bax, which also situated in the outer mitochondrial membrane, perhaps also at contact sites, could provide the gateway to cytosol for Cyt *c*. Again, Bcl-2 with its ability to block Bax pore formation under certain conditions could conceivably block release of Cyt *c* into the cytosol.

Lastly, the insertion of Bcl-2, Bax, and Bcl-X_L proteins into membranes may be of greater importance to their function as adaptor or docking proteins than for pore formation. Bcl-2 and Bcl-X_L have shown affinity for a host of proteins, among them the protein kinase Raf-1, the protein phosphatase calcineurin, as well as other proteins with ill-defined functions such as CED-4 and the Hsp70/Hsc90 modulating protein BAG-1 (reviewed in Häcker and Vaux, 1995). In contrast, Bax shows no affection for these proteins, perhaps due to its lack of a BH4 domain, which is important for several of these interactions (Wang *et al*, 1996). It is possible that the BH4 domain is tucked out of reach in the uninserted state of Bcl-2 and Bcl-X_L, but becomes accessible upon insertion of the central hydrophobic helices (Figure 2). Similarly, recent structural studies (Sattler *et al*, 1997) of the Bak BH3 peptide bound to the aforementioned groove suggest that the peptide insertion could prevent access or freeing of the BH3 domain for interaction with other BH3-containing proteins.

Much remains to be explored concerning pore formation by the trio of Bcl-2, Bcl-X_L, and Bax, and even whether the other members of the continually growing Bcl-2 family share the channel-forming trait. In this regard, it seems highly unlikely based on sequence comparisons and secondary structure predictions that the 'BH3-only' branch of the Bcl-2 family (Bik, Bad, Bak and Hrk) will form channels. Thus, these members of the Bcl-2 family seem likely to be relegated to the role of trans-dominant inhibitors of anti-apoptotic proteins such as Bcl-2 and Bcl-X_L. Of utmost importance will be the elucidation of the *in vivo* importance of the pores created by Bcl-2, Bcl-X_L, Bax and other structurally similar members of the Bcl-2 family. How these proteins make the transition from a soluble to membrane-inserted state, the dynamics and reversibility of the process, as well as which protein-protein interactions regulate this event are also critical questions. With continued investigations, however, the answers to these and other related questions are likely to shed bright light on one of the most important points for regulating the pathways of programmed cell death and apoptosis.

Acknowledgements

Research at the University of California San Diego is supported by NIH (GM-49711). We thank R Kodandapani for the modeling of Bax and Bcl-2 and S McDonald and M Hasham for their help in the preparation of Figure 2. SLS is supported by NIH Postdoctoral Training grant (1-T32 AG00252-01).

References

Achtman M, Mercer A, Kusecek B, Pohl A, Heuzenroeder M, Aaronson W, Surron A and Silver RP (1983) Six widespread bacterial clones among Escherichia coli K1 isolates. Infect. Immun. 39: 315–335

Antonsson B., Contin F, Ciavatta A, Montessuit S, Elwis S, Martinou I, Bernasconi L, Bernard A, Mermod J-J, Mazzei G, *et al.* (1997) Inhibition of Bax channel-forming activity by Bcl-2. Science 277: 370–372

Baffy G, Miyashita T, Williamson JR and Reed JC (1993) Apoptosis induced by withdrawl of interleukin-3 [IL-3] from an IL-3 dependent hematopoietic cell line is associated with repartitioning of intracellular calcium and is blocked by enforced Bcl-2 production. J. Biol. Chem. 268: 6511–6519

Boise LH, Gonzales-Garcia M, Postema CE, Ding L, Lindsten T, Turka LA, Mao X, Nunez G and Thompson CB (1993) Bcl-x a Bcl-2 related gene that functions as a dominant regulator of apoptotic cell death. Cell 74: 597–608

Borner C, Martinou I, Mattmann C, Irmler M, Schaerer E, Martinou J-C and Tschopp J (1994) The protein bcl2 does not require membrane attachment, but two conserved domains to suppress apoptosis. J. Cell Biol. 126: 1059–1068

Bullock JO, Cohen FS, Dankert JR and Cramer WA (1983) Comparison of the macroscopic and single channel conductance properties of colicin E1 and its COOH-terminal tryptic peptide. J. Biol. Chem. 258: 9908–9912

Chang BS, Minn AJ, Muchmore SW, Fesik SW and Thompson CB (1997) Indentification of a novel regulatory domain in Bcl-X_L and Bcl-2. EMBO J. 16: 968–977

Chittenden T, Harrington EA, O'Connor R, Flemington C, Lutz RJE and Guild BC (1995) Induction of apoptosis by the Bcl-2 homologue Bak. Nature 374: 733–736

Choe S, Bennett MJ, Fujii G, Curmi PMG, Kantardjieff KA, Collier RJ and Eisenberg D (1992) The crystal structure of diphtheria toxin. Nature 357: 216–222

Cramer WA, Heymann JB, Schendel SL, Deriy BN, Cohen FS, Elkins PA and Stauffacher CV (1995) Structure-function of the channel-forming colicins. Annu. Rev. Biophys. Biomol. Struct. 24: 611–641

de Jong D, Prins FA, Mason DY, Reed JC, van Ommen GB and Kluin PM (1994) Subcellular localization of the bcl-2 protein in malignant and normal lymphoid cells. Cancer Res. 54: 256–260

Diaz J-L, Oltersdorf T, Horne W, McConnell M, Wilson G, Weeks S, Garcia T and Fritz LC (1997) A common binding site mediates heterodimerization and homodimerization of Bcl-2 family members. J. Biol. Chem. 272: 11350–11355

Donovan JJ, Simon MI, and Montal M (1982) Insertion of diphtheria toxin into and across membranes: role of phosphoinositide asymmetry. Nature 298: 669–672

Elkins P, Bunker A, Cramer WA and Stauffacher CV (1997) A mechanism for toxin insertion into membranes is suggested by the crystal structure of the channel-forming domain of colicin E1. Structure 5: 443–458

Gonzalez-Garcia M, Perez-Ballestero RP, Ling L, Duan L, Boise LH, Thompson CB and Nunez G (1994) bcl-xl is the major bcl-x mRNA form expressed during murine development and its product localizes to mitochondria. Development 120: 3033–3042

Häcker G and Vaux DL (1995) A sticky business. Curr. Biol. 622–624

Hille B. (1984) Ionic Channels of Excitable Membranes. Sunderland, Massachusets, Sinauer Associates Inc.

Hockenberry DM, Oltvai ZN, Yin X-M, Milliman CL and Korsmeyer SJ (1993) Bcl-2 functions in antioxidant pathway to prevent apoptosis. Cell 75: 241–251.

Ichas F, Jouaville S and Mazat J-P (1997) Mitochondria are excitable organelles capable of generating and conveying electrical and calcium signals. Cell 89: 1145–1153

Jacobson MD and Raff MC (1995) Programmed cell death and Bcl-2 protection in very low oxygen. Nature 374: 814–816

Jonas EK, Knox RJ, and Kaczmarek LK. (1997) Giga-Ohm seals on intracellular membranes: a technique for studying intracellular ion channels in intact cells. Neuron 19: 7–13

Kagan BL and Sokolov Y. (1994) Use of lipid bilayer membranes to detect pore formation by toxins. Meth. Enzymol. 235: 691–705

Kane DJ, Sarafin TA, Auton S, Hahn H, Gralla FB, Valentine JC, Ord T and Bredesen DE (1993) Bcl-2 inhibition of neural cell death: decreased generation of reactive oxygen species. Science 262: 1274–1276

Kluck RM, Bossy-Wetzel E, Green DR and Newmeyer DD (1997) The release of cytochrome c from mitochondria: a primary site for Bcl-2 regulation of apoptosis. Science 275: 1132–1136

Korsmeyer SJ, Shutter JR, Veis DJ, Merry DE and Oltvai ZN (1993) Bcl-2/Bax: a rheostat that regulates an anti-oxidant pathway and cell death. Canc. Biol. 4: 327–332

Krajewski S, Tanaka S, Takayama S, Schibler JJ, Fenton W and Reed JC (1993) Investigation of the subcellular distribution of the bcl-2 oncoprotein: residence in the nuclear envelope, endoplasmic reticulum, and outer mitochondrial membranes. Canc. Res. 53: 4701–4714

Lam M, Dubyak G, Chen L, Nunez G, Miesfeld RL and Distelhorst CW (1994) Evidence that Bcl-2 represses apoptosis by regulating endoplasmic reticulum-associated Ca^{2+}-fluxes. Proc. Natl. Acad. Sci. U.S.A. 91: 6569–6573

London E. (1992) Diphtheria toxin: membrane interaction and membrane translocation. Biochim. Biophys. Acta. 1113: 25–51

Minn AJ, Velez P, Schendel SL, Liang H, Muchmore SW, Fesik SW, Fill M and Thompson CB (1997) Bcl-X_L forms an ion channel in synthetic lipid membranes. Nature 285: 353–357

Montal MO, Iwamoto T, Tomich JM and Montal M (1993) Design, synthesis and functional characterization of a pentameric channel protein that mimics the presumed pore structure of the nicotinic cholinergic receptor. FEBS Lett 320: 261–266

Montal M and Mueller P. (1972). Formation of bimolecular membranes from lipid monolayers and a study of their electrical properties. Proc Natl Acad Sci U.S.A. 69, 3561–3566

Moran O and Sorgato MC (1992) High-conductance pathways in mitochondrial membranes. J. Bioenerg. Biomembr. 24: 91–98

Muchmore SW, Sattler M, Hiang H, Meadows RP, Harlan JE, Yoon HS, Nettesheim D, Chang BS, Thompson CB, Wong S-L, *et al.* (1996) X-ray and NMR structure of human $BclX_L$, an inhibitor of programmed cell death. Nature 381: 335–341

Oh KJ, Zhan H, Cui C, Hideg K, Collier RJ, and Hubbel WL (1996) Organization of diphtheria toxin T domain in bilayers: a site-directed spin labeling study. Science 273: 810–812

Oltvai ZN, Millman CL and Korsmeyer SJ (1993) Bcl-2 heterodimerizes with a conserved homolog, Bax, that accelerates programmed cell death. Cell 74: 609–619

Parker MW, Postma JPM, Pattus F, Tucker AD and Tsernoglou D (1992) Refined structure of the pore-forming domain of colicin A at 2.4 Å resolution. J. Mol. Biol. 224: 639–657

Pugsley AP andOudega B (1987) Methods for studying colicins and their plasmids. In Plasmids: a practical approach. (ed.) Oxford: IRL Press.

Reed JC (1994) Bcl-2 and the Regulation of Programmed Cell Death. J. Cell Biol. 124: 1–6

Reynolds JE and Eastman A (1996) Intracellular calcium stores are not required for Bcl-2-mediated protection from apoptosis. J. Biol. Chem. 271:

Sattler M, Liang H, Nettesheim D, Meadows RP, Harlan JE, Matthias E, Yoon HS, Shuker SB, Chang BS, Minn AJ, *et al.* (1997) Structure of Bcl-Bak peptide complex: recognition between regulators of apoptosis. Science 275: 983–986

Schatz G (1993) The protein import machinery of mitochondria. Prot. Sci. 2: 141–146

Schendel SL and Cramer WA (1994) On the nature of the unfolded intermediate in the *in vitro* transition of the colicin E1 channel domain from the aqueous to the membrane phase. Prot. Sci. 3: 2272–2279

Schendel SL, Xie Z, Montal MO, Matsuyama S, Montal M and Reed JC (1997) Channel formation by anti-apoptotic protein Bcl-2. Proc. Natl. Acad. Sci. U.S.A. 93: 511–5118

Schlesinger PH, Gross A, Yin X-M, Yamamoto K, Saito M, Waksman G, Korsmeyer SJ. (1997) Comparison of the ion channel characteristics of proapoptotic BAX and antiapoptotic BCL-2. Proc. Natl. Acad. Sci. U.S.A. 94: 11357–11362

Schinder AF, Olson EC, Spitzer NC, and Montal M. (1996) Mitochondrial dysrfunction is a primary event in glutamate neurotoxicity. J. Neurosci. 16: 6125–6133

Sedlak TW, Oltvai ZN, Yang E, Wang K, Boise LH, Thompson CB and Korsmeyer SJ (1995) Multiple Bcl-2 family members demonstrate selective dimerizations with Bax. Proc. Natl. Acad. Sci. U.S. A. 92: 7834–7838

Shimizu S, Eguchi Y, Kamiike W, Waguri S, Uchiyama Y, Matsuda H, and Tsujimoto Y. (1996) Bcl-2 blocks loss of mitochondrial membrane potential while ICE inhibitors at a different step during inhibition of death induced by respiratory chain inhibitors. Oncogene 13: 21–29

Shin YK, Levinthal C, Levintahl F, and Hubbel WL. (1993) Colicin E1 binding to membranes: time-resolved studies of spin-labeled mutants. Science 259: 960–963

Strack PR, Frey MW, Rizzo CJ, Cordova B, George HJ, Meade R, Ho SP, Corman J, Tritch R, Korant BD. (1996) Apoptosis mediated by HIV protease is preceded by cleavage of Bcl-2. Proc. Natl. Acad. Sci. U.S.A. 93: 9571–9576

Thompson CB (1995) Apoptosis in the pathogenesis and treatment of disease. Science 267: 1456–1462

Tsujimoto Y, Cossman J, Jaffe E and Croce C (1985) Involvement of the bcl-2 gene in human follicular lymphoma. Science 228: 1440–1443

van der Goot FG, González-Mañas JM, Lakey JH and Pattus F. (1991) A 'molten-globule' membrane-insertion intermediate of the pore-forming domain of colicin A. Nature 354: 408–410

Wang HG, Rapp UR and Reed JC (1996) Bcl-2 targets the protein kinase Raf-1 to mitochondria. Cell 87: 629–638

Yin X-M, Oltvai ZN and Korsmeyer SJ (1994) BH1 and BH2 domains of Bcl-2 are required for inhibition of apoptosis and heterodimerization with Bax. Nature 356: 312–323

Zakharov SD, Heymann JB, Zhang Y-L and Cramer WA (1996) Membrane binding of the colicin E1 channel: activity requires an electrostatic interaction of intermediate magnitude. Biophys. J. 70: 2774–2783

Zamzani N, Marchetti P, Castedo M, Decaudin D, Macho A, Hirsch T, Susin SA, Petit PX, Mignotte B and Kroemer G. (1995) Sequential reduction of mitochondrial transmembrane potential and generation of reactive oxygen species in early programmed cell death. J. Exp. Med. 182: 367–377

Zha H, Aime-Sempe C, Sato T and Reed JC (1996a) Proapoptotic protein bax heterodimerizes with Bcl-2 and homodimerizes with Bax via novel domain (BH3) distinct from BH1 and BH2. J. Biol. Chem. 271: 7440–7444

Zha H, Fisk HA, Yaffe MP, Mahajan N, Herman B and Reed JC (1996b) Structure-function comparisons of the proapoptotic protein Bax in yeast and mammalian cells. Mol. Cell. Biol. 16: 6494–6508

Zoratti M and Szabo I (1995) The mitochondrial permeability transition. Biochim. Biophys. Acta. Rev. Biomembr. 1241: 139–176